Multimodal Proprioceptive Integration

in Sensorimotor Networks of an Insect Leg

Inaugural-Dissertation

zur

Erlangung des Doktorgrades

der Mathematisch-Naturwissenschaftlichen Fakultät

der Universität zu Köln

vorgelegt von

Corinna Gebehart

aus Köln

2021

Berichterstatter/in:

Prof. Dr. Ansgar Büschges

Prof. Dr. Silvia Daun

Prof. Dr. Harald Wolf

Tag der mündlichen Prüfung: 17. September 2021

Dedicated to my teachers,

past and present,

in science and life.

Contents

Abstract

An animal's nervous system monitors the actions of the body using its sense of proprioception. This information is used for precise motor control and to enable coordinated interaction with the animal's surroundings. Proprioception is a multimodal sense that includes feedback about limb movement and loading from various peripheral sense organs. The sensory information from distinct sense organs must be integrated by the network to form a coherent representation of the current proprioceptive state and to elicit appropriate motor behavior.

By combining intra- and extracellular electrophysiological recording techniques with precise mechanical sensory stimulation paradigms, I studied multimodal proprioceptive integration in the sensorimotor network of the stick insect leg. The findings demonstrate *where*, *when*, and *how* sensory feedback from load-sensing campaniform sensilla (CS) is integrated with movement information from the femoral chordotonal organ (fCO) in the sensorimotor network controlling movement of the femur-tibia (FTi) joint.

Proprioceptive information about distinct sensory modalities (load / movement) and from distinct sense organs of the same sensory modality (trochanterofemoral CS (tr/fCS) / tibial CS (tiCS)) was distributed into one network of local premotor nonspiking interneurons (NSIs). The NSIs' processing of fCO, tr/fCS, and tiCS was antagonistic with respect to a given NSI's effect on the motor output of extensor tibiae motor neurons (ExtTi MNs).

Spatial summation of load and movement feedback occurred in the network of premotor NSIs, whereas temporal summation was shifted between sensory modalities. Load feedback (tr/fCS / tiCS) was consistently delayed relative to movement signals (fCO) throughout the sensorimotor pathways of sensory afferents, premotor NSIs, and ExtTi MNs. The connectivity between these neuron types was inferred using transmission times and followed distinct patterns for individual sense organs. At the motor output level of the system, the temporal shift of simultaneously elicited load and movement feedback caused load responses to be superimposed onto ongoing movement responses.

These results raised the hypothesis that load could alter movement signal processing. Load (tiCS) affected movement (fCO) signal gain by presynaptic afferent inhibition. In postsynaptic premotor NSIs, this led to altered movement parameter dependence and nonlinear summation of load and movement signals. Specifically, the amplitude dependence of NSIs opposing ExtTi MN output was increased, and, consistently, the movement response gain of the slow ExtTi MN was decreased. Movement signal processing in the premotor network was altered depending on the proprioceptive context, i.e. the presence or absence of load feedback.

Lateral presynaptic interactions between load (tiCS) and movement (fCO) afferents were reciprocal, i.e. existed from fCO to tiCS afferents and vice versa, and also occurred between sensory afferents of the same sense organ. Additionally, a new type of presynaptic interaction was identified. Load signals increased the gain of directional movement information by releasing unidirectionally velocity- or acceleration-sensitive fCO afferents from tonic presynaptic inhibition. Paired double recordings showed lateral connectivity also at the level of the premotor NSI network. NSIs interacted via reciprocal excitatory connections. Additionally, the activity of individual NSIs was correlated in the absence of external stimuli, and specific types of NSIs showed rhythmic 30 Hz oscillations of the resting membrane potential, indicating an underlying mechanism of network synchronization.

Taken together, the results of this dissertation provide an understanding of the integration of multimodal proprioceptive feedback in the sensorimotor network by identifying neuronal pathways and mechanism underlying spatial and temporal signal summation. The local network uses multimodal signal integration for context-dependent sensory processing, thereby providing insights into the mechanism by which a local network can adapt sensory processing to the behavioral context. Initial results clearly highlight the necessity to consider lateral connections along sensorimotor pathways to unravel the complex computations underlying proprioceptive processing and motor control. The findings on the integration of proprioceptive signals, obtained in the resting animal, broaden our understanding of sensorimotor processing and motor control not only in the stationary, but also in the walking animal.

List of Abbreviations

CI_1	common inhibitor 1
CS	campaniform sensilla
ExtTi	extensor tibiae
eExtTi MNs	excitatory extensor tibiae motor neurons
fCO	femoral chordotonal organ
fCO afferents – A	acceleration-sensitive fCO afferent
fCO afferents – P	position-sensitive fCO afferent
fCO afferents – V	velocity-sensitive fCO afferent
FETi	fast extensor tibiae
FTi	femur-tibia
GABA	γ-aminobutyric acid
G6A / G6B	group 6A / group 6B
I	current
MN	motor neuron
ncr	nervus cruris
nl3	nervus lateralis 3
nl5	nervus lateralis 5
NSI	nonspiking interneuron
NSI – E	NSI with excitatory effects on SETi MN
NSI – I	NSI with inhibitory effects on SETi MN
PAD	primary afferent depolarization
PTX	picrotoxin
R	resistance
RetCx	retractor coxae
SETi	slow extensor tibiae
tiCS	tibial campaniform sensilla
tr/fCS	trochanterofemoral campaniform sensilla
V_m	membrane potential / voltage

1 Introduction

1.1 Proprioception

An animal's sense of proprioception is an essential requirement for precise motor control in changing and unpredictable surroundings. It enables closed loop neuronal control of movements by supplying the nervous system with feedback about the consequences of its own actions. Animals rely on their sense of proprioception to stabilize locomotion, to respond to external perturbations, and even during the seemingly simple task of standing still and maintaining a fixed posture (Zill et al., 2004; Deliagina et al., 2012; Proske and Gandevia, 2012; Edwards and Prilutsky, 2017). Proprioceptive feedback from mechanosensory structures provides information about the state of the body, for example, with regard to limb movement, joint position, and muscle force. Additionally, it supplies information about the body's interaction with its surroundings by signaling external perturbations or deviations from a planned motor action caused by unexpected features of the environment (Sherrington, 1907; Proske and Gandevia, 2012; Tuthill and Azim, 2018).

Proprioceptive feedback is a ubiquitous element of motor control, with common principles found between vertebrates and invertebrates (Pearson, 1995a; Tuthill and Azim, 2018; Dallmann et al., 2021). Despite differences in the anatomy of their bodies and the structure of their nervous systems, both vertebrates and invertebrates make use of sensory structures signaling limb loading, movement, and position to coordinate their movements and maintain their posture. To achieve postural stability, proprioceptive signals from peripheral sense organs are integrated with the central motor programs carried out during locomotion (Bidaye et al., 2018). They interact with central pattern generating networks to stabilize movements, coordinate phase timing and transition, and enable rapid responses to perturbations (e.g. Hess and Büschges, 1999; Noah et al., 2001; Akay et al., 2014; Mulloney et al., 2014). Not only the rhythmic patterns of locomotion are shaped by proprioceptive feedback, but also planned motor tasks such as targeted reaching movements depend on these signals (Fink et al., 2014; Weiler et al., 2021). In both the presence or absence of active movement, proprioception is essential for establishing and maintaining an upright posture (Bässler, 1993; Deliagina et al., 2012; Grillner and El Manira, 2020). The relevance of proprioception becomes especially obvious when it is disturbed by experimental design or in disease, with effects ranging from altered walking kinematics (Ivanenko et al., 2000; Mendes et al., 2013) to deficient motor control (Graham and Bässler, 1981), and symptoms of complex disorders like Parkinson's disease (e.g. Zia et al., 2000) and schizophrenia (Frith et al., 2000).

The sense of proprioception differs from other senses such as vision or olfaction as it combines multiple sensory modalities from distinct sense organs and is not limited to a single type of sensory structure. In legged animals, the two main sources of proprioceptive feedback from the limbs are

constituted by the senses of load and movement. Load sensors provide information about forces acting on, or within, the limb, caused by self-generated muscle forces, external forces such as gravity, or external perturbations that act on the limb or that the moving limb encounters (Zill et al., 2004; Windhorst, 2007). In vertebrates, Golgi tendon organs within the limbs are located in parallel with tendons and muscles and measure changes in tendon length as a proxy for muscle load and force (Jami, 1992; Proske and Gandevia, 2012). In insects, campaniform sensilla (CS) are embedded into the cuticle of the legs and measure force and load as distortions of the cuticular exoskeleton (Pringle, 1938; Zill and Moran, 1981a; Zill et al., 2004). CS can be directionally sensitive and are typically found in groups with similar directional preference. Several of these groups are distributed on the segments of the insect leg (Zill and Moran, 1981a; Hofmann and Bässler, 1982; Zill et al., 2011; Dinges et al., 2021).

The second source of proprioceptive feedback from the limbs are movement-sensing organs that provide information about joint position or movement, and its derivatives, i.e. velocity and acceleration. Muscle spindles are embedded into the vertebrate muscle and measure changes in muscle fiber length, whereas in insects chordotonal organs, mechanosensory hairs or bristles, and hair plates measure joint angle and its extreme positions (Field and Matheson, 1998; Büschges and Gruhn, 2007; Windhorst, 2007; Tuthill and Wilson, 2016a).

In insects and vertebrates alike, load and movement are perceived by distinct sensory structures that reside within the same limb and which are activated by stimuli that typically are a mixture of both sensory modalities, thus activating both types of sense organs in parallel. A monkey that moves an object requires shortening of muscle fibers in its arm, sensed by the embedded muscle spindles, while the weight of the object and the generated muscle force pull on tendons and thereby activate Golgi tendon organs. Similarly, a leaf moving beneath the tarsus of a still-standing stick insect will affect joint angles, and muscle forces generated to keep the leg in position against the moving leaf will distort the cuticle. As these examples demonstrate, the different proprioceptive senses typically act in parallel, and in many cases elicit reflex responses in the same muscles. In stick insects, load or other forces acting on a group of CS on the proximal tibia (tibial CS (tiCS), group 6) elicit responses in motor neurons (MNs) innervating the extensor tibiae (ExtTi) muscle (Zill et al., 2011). The same MNs respond to signals from the femoral chordotonal organ (fCO), the movement sensor of the femur-tibia (FTi) joint that is moved by the ExtTi muscles (Bässler, 1983a). Similar examples can be found in the reflex pathways of vertebrates (Jankowska, 2013b).

Proprioception as a multimodal sense in the context of motor control therefore requires the convergence of load and movement signals in the nervous system. In this dissertation, I have made use of the well-studied sensorimotor system of the stick insect (Bässler, 1993; Bässler and Büschges, 1998; Büschges and Gruhn, 2007) to study proprioceptive integration of load and movement feedback in the

neuronal control loop of the FTi joint, with a specific focus on spatial and temporal summation of proprioceptive signals, and their interaction within the processing networks.

1.2 Spatial Summation of Multimodal Proprioceptive Feedback

The first part of this dissertation will focus on spatial summation of load and movement signals, i.e. the question *where* in the network these signals converge. As described above, proprioceptive signals from different sense organs are often present at the same time and act on the same muscles. Signals from load and movement sense organs must therefore interact to form a coherent proprioceptive representation of a limb's position in space and its interaction with the environment. Interneurons located within the spinal cord of vertebrates are known to be major sites of signal integration (Czarkowska et al., 1981; Jankowska and McCrea, 1983; Jankowska, 2013a, b). Similarly, in insects, local interneurons in the ventral nerve cord integrate intersegmental and sensory signals with inputs from other sources (Burrows, 1996). Studies on large insects additionally benefit from direct experimental measurements of neuronal activity, since the neuropilar arborizations of neurons are accessible to single neuron intracellular recordings. Specifically the premotor network of the FTi joint has been the subject of extensive studies on sensorimotor control (e.g. Büschges, 1990; Sauer et al., 1995; Wolf and Büschges, 1995; Driesang and Büschges, 1996; Sauer et al., 1996), resulting in detailed knowledge about the neuronal pathways that integrate proprioceptive movement feedback and coordinate movement of the tibia. The position of and movement around the FTi joint, i.e. extension and flexion of the tibia relative to the femur, is monitored by the fCO, whose signals are distributed into an antagonistic network of individually identifiable, local premotor nonspiking interneurons (NSIs, Büschges, 1990, 1994; Sauer et al., 1996). The NSIs, in turn, either drive or inhibit activation of ExtTi MNs, which control extension of tibia. In the locust, NSIs, albeit not individually identified, were found to respond to load activation of CS (Burrows and Pflüger, 1988; Laurent and Burrows, 1988). This led to the hypothesis that local premotor NSIs of the FTi joint control loop, which process movement feedback from the fCO, are the point of convergence for multiple proprioceptive modalities. To test this hypothesis, intracellular sharp electrode recordings of local premotor NSIs were combined with mechanical stimulation of the fCO and groups of CS located on the trochanterofemur (tr/fCS, groups 1-5) and the tibia (tiCS, groups 6A & B (G6A, G6B)). The results presented in Chapter 2 demonstrate that local premotor NSIs of the FTi joint control loop are the point of convergence for signals from movement and multiple load sense organs. More particularly, this was true for every single NSI that was found in this study, with no exceptions of NSIs processing signals only from only a subset of the examined sense organs. Load and movement signals were distributed into, and processed by, a single, antagonistic network of NSIs and no NSI was specifically dedicated to one sensory modality alone.

1.3 Temporal Summation of Multimodal Proprioceptive feedback

Multimodal proprioceptive signal integration is not only determined by spatial summation, i.e. *where* signals converge along the neuronal pathways from sense organs to MNs, but also by temporal summation, i.e. *when* signals converge. Does the nervous system have access to the same temporal state of load and movement information at any given point in time, or do signals from one sensory modality reach the network faster than from the other? This is of especial relevance for proprioception as a multimodal sense whose signals, e.g. in the motor control of the leg, are relayed from sense organs that are located spatially apart at distant positions on or in the leg (cf. Chapter 1.1). A shift in balance, and thus in weight distribution, from one leg to another, for example, will simultaneously stimulate load and movement sense organs, whose electrical signals will then be transmitted from different starting points (the sensory structures) along initially separate neuronal pathways (sensory afferents and their postsynaptic neurons) to finally converge in the nervous system (e.g. Jankowska and McCrea, 1983; Burrows, 1996; Schmitz and Stein, 2000). It was therefore hypothesized that the transmission distance for an individual sensory signal, in terms of the length of the neuronal projections and the number of postsynaptic synapses and neurons, will differ between sensory modalities. If differences in signal timing in neural networks are not compensated for by other properties of the nervous system, they may have functional effects on signal integration (Hodgkin, 1954; Hartline and Colman, 2007; Thoreson and Mangel, 2012; Hedwig and Sarmiento-Ponce, 2017).

The stick insect is a particularly useful model organism for this type of question. As an invertebrate, it does not possess myelinated axons. Therefore, and because of its size, the distances between sense organs, and between the sense organs and the nervous system, are sufficiently large to potentially cause functionally meaningful, and experimentally measurable signal latencies. In Chapter 3, the timing and latencies of sensory signals and their elicited responses in the network were measured using intra- and extracellular recordings from CS and fCO sensory afferents, local premotor NSIs, and MNs. Using signal timing to distinguish between short- and long-latency connections from sensory afferents to postsynaptic neurons enabled the inference of network connectivity, i.e. mono- and polysynaptic connections. In combination with the absolute time from stimulus onset to responses within the network, this allowed for comparison between load and movement signal timing and processing. The data revealed a consistent shift between both proprioceptive modalities, observable by load signaling being delayed in comparison to movement. The effect persisted from the sensory afferent input into the system via the interneuronal and motor neuronal network to its output and the resulting muscle force.

1.4 Integration of Multimodal Proprioceptive Feedback

Spatial and temporal summation of multimodal proprioceptive feedback establish the essential framework that is underlying proprioceptive integration. Proprioceptive signals from distinct sense organs,

however, do not only run in parallel through the same network. They shape each other's processing and the resulting motor output, for example, by altering the strength of reflex responses, the precision of postural control, or the likelihood of occurrence of reflex reversals (Schmitz and Stein, 2000; Akay and Büschges, 2006; Kistemaker et al., 2013). To understand how signals from distinct proprioceptive modalities intertwine to form a coherent representation of the leg's proprioceptive space, therefore, requires not only knowledge about *where* and *when* signals interact, but also *how* these interactions shape signal integration.

The concept of proprioception as one single, multimodal sense raises the question how multimodal signals interact and how they may affect each other's processing. Load and movement feedback in general are often present at the same time, while consisting of different combinations of specific load and movement signals. For example, moving a leg backwards during stance phase of walking and a backward movement caused by an external perturbation exerting force on the anterior side of the leg may result in similar movement, but very different load signals. They will in turn require different motor responses. Similarly, during walking, body weight should be shifted onto a leg that is terminating swing phase only if this leg has made ground contact. If a leg steps into a hole, no load feedback signaling ground contact will occur. Shifting body weight onto this leg could result in loss of stability and falling and should therefore be prevented (Szczecinski et al., 2018). Thus, hypothetically, one important aspect of load and movement feedback integration could be to contextualize each other, i.e. to change the relevance or meaning of one modality in the presence or absence of the other.

The results presented in the following Chapters 2 and 3 demonstrate that load and movement feedback were combined within the same network of NSIs but with a constant shift in timing that resulted in a delay of load signals with respect to movement feedback. These findings led to the hypothesis that load signals may reach the network in time to tune an ongoing movement response within the network, i.e. to alter movement signal processing in the context and presence of load feedback. In Chapter 4, this hypothesis was tested by combining load and movement stimuli while recording from the different elements of the sensorimotor network. The effects of multimodal signal integration were examined in the network of interneurons that was identified as a point of multimodal convergence in Chapters 2 and 3. Additionally, it was analyzed at the level of the sensory afferent input to the network and its motor output, following indications from previous studies of multimodal signal integration at these levels of the sensorimotor network of the stick insect leg (Stein and Schmitz, 1999; Schmitz and Stein, 2000; Akay and Büschges, 2006).

Across vertebrates and invertebrates, presynaptic inhibition between sensory afferents is a ubiquitous mechanism for filtering of sensory input and the avoidance of sensory overload by controlling the gain of sensory signals (Dudel and Kuffler, 1961; Clarac and Cattaert, 1996; Azim and Seki, 2019). Making

use of the accessibility of all these elements in the stick insect sensorimotor network, in combination with the possibility to specifically target individual sense organs with precisely controlled stimuli, allowed for tracing of the effects of multimodal sensory integration throughout the network. Presynaptic inhibition from a distinct group of CS (tiCS, group 6) onto fCO afferents was identified. Combined load and movement stimuli led to an altered gain of movement signal responses in local premotor NSIs, including those that are monosynaptic targets of fCO afferents (cf. Sauer et al., 1996). A specific upregulation of the gain of NSIs that are known to oppose the resistance reflex in the ExtTi MNs (Büschges, 1990; Sauer et al., 1996) was consistent with the effects of combined load and movement stimuli on the slow ExtTi MN (SETi) at the level of the neuronal motor output. The results presented in Chapter 4 provide the neuronal base for a mechanism by which presynaptic inhibition between sensory afferents of different modalities can shift the balance of an antagonistic, distributed network to alter the motor output of the system in a sensory context-dependent manner.

The mechanism of sensorimotor gain control based on presynaptic afferent inhibition identified in this dissertation highlights the relevance of lateral connectivity within the premotor network. The network does not solely consist of parallel, independent pathways that process proprioceptive signals in a purely feedforward way. To understand proprioceptive integration, and the mechanisms underlying the internal representation of the animal's current proprioceptive state, information about lateral connections at different levels of the network will be essential. In Chapter 5, initial data on two aspects of lateral connectivity, namely at the level of sensory afferents and within the premotor network, will be presented to provide an outlook and a basis for future investigations. Lateral connectivity between load and movement sensory afferents was analyzed in detail, and a new mechanism for upregulating the sensory signal gain of specific sensory afferents was identified. In the premotor NSI network, lateral connectivity was analyzed using paired double recordings of identified NSIs. The recorded NSIs were connected by reciprocal, excitatory connections. Additionally, specific types of NSIs were found to have correlated, and in some cases synchronized oscillatory, fluctuations in membrane potential in the absence of external stimuli. The results indicate that lateral connections between NSIs might play an important role in strengthening network coupling and proprioceptive processing. Based on the findings presented in Chapters 2, 3, and 4, analyzing the relevance of the pathways and mechanisms of lateral connectivity in the premotor network will further advance our understanding of multimodal proprioceptive signal integration and, ultimately, how the sense of proprioception arises and is used by premotor networks for stable, yet flexible, motor control.

2 Distributed Processing of Multimodal Proprioceptive Feedback

2.1 Distributed Processing of Load & Movement Feedback in the Premotor Network Controlling an Insect Leg Joint

Gebehart, C., Schmidt, J., Büschges, A.

In Chapter 2, the spatial summation of load (tr/fCS & tiCS) and movement (fCO) proprioceptive feedback in the distributed, antagonistic network of local premotor NSIs of the stick insect FTi joint control loop is described. It thereby establishes the neuronal basis of multimodal proprioceptive integration in the sensorimotor network of an insect leg by identifying the network responsible for of spatial sensory signal summation.

The results on NSI responses to tr/fCS stimuli include a small number of experiments that I performed as part of my Master's Thesis (Gebehart, 2018). Specifically, initial data on NSI responses to stimulation of tr/fCS was collected during the Master's Thesis. These experiments were repeated and extended as part of my PhD dissertation.

This study was published in 2021 in *Journal of Neurophysiology*, 125: 1800 - 1813.

doi:10.1152/jn.00090.2021

NSIs were stained for morphological characterization. Exemplary stainings of recorded and identified NSIs that were characterized in previous studies are shown in Supplementary Figure 2.1.

2.2 Author Contributions

Conceived & designed experiments:

Corinna Gebehart, Joachim Schmidt, Ansgar Büschges

Performed experiments, analyzed data & prepared figures:

Corinna Gebehart

Interpreted experimental results:

Corinna Gebehart, Joachim Schmidt, Ansgar Büschges

Drafted manuscript:

Corinna Gebehart, Ansgar Büschges

Edited & revised manuscript & approved final version:

Corinna Gebehart, Joachim Schmidt, Ansgar Büschges

J Neurophysiol 125: 1800–1813, 2021.
First published March 31, 2021; doi:10.1152/jn.00090.2021

american physiological society

JNP JOURNAL OF NEUROPHYSIOLOGY

RESEARCH ARTICLE

Control of Movement

Distributed processing of load and movement feedback in the premotor network controlling an insect leg joint

Corinna Gebehart, Joachim Schmidt, and Ansgar Büschges

Department of Animal Physiology, Institute of Zoology, Biocenter Cologne, University of Cologne, Cologne, Germany

Abstract

In legged animals, integration of information from various proprioceptors in and on the appendages by local premotor networks in the central nervous system is crucial for controlling motor output. To ensure posture maintenance and precise active movements, information about limb loading and movement is required. In insects, various groups of campaniform sensilla (CS) measure forces and loads acting in different directions on the leg, and the femoral chordotonal organ (fCO) provides information about movement of the femur-tibia (FTi) joint. In this study, we used extra- and intracellular recordings of extensor tibiae (ExtTi) and retractor coxae (RetCx) motor neurons (MNs) and identified local premotor nonspiking interneurons (NSIs) and mechanical stimulation of the fCO and tibial or trochanterofemoral CS (tiCS, tr/fCS), to investigate the premotor network architecture underlying multimodal proprioceptive integration. We found that load feedback from tiCS altered the strength of movement-elicited resistance reflexes and determined the specificity of ExtTi and RetCx MN responses to various load and movement stimuli. These responses were mediated by a common population of identified NSIs into which synaptic inputs from the fCO, tiCS, and tr/fCS are distributed, and whose effects onto ExtTi MNs can be antagonistic for both stimulus modalities. Multimodal sensory signal interaction was found at the level of single NSIs and MNs. The results provide evidence that load and movement feedback are integrated in a multimodal, distributed local premotor network consisting of antagonistic elements controlling movements of the FTi joint, thus substantially extending current knowledge on how legged motor systems achieve fine-tuned motor control.

NEW & NOTEWORTHY Proprioception is crucial for motor control in legged animals. We show the extent to which processing of movement (fCO) and load (CS) signals overlaps in the local premotor network of an insect leg. Multimodal signals converge onto the same set of interneurons, and our knowledge about distributed, antagonistic processing is extended to incorporate multiple modalities within one perceptual neuronal framework.

leg muscle control system; motor control; multimodal integration; posture control; sensorimotor processing

INTRODUCTION

Animals in their natural environment need to control both, body posture and movements at all times to perform precisely tuned and contextually appropriate motor behaviors, being it maintenance of a specific body posture at rest or active movements of their appendages during behavioral tasks. In legged animals, vertebrates and invertebrates alike, body posture is maintained against gravity and external perturbations by the leg muscle control system generating postural reflexes in response to proprioceptive sensory feedback [reviews in Bässler (1), Burrows (2), Deliagina et al. (3), Grillner and El Manira (4)]. In vertebrates, this feedback is provided by Golgi tendon organs and muscle spindles [reviewed in Jami (5), Windhorst (6)]. In insects, proprioceptive feedback is provided by functionally analogous sense organs, that is, hair plates or chordotonal organs and campaniform sensilla (CS) that are distributed in and on the legs (7–11). The former provide information on joint position and movement, CS monitor forces generated by external perturbations or internal muscle strains. These signals are used by local motor networks to control timing and strength of motor activity via the activation of motor neurons (MNs) that target limb muscles to maintain a stable body posture (1, 2, 12). To form a coherent representation of the proprioceptive context of a limb and thus enable skilled and precise postural control, the different, usually

Correspondence: A. Büschges (ansgar.bueschges@uni-koeln.de); C. Gebehart (c.gebehart@uni-koeln.de).
Submitted 1 March 2021 / Revised 29 March 2021 / Accepted 30 March 2021

concurrently activated, types of sensory feedback, that is, movement and load, need to be integrated in the premotor network of the leg muscle control system. Despite detailed knowledge of the topology of neuronal pathways processing individual aspects of proprioceptive feedback [e.g., Büschges (13), Laurent and Burrows (14)], little is known about how multimodal proprioceptive feedback, for example, feedback arising from movement and load sensing organs in and on the legs, is integrated in the local networks that control limb movements (15).

In arthropods, neural pathways processing proprioceptive signals to control motor activity consist of direct, monosynaptic connections between sensory neurons and leg MNs (16, 17), acting in parallel with polysynaptic pathways comprised of local interneurons [reviews in Bässler and Büschges (18), Edwards and Prilutsky (19); Laurent and Burrows (14); Sauer et al. (20)]. The neural network topology consisting of polysynaptic pathways that operate by means of parallel, distributed processing is well established for sensory signals reporting position and movement of a limb (1, 18, 20–22). In distributed networks, information processing along each individual channel does not necessarily support the generated overall motor activity, but may also generate an opposing synaptic drive to the MNs (stick insect: 22–24, locust: 12, 21).

A well-studied case in this respect is the neural network controlling the activity of MNs supplying the extensor tibiae (ExtTi) muscle of the femur-tibia (FTi) joint in the stick insect. This network processes sensory signals from the femoral chordotonal organ (fCO), which provides information on position and movement of the tibia in relation to the femur (25, 26). Besides direct connections from fCO sensory neurons to ExtTi MNs, individual polysynaptic pathways via more than 10 types of identified local nonspiking interneurons (NSIs) between the fCO and ExtTi MNs have so far been identified (13, 22, 27). Given their specific synaptic inputs from fCO afferents, for example, during tibial flexion, and their synaptic drive to ExtTi MNs, individual premotor NSIs support the postural reflex muscle activation, that is, activation of these MNs, whereas others oppose it. The network of NSIs within the control loop of the FTi joint thus presents an example of parallel, distributed processing (18, 22). Subsequent modeling studies verified the functional sufficiency of this kind of proprioceptive information processing by emphasizing its significance for task-specific modulation of gain and sign of reflex responses (22, 28).

For a more complete picture of the network architecture and function underlying postural control, however, it is necessary to investigate the identified sensory processing in the context of more complex conditions. Outside of experimental conditions proprioceptive feedback from multiple sense organs will not occur separately and movement signals have to be integrated with other types of input. More specifically, perturbations of limb posture are not represented by changes in the position of a leg segment only, as they always concur with forces acting on the limb through external load and/or internally generated muscle forces, thereby establishing a behavioral meaningful representation of a leg's sensory context (29). Multimodal integration presents a basis for context-dependent motor responses at the level of the local network, for example, contributing to postural control in the resting and the walking animal. In the insect leg, this relates to the concurrent processing of movement signals from the fCO with load feedback from groups of CS located at specific locations of the segments of each leg (10, 30–32). Given the simultaneous presence of this bimodal proprioceptive feedback in the local network and the contribution of both movement and load/force sensors to stable posture, investigating their integration and the underlying processing principles is essential for our understanding of the operation of motor control systems not only in an insect but also in other animals.

In the present study, we investigated multimodal sensory processing specifically for the integration of movement and load feedback in the middle leg FTi joint premotor network of the stick insect, *Carausius morosus*. The size of these insects allows precise, individual or concurrent mechanical stimulation of multiple sense organs. We studied how signals from the fCO and load signals from tibial and trochanterofemoral CS (tiCS, tr/fCS) are processed in the premotor network controlling MNs that innervate ExtTi muscles. Previous studies have shown that signals from tiCS contribute to the control of the activity of ExtTi MNs (33, 34). Forces acting on the immobile tibia in the direction of flexion induce a reflex activation in ExtTi MNs, whereas forces acting on the tibia in the opposite direction have the opposite influence. Although previously shown to have smaller or no influence on the activity of ExtTi MNs, we included tr/fCS in our stimulation paradigm (31, 35, 36). The position of these proximal CS has been hypothesized to endow them with the ability to integrate forces acting along the entire leg, implicating a functional role of tr/fCS for coordination of multiple leg joints, including the FTi joint [discussed in Akay et al. (37), Höltje and Hustert (38), Zill et al. (39)].

We combined mechanical sensory stimulation of tiCS, tr/fCS, and the fCO with extracellular recordings from lateral motor nerves and intracellular recordings from neuropilar arborizations of NSIs and MNs. We show the individual and combined effects of load and movements stimuli in these neuron types and identify three previously unpublished types of NSIs. We find that the same set of premotor interneurons integrates both load and movement feedback in a distributed, antagonistic fashion, and that individually identifiable interneurons show similar response characteristics for bimodal and distributed sensory integration of movement and load/force signals.

MATERIALS AND METHODS

Animals

Experiments were performed at room temperature (20°C–24°C) on adult female stick insects, *C. morosus*, from the parthenogenetic colony at the University of Cologne. Animals were provided with blackberry leaves ad libitum and kept in a 12-h light/dark cycle at 23°C–27°C and 50% humidity. We confirm that all animals were kept and handled according to the pertinent guidelines.

Dissection

All legs except the right mesothoracic leg were removed. The coxa-trochanter joint was immobilized by inserting a

minuten pin into the cuticle of the ventral trochanter and both the coxa-trochanter, and the thorax-coxa joints were fixated with light-curing glue (3 M ESPE Sinfony, Neuss, Germany), setting the trochanterofemur at 90° to the body long axis (40).

tr/fCS and tiCS were stimulated in separate experiments. For stimulation of tr/fCS, the animal was positioned dorsal side up on a platform with the femur suspended in midair. For tiCS stimulation, the FTi joint, in addition to the other two joints, was fixed to 90°–110° and the distal femur was glued to the platform with the tibia protruding over the edge.

The mesothoracic ganglion was exposed by a dorsal midline incision, intestines, and main trachea were left intact. Contralateral mesothoracic nerves were squeezed, the ipsilateral nervi anterior, posterior, and transversalis were cut [nomenclature according to Marquardt (41)]. The ganglion was placed on a wax-coated steel platform, its surrounding connective tissue pinned with cactus spines according to established procedures [e.g., Büschges (13), Driesang and Büschges (42)]. To enable electrode penetration, Pronase E crystals (VWR, Darmstadt, Germany) were placed on the ganglion for 45 s, followed by rinsing with extracellular saline [178.54 mM NaCl, 17.61 mM KCl, 7.51 mM $CaCl_2$, 25 mM $MgCl_2$, 10 mM HEPES buffer, set to pH 7.2 with NaOH (43)]. Experiments were performed in inactive, that is, resting, animals [for definition of behavioral states and review see Bässler (1)].

Electrophysiological Recordings

Sharp microelectrodes (resistance 25–35 MΩ) were fashioned from borosilicate glass capillaries (8GB100TF-8P, Science Products, Hofheim, Germany) with a micropipette puller (P-1000, Sutter Instruments, Novato, CA). Electrodes contained a chlorinated silver wire and intracellular saline [1 M KAc, 0.1 M KCl, 5% neurobiotin tracer (Vector Laboratories, Burlingame, CA)]. Intracellular recordings were made from neuropilar arborizations of premotor NSIs and MNs in the ipsilateral hemiganglion. Interstitial potentials (5–20 mV) were compensated (44). Intracellular signals were amplified (gain ×20, highcut filter 3 kHz, SEC-06 preamplifier, SEC-10LX single electrode clamp amplifier, npi, Tamm, Germany), current injection pulses were controlled with a digital stimulator (MS501, Electronics Workshop Animal Physiology, University of Cologne, Germany).

Extracellular signals from lateral nerves were recorded with hook electrodes (45). Activity of ExtTi MNs was recorded from nerve F2 in the femur (Figs. 1 and 4) or nl3 (Fig. 2). Retractor coxae (RetCx) MN activity was monitored on nl5. Extracellular signals were amplified (gain ×2,000, lowcut filter 0.3 kHz, highcut 2.5 kHz, notch filter 50 Hz, MA101 preamplifier and MA102 differential amplifier, Electronics Workshop, University of Cologne). Signals were digitized and stored using Spike2 (sampling rate 12.5 kHz for extracellular, 6.25 kHz for intracellular signals, ADC Micro1401 mkI, Spike2 v7.16, CED, Cambridge, UK).

Mechanical Stimulation of Sense Organs

For stimulation of CS, a metal probe exerted force on the medial femur, pushing it into an anterior or posterior direction [tr/fCS; e.g., Haberkorn et al. (40)] or on the proximal tibia into dorsal or ventral direction [tiCS; see also Zill et al. (34), Haberkorn et al. (40)]. The respective leg segment was displaced by 50 μm with ramp-and-hold stimuli, ramp rise and fall time was 0.1 s, hold duration 1.1 s. The rising phase of each stimulus increased leg loading, the return to prestimulus levels released leg loading. Unloaded trochanterofemur and tibia were immobilized at 90° angle to the body long axis (tr/fCS stimulation) or the femur (tiCS), respectively. Minimum interstimulus interval for these and all following stimuli was 2.6 s.

To stimulate the fCO, we used two different types of experimental paradigms: *1*) In experiments with tiCS stimulation, the dorsal femur was opened and the fCO receptor apodeme was clamped according to established procedures (23, 26). Linear elongation and relaxation of the apodeme mimicked tibial flexion or extension, respectively, starting FTi joint angle in all fCO stimulation paradigms was 90°–110°. fCO ramp-and-hold stimuli consisted of 0.2 s apodeme elongation by 300 μm, corresponding to 60° of tibial flexion, a hold phase of 1 s, and 0.2 s relaxation back to the starting position (46). fCO clamp and CS stimulators were moved by custom-built linear motors (lowpass filter 1 kHz, VCM Controller/Power Amplifier, Electronics Workshop, University of Cologne), controlled with Spike2 (CED) or a digital stimulator (MS501). *2*) In experiments with tr/fCS stimulation, the femur was left intact and tiCS were ablated with a heated metal probe. To stimulate the fCO, the tibia was moved using a forked metal probe positioned around the tibia. Movements were driven by a rotational stepper motor, controlled with Mach3 (v7.13, CNC Steuerung, Bocholt, Germany). In this setting, the motor and positioning of the animal imposed constraints on ramp-and-hold stimulus parameters, which were set to approximate those of the fCO clamp stimulation. Velocity of tibial flexion and extension was set to 300°/s, final movement angle 50°, resulting in an approximate ramp duration of 0.2 s. The position was held for 1 s. During combined fCO and CS stimulation, the CS stimulus started 50 ms after the onset of the fCO stimulus ramp to synchronize holding phases.

Identification of NSIs

NSIs were identified based on established physiological and morphological characteristics. Their effect on ExtTi and RetCx MN activity was determined by de- and hyperpolarizing current injections, and NSI responses to fCO elongation and relaxation were compared with those of previously published NSIs (13, 22). Neurons were considered nonspiking if no action potentials were observed throughout the experiment, including periods of depolarizing current injection, tactile stimulation of the animal, tiCS, tr/fCS or fCO stimulation, or when the animal was actively moving (13, 47). For morphological identification, neurobiotin tracer was iontophoretically injected using positive current pulses (2 nA, 400 ms pulse duration, 1 Hz) for 10–15 min following each experiment (48). After 30–60 min tracer diffusion, the ganglion was removed, prefixated in 4% paraformaldehyde [in PBS, 5% Triton X-100 (Merck, Darmstadt, Germany)] for 20 min and fixated in 4% paraformaldehyde in PBS for 2–16 h at 4°C. Ganglia were washed three times in PBS, 10 min each, incubated in Cy3- or Cy5-conjugated streptavidin [Jackson ImmunoResearch Laboratories, Baltimore Pike, PA,

1:500 in PBS, 0.5% Triton X-100, 2% normal goat serum (Vector Laboratories)] on a shaker at 4°C overnight, washed three times in PBS for 10 min, and dehydrated in an ascending ethanol series (50%/70%/90%/100%/100%, 10 min each) before mounting in methyl salicylate (Sigma-Aldrich). Samples were imaged using a fluorescent microscope (Axio Imager.Z2 with ApoTome, Carl Zeiss Microscopy, Jena, Germany) and processed with ImageJ (1.51w, NIH).

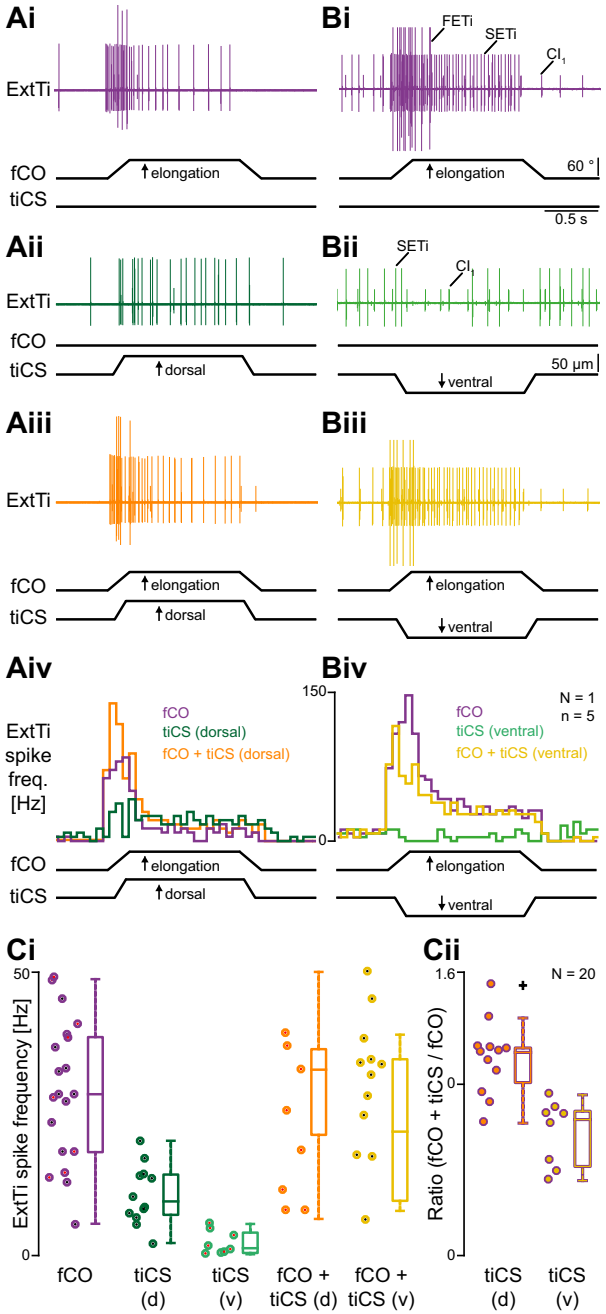

Data Analysis

MN action potential frequencies were calculated over the entire ramp-and-hold stimulus of five consecutive stimuli. Peristimulus time histograms were generated from means of five consecutive stimuli from the same experiment (bin size 50 ms). Boxplots show median, 25th, and 75th percentiles, values that exceed the distance of 1.5 times the interquartile length from the box edges were defined as mathematical outliers. MN action potentials in Fig. 5*C* were cut using a custom-written Spike2 script (peak detect amplitude 10 mV, 9 ms windows cut around each peak). Each stimulation was repeated at least five times per recording. Intracellular traces show five response sweeps of consecutive stimuli with DC offset subtracted to show response consistency if not indicated otherwise. Extracellular traces show single sweeps. Figures were created with MATLAB (R2018b, MathWorks), Spike2, and Adobe Illustrator CS6 (v16, Adobe Systems). Only those experiments and data were taken into consideration which were collected when the animal was in the inactive, that is, resting behavioral state, generating MN responses to sensory stimulation as shown in Figs. 1 and 2.

RESULTS

Individual and Combined Effects of Load and Movement on ExtTi MNs

To identify mechanisms of integration and processing of load and movement sensory feedback in the local premotor network of ExtTi MNs, we first examined the motor output that the system produces when presented with these sensory signals. We therefore investigated the individual and combined effects of movement and load feedback signals from the fCO and tiCS, respectively, on ExtTi MNs in the resting animal (Fig. 1).

Elongation of the fCO, mimicking flexion of the FTi-joint, induces the well-studied excitatory phasic-tonic response in ExtTi MNs, a resistance reflex that opposes the imposed movement (Fig. 1, *Ai* and *Bi*). Stimulation of tiCS elicited changes in spike frequency that were dependent on the direction of stimulation, that is, the activated subgroup of tiCS (Fig. 1, *Aii* and *Bii*). Dorsally directed forces pushing on the tibia activate tiCS group 6B afferents and increased ExtTi MN frequency (Fig. 1*Aii*; 33), whereas the opposite stimulus direction, that is, ventrally directed stimuli that activate tiCS

Figure 1. Load (tiCS) signals alter the strength of the resistance reflex against movement (fCO) signals; effect shown on the level of the activity of ExtTi MNs monitored by extracellular recordings of their activity. Stimulation of tiCS into dorsal (*A*) and ventral (*B*) direction causes opposing, that is, excitatory or inhibitory, changes in ExtTi MN frequency. ExtTi responses to fCO (*i*), tiCS (*ii*), and simultaneous fCO and tiCS (*iii*) ramp-and-hold stimuli; *top traces*: extracellular nerve recording, *bottom two traces*: stimulation. Peristimulus time histograms of ExtTi MN frequency to individual and combined stimuli (*iv*). Exemplary data from two different animals (*A* and *B*). Initial FTi joint angle in these and all following experiments was set to 90°–110°. *C*: individual data and boxplots of absolute ExtTi MN spike frequencies (*i*) and ratio between frequency of combined stimuli and exclusive fCO stimulation (*ii*), differentiated between dorsal (d) and ventral (v) load stimulus directions. +, Mathematical outlier. ExtTi, extensor tibiae; fCO, femoral chordotonal organ; FETi, fast extensor tibiae; FTi, femur-tibia; MN, motor neuron; SETi, slow extensor tibiae; tiCS, tibial campaniform sensilla.

group 6A afferents, reduced ExtTi MN frequency (Fig. 1*Bii*; 33). We next tested for combining both stimulus modalities by concurrent stimulation of the fCO and tiCS (Fig. 1, *Aiii* and *Biii*). Comparison of the raw data traces and peristimulus time histograms (Fig. 1, *Aiv* and *Biv*) revealed clear effects of load signals on the strength, that is, spike frequency, of the phasic component of movement-elicited resistance reflexes that were in accordance with the effects of exclusive load stimuli. Figure 1*Ci* summarizes the range of ExtTi MN frequencies measured during fCO, tiCS, and combined stimuli, with a distinction between dorsally and ventrally directed load stimuli. Note that movement signals elicited higher frequencies than load (Fig. 1*Ci*, *first panel*).

Frequencies during exclusive load stimulation clustered into two groups caused by the differential, that is, excitatory or inhibitory, effects of tiCS groups 6B and A, respectively (Fig. 1*Ci*, *second* and *third panel*). Effects of combined stimuli were not clustered when comparing absolute frequencies, as the decrease or increase caused by tiCS depended on the initial strength of the fCO-based resistance reflex in each animal (Fig. 1*Ci*, *fourth and fifth panel*). Comparing the relative change between frequencies of fCO-elicited responses with and without concurrent tiCS stimulation into the two different directions, however, demonstrates the relative increase with dorsally directed and decrease with ventrally directed load. In the following, we will first focus on individual effects of either load or movement signals, before returning to the question of their summation at the neuronal level.

Load and forces acting on different parts of the insect leg may be distributed to spatially more distant groups of CS by means of cuticular distortion (38, 39). We therefore also tested for influences of the more proximal tr/fCS groups 1–5 by applying anteriorly and posteriorly directed load to the trochanterofemur in a separate set of experiments (Fig. 2*A*). Anterior loading did not affect ExtTi MN frequency, whereas a weak phasic activation of ExtTi MNs could be seen in some of the recordings in response to posteriorly directed stimuli. This is in accordance with previous studies that found little to no effect of tr/fCS on ExtTi MNs (31, 35). In contrast, posteriorly directed tr/fCS stimulation consistently elicited phasic increases in RetCx MN frequency (Fig. 2*B*; 15, 49), whereas these MNs showed no consistent responses to stimulation of tiCS or the fCO (Fig. 2, *C* and *D*). In the following, we will include tr/fCS stimuli to provide a reference point outside the FTi control loop and to extend the analysis of load feedback integration from forces acting parallel to the leg reference frame to those orthogonal to it (39).

As extracellular recordings do not detect subthreshold synaptic inputs to MNs, we used intracellular recordings to verify whether MNs that were not activated above spiking threshold showed qualitatively the same responses as those caught on the extracellular recordings. Recordings from the slow and fast extensor tibiae (SETi, n = 3; FETi, n = 3) MNs revealed qualitatively similar influences of both types of proprioceptive feedback signals on the two MNs providing excitatory drive to the ExtTi muscle (Fig. 2, *E*–*G*). Note the

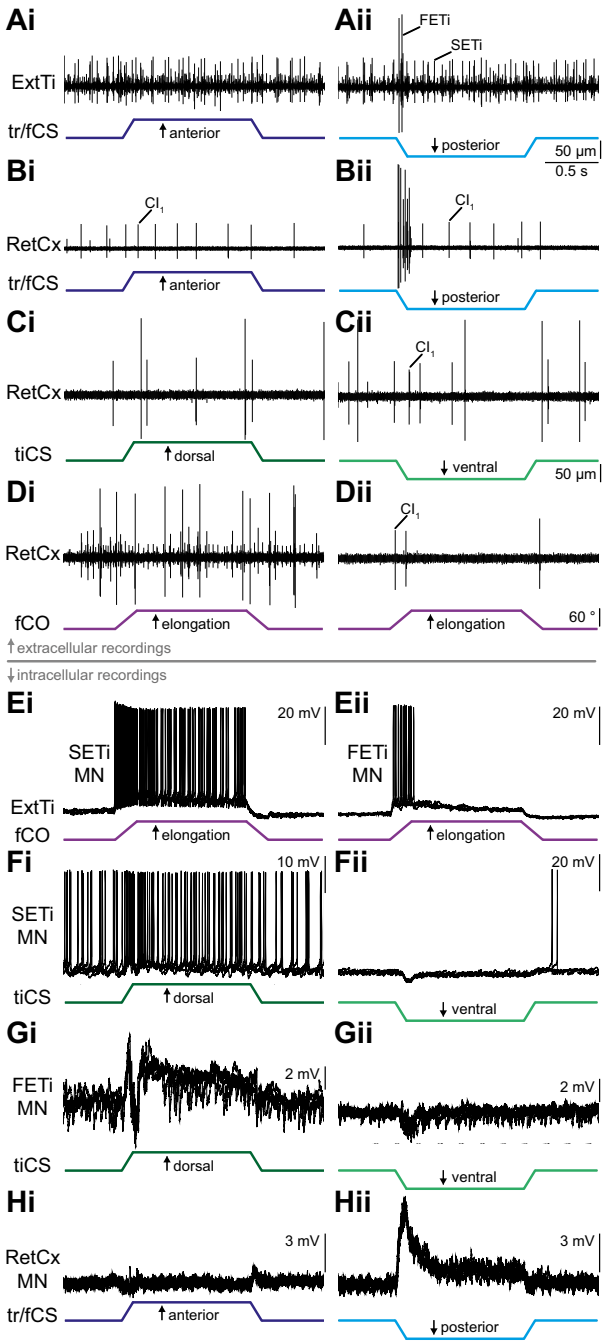

Figure 2. Extracellular (*A*–*D*) and intracellular (*E*–*H*) ExtTi and RetCx MN responses to movement (fCO) and load (tiCS/tr/fCS) stimuli in different directions (*i* and *ii*). ExtTi MNs responded to posteriorly directed tr/fCS stimulation (*A*), for responses to tiCS and fCO stimuli see Fig. 1; RetCx MNs responded to posteriorly directed tr/fCS stimuli (*B*), but showed no changes in frequency during tiCS (*C*), and fCO stimulation (*D*). SETi and FETi responses to fCO (*E*) and tiCS (*F* and *G*) stimulation were qualitatively similar. Responses of a RetCx MN that remained subthreshold during tr/fCS stimulation (*H*). *Top traces*: extra- or intracellular MN recordings, *bottom traces*: stimulation. Responses in *Ei*/*Fii*, *Eii*/*Gii*, *Hi*/*Hii*, respectively, were recorded in the same experiment. ExtTi, extensor tibiae; fCO, femoral chordotonal organ; FETi, fast extensor tibiae; FTi, femur-tibia; MN, motor neuron; RetCx, retractor coxae; SETi, slow extensor tibiae; tiCS, tibial campaniform sensilla; tr/fCS, trochanterofemoral campaniform sensilla.

complex response, consisting of a sequence of depolarization, hyperpolarization, depolarization, of the ExtTi MNs to dorsally directed tiCS stimulation (Fig. 2, *Gi* and *Fi*). Though this pattern was not observed in all recordings (cf. Fig. 5*C*), it could indicate an intricate connectivity pattern of faster excitation, followed by delayed inhibition, and another lasting excitatory input to the ExtTi MNs that remain to be investigated.

The extracellular response in RetCx MNs to posteriorly directed tr/fCS stimulation typically consisted of only a subset of all ~17 individual MNs innervating the RetCx muscle (Fig. 2*Bii*; 50). Intracellular recordings revealed qualitatively similar responses in those RetCx MNs whose responses remained subthreshold (Fig. 2*H*, $n = 6$). All intracellular responses depicted here were recorded at resting membrane potential and demonstrated a strong directional specificity in MNs for dorsal tiCS (SETi, FETi) or posterior tr/fCS (RetCx) stimuli. This specificity resembled the directionality dependency shown by CS (11) and has been observed in other studies (15, 40). We therefore investigated whether the same response specificity would also emerge at the level of the premotor local NSIs.

Movement and Load Signals Are Processed and Integrated in a Common Distributed Network of Local Premotor NSIs

Sensorimotor pathways contributing to reflex action of the FTi joint in the stick insect and in other insects not only consist of monosynaptic connections from sensory afferents to MNs, but also of polysynaptic pathways by means of distributed processing (2, 13, 18, 22). To assess the contribution of premotor interneurons to the reported responses in the MNs, we studied the processing of both types of proprioceptive feedback in the population of local premotor NSIs of the FTi control loop. Two plausible alternative architectures might be implemented in the local premotor network: load and movement signals could either be processed in parallel by modality-specific pathways or they might share common sensorimotor pathways. The former would necessitate the integration of both modalities at a later stage in the network, for example, at the level of the MN membrane. The latter hypothesis raises the question to which extent these pathways overlap and how signals from different modalities interact with each other at different points in the premotor network.

We searched for premotor NSIs providing synaptic drive to ExtTi MNs and tested all of them for synaptic inputs from tiCS afferents and fCO afferents by mechanical stimulation according to the stimulus regimes described above (Fig. 3). Due to the fact that using sharp electrodes to record interneurons in the neuropil of the mesothoracic ganglion does not allow for visual targeting of neurons, we took care not to restrict our search to specific neuropil regions. Unexpected and important to note is the fact that we did not record a single interneuron, out of a sample of altogether 131 recorded neurons, which was affected by only one of the two sensory modalities. Of those 131 recorded NSIs, 85 were identified and recorded in sufficient numbers to be included in this study (Supplemental Table S1; all Supplemental Material is available at https://doi.org/10.6084/m9.figshare.14130020).

The effects of sensory signals from fCO and tiCS were recorded and analyzed in detail in five NSI types providing excitatory drive onto SETi (E1, E2, E3, E4, E9; Fig. 3) and in four NSI types providing inhibitory synaptic drive to SETi (I1, I3, I4, I5; Fig. 3). NSIs E9, I3, and I5 have not been described before and will be further characterized in Fig. 4. Numbers of recorded NSIs are indicated in Supplemental Table S1.

Response amplitudes to sensory stimulation ranged from 1 mV to 15 mV between and even within the same NSI type, for example, NSI I5 was strongly depolarized by synaptic inputs arising from dorsal load stimuli activating tiCS, but only weakly from ventrally directed load to tiCS (Fig. 3, I5, *ii* and *iii*). Effects of fCO and tiCS signals to the NSIs were qualitatively consistent in a given NSI type for all stimulus qualities tested, that is, sign of the change in membrane potential and presence of phasic and tonic components. NSI E4 was an exception; a minority of recordings showed qualitatively different responses to some stimuli (Supplemental Table S1). Note that response amplitudes, especially of tonic components, could vary to some degree in all types of NSIs.

NSIs received synaptic input from the fCO and tiCS, and, in turn, provided synaptic drive to ExtTi MNs. Interestingly, when comparing the synaptic sensory input to a given NSI with the effects of the same sensory stimulation on ExtTi MNs themselves, only a single type of NSI, that is, E3, was supporting ExtTi MN responses during fCO and tiCS activation. NSI E3 was phasically depolarized by dorsal loading of tiCS (Fig. 3, E3 *ii*) and hyperpolarized by ventral loading (Fig. 3, E3 *iii*), thereby supporting the influence of tiCS signals on ExtTi MN activity (ExtTi MN, Fig. 3, E3 *ii* and *iii*). E3 was phasic-tonically depolarized by a mimicked flexion (fCO elongation) of the FTi joint, and hyperpolarized by a mimicked extension (fCO relaxation, Fig. 3, E3 *i*). The synaptic inputs to E3 during fCO stimulation thus supported reflex activation and inactivation of ExtTi MNs upon flexion and extension signals from the fCO in the resting animal (13). The situation differed drastically in the other types of NSIs (Fig. 3). Comparing the synaptic drive from dorsal and ventral loading of the tibia, resulting in activation of tiCS groups 6B and A, with the NSI's specific influence on ExtTi MN activity revealed that for most NSIs, synaptic drive from tiCS did not match their influence on these MNs. For example, NSIs E1, E4, and E9 were tonically depolarized by ventral loading of the tibia, thereby opposing the decreased activity of ExtTi MNs induced by the same sensory stimulus (Fig. 3, E1, E4, and E9 *iii*). The same held for NSIs I1 and I4 for the case of ventral loading (I1, I4 *iii*) and for NSI I5 for dorsal loading of the tibia (Fig. 3, I5 *ii*) when compared with the responses of the ExtTi MNs. In summary, load and movement feedback were found to be distributed to and integrated by the same set of local premotor NSIs whose responses to sensory signals were diverse but consistent.

This finding was clearly confirmed by comparing the influence of load activation of tr/fCS on premotor NSIs with the effects of the same stimuli on ExtTi MNs (Fig. 3, *iv* and *v*). Although ExtTi MN responses to tr/fCS stimulation were weak or nonexistent (Fig. 2*A*), all NSIs of the FTi control loop received synaptic inputs upon stimulation of tr/fCS. These responses, similar to those reported for tiCS stimulation, were not necessarily in accordance with the respective NSI's

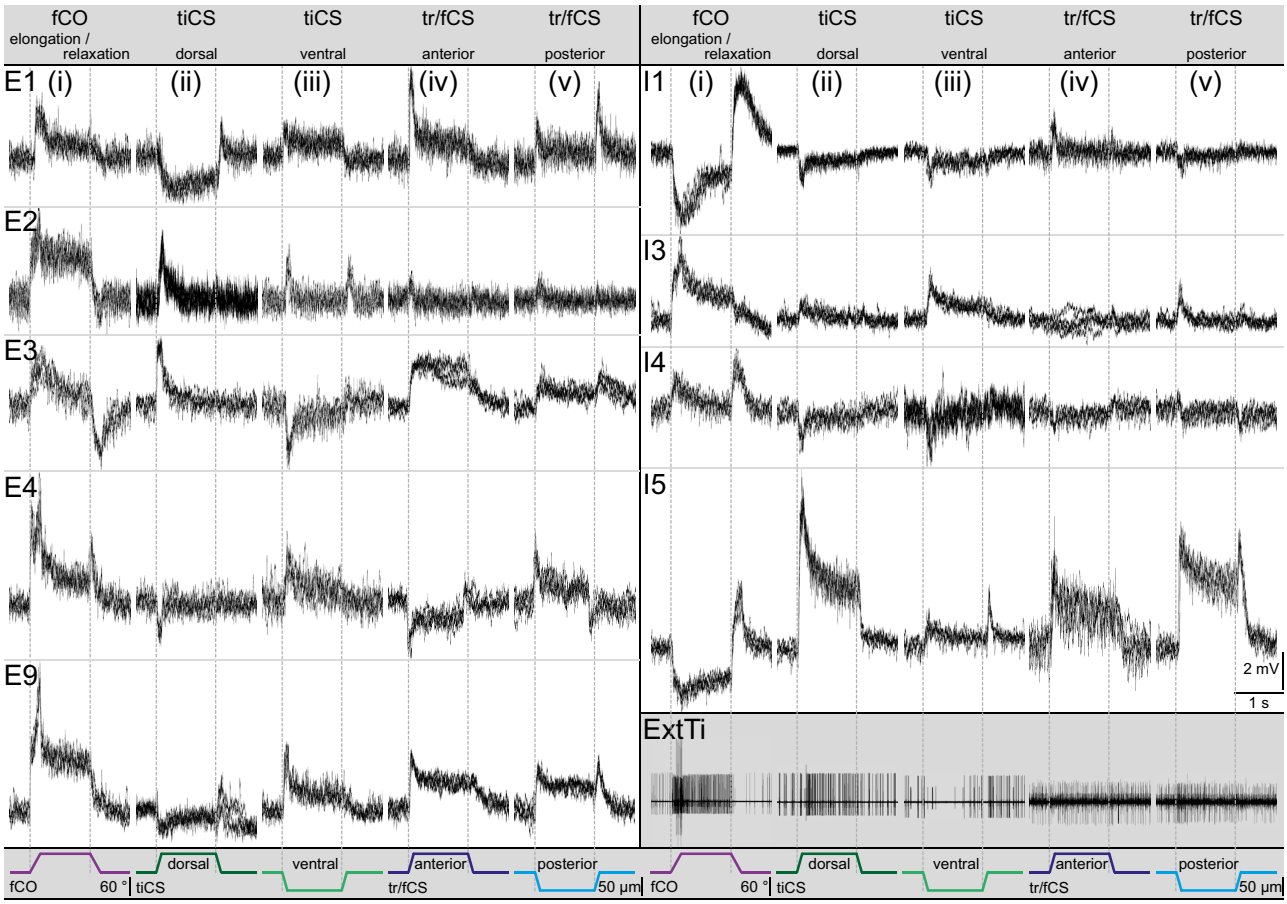

Figure 3. Distributed parallel processing of multimodal proprioceptive synaptic inputs in identified local premotor NSIs. Intracellular responses to movement [fCO (*i*)] and different directions of load [tiCS (*ii* and *iii*)/tr/fCS (*iv* and *v*)] stimulation in NSIs with excitatory (E1, E2, E3, E4, E9) or inhibitory (I1, I3, I4, I5) effects on SETi, superimposed traces of five consecutive stimuli each. Onset of each rising and falling ramp indicated by dashed lines. *Bottom trace*: stimulation; *bottom right panel*: extracellular ExtTi responses as reference. ExtTi, extensor tibiae; fCO, femoral chordotonal organ; NSI, nonspiking interneuron; RetCx, retractor coxae; SETi, slow extensor tibiae; tiCS, tibial campaniform sensilla; tr/fCS, trochanterofemoral campaniform sensilla.

effects on and the (weak) responses of the ExtTi MNs. Responses in NSIs and MNs shown in Figs. 2 and 3 to anteriorly and posteriorly directed forces on the trochanterofemur were qualitatively and quantitatively similar to the responses to dorsal and ventral stimuli. Therefore, the latter are not included in this study.

We identified three new types of premotor NSIs, which were named NSIs E9, I3, and I5 (Fig. 4), all of which received synaptic inputs upon load and movement stimulation. NSI E9 had a contralateral, posterior soma and was driving SETi activity (Fig. 4*A*). The somata of NSIs I3 and I5 were located in the anterior and posterior part of the ipsilateral hemiganglion, respectively, and inhibited SETi activity (Fig. 4, *B* and *C*). In addition, NSI I3 was increasing the spike frequency of the common inhibitor 1 (CI_1), decreasing RetCx MN frequency, and regularly elicited rebound activation of SETi upon termination of depolarizing current injection. In two recordings, NSI I3 was found to increase FETi frequency and in one experiment, NSI I5 decreased CI_1 firing. All inputs from NSIs onto MNs were transmitted by means of subthreshold, graded potentials, and no action potentials were observed in any recording.

The overall effects of each NSI on FTi motor activity can be qualified as supporting or opposing. Table 1 categorizes the role of each NSI based on the data shown in Fig. 3 and from further recordings (cf. Supplemental Table S1). Synaptic inputs to the different identified premotor NSIs could either be in accordance with the observed change in ExtTi MN activity induced by the same sensory stimulus, that is, NSIs were supporting the stimulus-induced change in motor activity, or they could differ from it, resulting in a synaptic drive to ExtTi MNs opposing their response to that stimulus. These classifications consider the sign of the individual NSI's drive to SETi. In Table 1, the NSIs' overall responses to a given sensory stimulation are classified as supporting (+) or opposing (−) the stimulus-elicited ExtTi MN activity. Every change in activity of ExtTi MNs induced by movement or load feedback was supported or opposed by at least one type of NSI. Conversely, all NSIs supported and opposed at least one of the sensory induced changes in

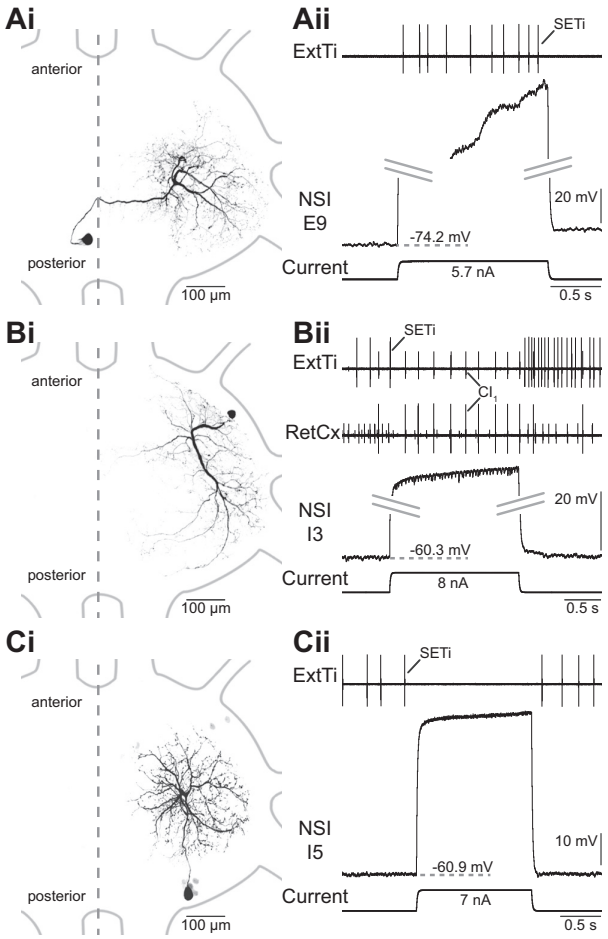

Figure 4. Three previously uncharted local premotor NSIs of the FTi control loop. E9 (*A*), I3 (*B*), and I5 (*C*) were characterized by their morphology (*i*), effects on monitored MN pools (*ii*), and by synaptic inputs from tiCS, tr/fCS, and the fCO (Fig. 3). *Top traces*: extracellular MN recordings; *middle traces*: intracellular NSI recordings; *bottom traces*: current injection. Dashed vertical line (*i*): midline; dashed horizontal line (*ii*): resting membrane potential. ExtTi, extensor tibiae; NSI, nonspiking interneuron; RetCx, retractor coxae; SETi, slow extensor tibiae.

motor activity, with no apparent correlation to the type of NSI or their response shapes.

The results presented in Fig. 3 and Table 1 delineate a set of NSIs into which sensory feedback from distinct modalities (load/movement) and from different sense organs of the same modality (tiCS/tr/fCS) was distributed. Even though we did not select for multimodality and including additional types of NSIs that are not presented in this study due to lower recording numbers, all NSIs were found to process inputs from the fCO, tiCS, and tr/fCS. These signals were all processed along antagonistic pathways, with effects of load signals adding to our previous knowledge on the complexity of movement signal processing.

Load Signals Affect Movement-Elicited Reflex Responses at the Level of Single Neurons

Our initial experiments had shown that the presence of load could affect the strength of movement-based reflex responses in ExtTi MNs (Fig. 1). Analysis of premotor local identified NSIs revealed that the different proprioceptive modalities are processed by and distributed into a single set of NSIs (Fig. 3). None of our results indicated the presence of NSIs dedicated to the processing of one modality alone. Thus, the combined effects of load and movement feedback on the extracellularly recorded motor output are likely to arise within the premotor network, including NSIs, not by solely combining load and movement effects at the MN membrane. We tested this hypothesis with intracellular recordings of NSIs and FETi while stimulating tiCS or tr/fCS and the fCO individually and simultaneously (Fig. 5). Exemplary data for NSIs I1, E9, and E4 are shown and equivalent effects were found in all NSIs tested.

Signals from tiCS, which are part of the FTi joint control loop that includes the fCO and the NSIs analyzed in this study, and from tr/fCS, which measure forces proximal to a different joint, were able to alter fCO-elicited responses in NSIs (Fig. 5, *A* and *B*). Note that these effects were not specific for an individual group of CS and a given type of NSI. NSI I1's movement response was affected by tiCS and tr/fCS alike (Fig. 5, *Ai* and *Bi*, see also *inset*). CS signals could enhance ongoing changes in NSI membrane potential, for example, by increasing the fCO-elicited depolarization in NSI E9 (Fig. 5*Aii*) or disrupt ongoing changes. The latter was observed in NSI E4, where the tr/fCS-induced hyperpolarization interrupted a fCO-based depolarization (Fig. 5*Bii*). These effects could occur in both excitatory and inhibitory NSIs, that is, in NSIs with opposing effects on ExtTi activity (e.g., Fig. 5, *Bi* and *Bii*). We also tested the effects of combined stimuli while intracellularly monitoring FETi and found similar effects (Fig. 5*C*). Taken together, these results reveal a high degree of interaction of two distinct proprioceptive modalities, load and movement, at the level of the premotor network and within single neurons.

DISCUSSION

We investigated the processing of CS signals to identify the pathways underlying the control of ExtTi MN activity in the resting stick insect, *C. morosus*. In all experiments, we combined the stimulation of load sensors with the stimulation of the fCO. This allowed us to compare the recorded neurons within the FTi premotor network with those which have been previously identified and which process movement related sensory feedback provided by the fCO [e.g., Sauer et al. (22)].

Multimodal sensory integration is a ubiquitous feature of the nervous system and key to understanding how motor networks coordinate muscle activity while allowing for finely tuned interactions of the body with its surroundings (51–54). The degree to which the networks processing individual proprioceptive modalities overlap is an essential aspect to understanding integrative processes in premotor networks occurring during natural behaviors such as walking and posture control. In a previous study by Schmitz and Stein (15) on the thorax-coxa joint control loop, the convergence of load and movement feedback was explored at the level of the MN membrane. The authors reported, similar to our results (Fig. 1), the strength of a movement related postural reflex to be

Table 1. *Antagonistic multimodal distributed processing in identified local premotor NSIs of the FTi control loop*

	Stimulus					
	fCO		tiCS		tr/fCS	
NSI	Elongation	Relaxation	Dorsal	Ventral	Anterior	Posterior
E1	+	+	−	−	−	+
E2	+	+	+	−	−	+
E3	+	+	+	+	−	+
E4	+	−	−	−	+	+
E9	+	+	−	−	−	+
I1	+	+	+	−	+	+
I3	−	+	−	+	+	−
I4	−	+	+	−	−	−
I5	+	+	−	+	+	−
ExtTi	Excitation	Inhibition	Excitation	Inhibition	No effect	Excitation

Overall synaptic inputs during each sensory stimulation to NSIs as shown in Fig. 3 classified as supporting (+) or opposing (−) the respective response in ExtTi MNs (bottom). + NSI supports ExtTi MN activity. − NSI opposes ExtTi MN activity. ExtTi, extensor tibiae; fCO, femoral chordotonal organ; FETi, fast extensor tibiae; FTi, femur-tibia; MN, motor neuron; NSI, nonspiking interneuron; tiCS, tibial campaniform sensilla; tr/fCS, trochanterofemoral campaniform sensilla.

affected by load signals. However, the individual underlying pathways were not identified.

Focusing on the FTi joint control loop, we extended our investigation to include tr/fCS and RetCx MNs. This extension provided a reference point for assessing effects within the FTi control loop, and another degree of complexity of sensory integration, as tr/fCS measure forces orthogonal to the leg plane of tiCS and the FTi joint.

We then addressed integration of information in premotor interneurons and showed that multimodal sensory signals are distributed into a set of identified local premotor NSIs whose outputs have antagonistic effects on the same MNs (Fig. 3). We specifically focused on NSIs with synaptic drive to the ExtTi MNs, as they are known to be points of sensory and intersegmental signal integration in the leg motor control system of insects [reviewed in Burrows (2), Bässler and Büschges (18), Siegler (55)]. Previous studies in the locust have found synaptic drive from CS to NSIs, however, without testing for effects of movement feedback, for example, from the fCO, in the same neurons (14, 17). We found that all recorded NSIs process information from the fCO and CS located on the tibia and the trochanterofemur, thus not only receiving load and movement feedback from the target joint of their MN effects (FTi), but also from more proximal ones.

This is emphasized by the fact that we identified three new types of NSIs in the FTi control loop, that is, NSIs E9, I3, and I5 (Fig. 4). An NSI with a morphology similar to I3 had previously been reported from a single recording (56). Akay (56) and Berg (57) previously reported two types of NSIs with morphologic and physiological characteristics similar to each other, named E9 and E10, respectively, which differ from the unidentified excitatory NSI found in this study. To maintain a systematic nomenclature and based on the number of publications, recordings, and the NSIs' characteristics, we decided to follow Berg's nomenclature. Akay's E9 was renamed to E10, and the NSI characterized in this study was named E9.

Distributed Processing of Proprioceptive Signals in the Premotor Network Controlling Tibial Movements

Distributed antagonistic processing is the divergence of a given signal onto a set of neurons which in turn have opposing effects on a downstream effector. Such neuronal pathways for example underly movement signal processing in the stick insect (13, 22), mechanosensation in the lobster stomatogastric ganglion (58), and have been hypothesized in spinal circuits of cats and humans (59, 60). A network's output is changed by adjusting the balance between opposing pathways, in extreme cases causing a reflex reversal (61). This endows a limited set of neurons with flexibility that separate, hard-wired supporting and opposing pathways would lack. In addition, the output of a distributed network is not an either/or function, but can be graded depending on how strong the balance between pathways is tipped toward either side, an aspect that is reinforced even more in the case of NSIs, which communicate solely via graded potentials. Previous studies on antagonistic distributed processing focused on feedback from single sensory structures alone.

The present work is based on a sample of 131 recorded NSIs, all of which received synaptic inputs upon load and movement stimulation and 85 of which are included in this study based on their role in the FTi control loop, unequivocal identification, and sample size for each type of NSI. All of the recorded NSIs received synaptic drive upon stimulation of CS and the fCO and all of the included NSIs provided either excitatory (e.g., E4) or inhibitory (e.g., I3) synaptic drive to ExtTi MNs. Importantly, none of the recorded NSIs received synaptic input from only one or two of the three examined sense organs, that is, fCO, tiCS, tr/fCS, leading us to the conclusion that information about leg movement and loading is processed by a single, common premotor network (Fig. 6*A*). We have shown in Table 1 the antagonism the individual elements of the premotor network show in supporting or opposing the individual motor responses to each respective sensory input. Broadening this finding, and supposing that a motor network's main purpose is to impose and control movements, are NSI responses to CS input still antagonistic when relating them not to the motor output caused by the respective individual sensory stimulus, but to the movement resistance reflex itself? In other words, if a given NSI's response to fCO inputs and its effects on ExtTi MNs opposes the reflex activation of these MNs, does the additional input from CS to the NSI, which is likely to occur simultaneously under natural conditions, enhance or reduce the NSI's antagonistic effect?

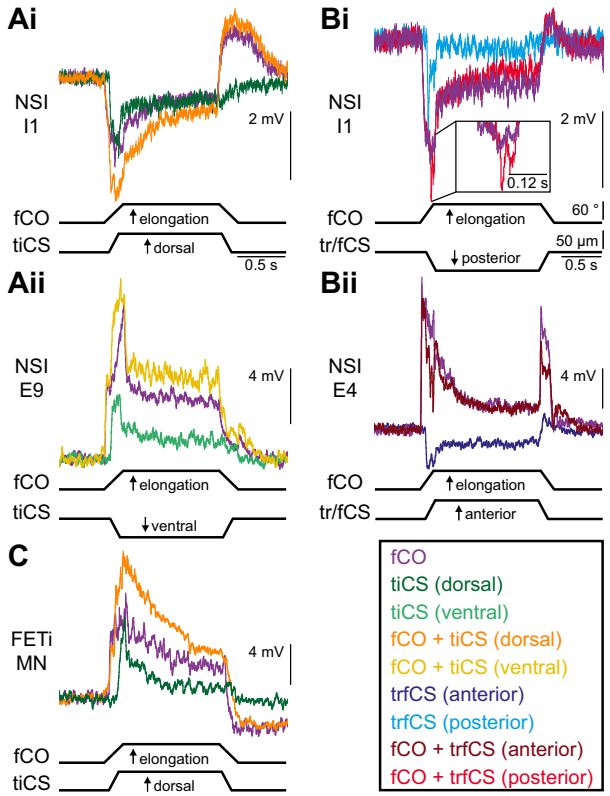

Figure 5. Load signals interrupt or enhance ongoing movement-elicited changes in membrane potential in NSIs and MNs. Effects of combined movement (fCO) and load (tiCS/tr/fCS) stimuli on the intracellular membrane potential of individual NSIs (*A* and *B*) and FETi (*C*). *Top traces*: intracellular recording, mean of five consecutive stimuli; *bottom traces*: stimulation. FETi action potentials in *C* were cut to avoid distortion of the mean traces (see METHODS). fCO, femoral chordotonal organ; FETi, fast extensor tibiae; MN, motor neuron; NSI, nonspiking interneuron; tiCS, tibial campaniform sensilla; tr/fCS, trochanterofemoral campaniform sensilla.

We show these considerations for four exemplary NSIs (Fig. 6, *B–E*). NSI I1 is hyperpolarized upon elongation of the fCO (Fig. 6*Bi*), and, as I1 has an inhibitory effect on ExtTi MNs (Fig. 6*Bii*) that is thus reduced, this results in an overall supporting influence on the ongoing MN reflex activation (Fig. 6*Biii*). Supposing a ventral tiCS and posterior tr/fCS activation similar to the stimuli used in our study, these sensory signals would result in an additional hyperpolarization of I1 (Fig. 6*Bi*), thus enhancing the overall supporting effect on MN activation (Fig. 6*Biii*, shaded green bars). Conversely, CS activation would enhance I3's opposing effects (Fig. 6*C*), whereas I5's supporting influence would be decreased by load (Fig. 6*D*), and E4 even receives contradictory CS inputs (Fig. 6*E*). These examples emphasize the complexity of the antagonistic, distributed processing in the local premotor network, and show the need for further studies investigating which sense organs are activated simultaneously under natural conditions.

We broaden the existing knowledge on distributed processing of fCO-based movement signaling in the local locomotor network of the stick insect (20, 22, 27, 62, 63) by adding load signals from multiple load sensors, effectively increasing the dimensionality of antagonistic distributed processing in a local network to a multimodal perspective.

Load signals did not help to sort the antagonistic movement-signaling pathways within the NSI network, for example, by inhibiting NSIs supporting the resistance reflex and thus shifting the balance toward an assisting response. Instead, load feedback from different groups of CS on the leg is itself processed along antagonistic, distributed pathways. The question, therefore, remains as to how a distributed, antagonistic network can generate strong and stereotyped motor reflexes. Previous modeling studies have shown, though only for the generation of postural reflexes linked to a single sensory modality, that neural circuits with distributed information processing, for example, in the stick insect (22) or the leech (64, 65), can fulfill this function without any

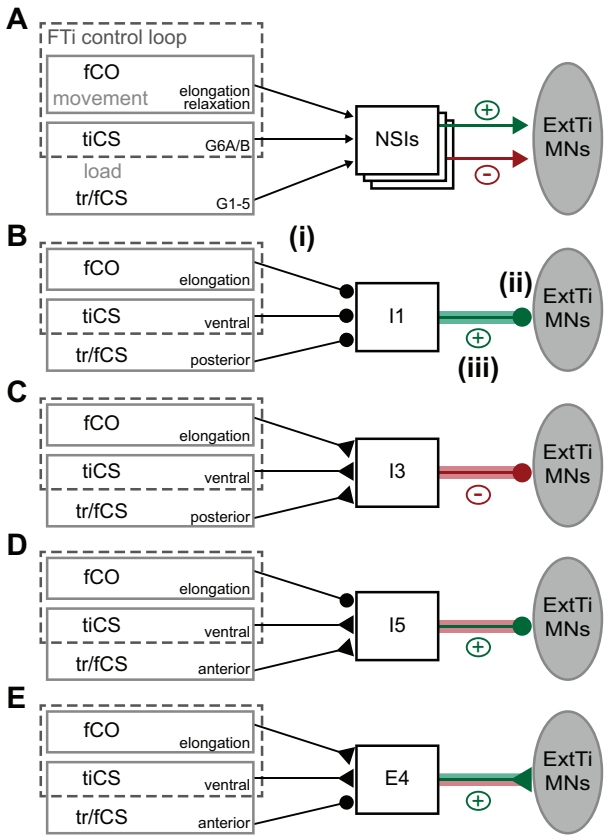

Figure 6. Network schematic of multimodal distributed, antagonistic processing. Antagonistic effects of load inputs on the supporting/opposing drive of NSIs to ExtTi MNs during the movement resistance reflex. *A*: local premotor NSIs integrate proprioceptive signals of different modalities (load/movement) and from different sense organs of the same modality (tiCS/tr/fCS). Signals from within the FTi control loop (fCO/tiCS) and from an adjacent joint (tr/fCS) are combined and support (+, green) or oppose (−, red) the motor output of ExtTi MNs. *B–E*: exemplary combinations of sensory stimuli and NSI types. *i*: sign of sensory synaptic drive to the NSI. *ii*: sign of the NSI's synaptic drive to ExtTi MNs. *iii*: supporting (+) or opposing (−) contribution of the NSI to the ExtTi MN movement resistance reflex in response to fCO stimulation is weakened (shaded red bar) or strengthened (shaded green bar) by load. ExtTi, extensor tibiae; fCO, femoral chordotonal organ; FTi, femur-tibia; MN, motor neuron; NSI, nonspiking interneuron; tiCS, tibial campaniform sensilla; tr/fCS, trochanterofemoral campaniform sensilla.

mechanism of emphasizing the gain of supporting pathways versus opposing ones. This gives rise to the current conclusion that it is the summation of synaptic input signals at the MN membrane that generates the observed motor output. Resolving this level of processing to a more detailed extent will be important for our understanding of distributed antagonistic networks and will have to be addressed in future studies.

Multimodal Processing in Premotor Networks

The integration of sensory signals from load and movement sensors in the leg is a task that is common to motor control of both vertebrates and invertebrates. It is achieved at multiple stages of the network, that is, in the sensory afferents themselves [66 (vertebrates), 67 (stick insect)], and at later stages in the local networks of the spinal cord (68) or the ventral nerve cord (present study, 69). In insects, the individual processing pathways of sensory signals in leg motor control have been and are subject to extensive studies, especially in the premotor network of locusts, stick insects, and, increasingly, the fruit fly (12–14, 17, 70). The network topology underlying integrative processing of load and movement signals, however, has received little attention.

According to our results NSIs constitute a major interface for the integration of proprioceptive signals from different sense organs on the leg. This seems to be a consistent feature of the network because every NSI was found to receive signals from all examined types of sense organs (fCO, tiCS, tr/fCS). Similarly, in the cat spinal cord, specific interneurons were found to integrate load and movement feedback from the limb, but vertebrate experimental restrictions prevented an in-depth identification of the underlying network (68, 71).

Several mechanisms for encoding multisensory information in a distributed network have been suggested, including a rate or combinatorial code (72). Rate coding is not applicable in this case, for the obvious reason of the examined integrative neurons being nonspiking. Combinatorial codes, transmitting categorical information about the presence or absence of individual sensory inputs, are mediated, in the strict sense, by distinct combinations of neurons being activated by individual or concurrent sensory stimuli. There is no indication for such a selective targeting of NSIs in the insect premotor network, as all NSIs were found to be influenced by all types of stimuli. Stein et al. (28), however, elicited reflex reversal in a model of the premotor network of the FTi joint by applying a combinatorial code that only shifts the weighting of or the synaptic inputs to concurrently activated pathways. Adjusting the strength of individual pathways to enable flexible system output has been suggested to be implemented in the biological FTi control loop (18, 27) and may explain how the diverse synaptic inputs found in this study are shaped into different motor outputs.

The diverse shapes of these graded responses may hint at a more complex computational mechanism in the processing of signals than could be accomplished by a similar number of spiking neurons and indicate that the network of NSIs provides the nervous system with an integrated representation of the leg's sensory and motor context, including self-generated movements and the resulting sensory feedback, perturbations, and ground contact.

Functional Implications for Sensorimotor Processing

Multimodal integration at the level of single neurons and pathways has been found in interneurons that are part of the vertebrate spinal cord motor networks [reviewed in Jankowska (73)]. Kistemaker et al. (29) highlight the advantages of combining movement and load feedback from muscle spindles and Golgi tendon organs for precise motor control. These aspects of motor control are comparable to the tasks faced by insect motor networks during walking and posture control, for which load and movement feedback are considered essential, and in which NSIs have been implied to play a major role (24, 74–77). The sensory signals evoked in this study include multimodal feedback (movement/load), and unimodal feedback from tiCS and tr/fCS. Thus, NSIs affecting movements within the leg plane (FTi joint) integrate sensory information not only within (tiCS), but also orthogonal (tr/fCS) to the leg plane (34, 39). Although little is known about the neural mechanisms underlying the concerted action of the different sense organs on the leg during stepping or when controlling posture, it has to be assumed that simultaneous activation of multiple sense organs or modalities is a common occurrence. It may even be hypothesized that under natural conditions, load always concurs with movement feedback and both are to be made sense of by the nervous system only in the context of each other (Zill, personal communication). This view is supported by our finding of a completely distributed multimodal network that integrates both types of proprioceptive feedback into one common framework. The relevance of distributed networks for sensory integration and in the generation of reflex responses is emphasized by the absence of monosynaptic connections from tiCS onto SETi in the hindleg of the locust (17), and the middle leg of the stick insect (Gebehart et al., unpublished observations).

From our results we conclude that the distributed, antagonistic premotor network of the FTi control loop integrates proprioceptive signals from movement and multiple load sensors. The importance of multimodal integration is evident from the absence of any NSI recording during an unbiased search that would only show responses to one type of sensory stimulus. Questions which future studies will have to address include first the identification of putative lateral synaptic connections between NSIs. The existence of such connections has been shown, although the degree of this interconnectivity, and the identity of the individual interconnected NSIs, remains open (2, 12). Second, harking back to Stein et al. (28) and the weighting of distributed pathways, how do connections from individual NSIs to MNs differ in their synaptic strength, and is their strength altered depending on the behavioral context? Last, is the multimodal distributed processing of sensory inputs we find in the resting animal comparable to the situation in the active animal, or is it even a prerequisite for the distributed outputs reported by previous studies [e.g., Kittmann et al. (78), Wolf and Büschges (79)]? In the animal generating active leg movements, reflex reversal occurs to movement signals such that ongoing movements are assisted [review in Bässler and Büschges (18)], the same mechanism has been reported for load feedback (39, 80). Akay et al. (35) showed that the effects of CS

stimulation to forces applied in a posterior direction to the trochanterofemur differed dramatically in animals that were active: responses in the tibial flexor muscle changed from small (minor) discharges in inactive animals to intense bursting in active animals. Furthermore, in its antagonist, discharges in both the SETi and FETi MNs were strongly inhibited following CS stimulation when animals were active (ibid. Fig. 3*A*) while the same stimuli elicited excitation spikes nondirectionally when animals were inactive (ibid. Fig. 3*B*). Similar plasticity in responses of active animals were observed to forces applied to the trochanter in the direction of flexion using ramp-and-hold functions (39) and "naturalistic" stimuli of joint torques (81). Most importantly in the context of multimodal sensory integration, load signals have been shown to shift the tuning of the network from a resisted movement to an assistance reflex (36). The specific mechanisms underlying these changes, either by facilitation of select pathways or changes in synaptic weighting, have not been investigated in detail so far. However, neuromodulation, for example, via octopaminergic descending neurons, is likely to mediate such task-specific modifications in sensorimotor processing (82). One such example is the state-dependent reversal of the resistance reflex, the neural basis for which can be traced back to individual premotor NSIs whose synaptic inputs from sense organs have been shown to change (61). Future studies will have to investigate, whether the relative weighting of the synaptic inputs from movement and force sensors depends on the behavioral state, for example, is different at rest compared to an active animal and whether load potentially functions as a mechanism for tuning individual pathways. These questions may give insight into how a multimodal, distributed network can produce precise changes in output when they are behaviorally relevant.

ACKNOWLEDGMENTS

The authors gratefully acknowledge technical support provided by Mehrdad Ghanbari and Michael Dübbert, and thank Nicholas S. Szczecinski and Sasha N. Zill for helpful comments and discussions.

GRANTS

This study was funded by a grant from the Deutsche Forschungsgemeinschaft (DFG, German Research Foundation) 233886668/GRK1960 (to A.B. and C.G.) and supported by the Studienstiftung des deutschen Volkes (to C.G.).

DISCLOSURES

No conflicts of interest, financial or otherwise, are declared by the authors.

AUTHOR CONTRIBUTIONS

C.G., J.S., and A.B. conceived and designed research; C.G. performed experiments; C.G. analyzed data; C.G., J.S., and A.B. interpreted results of experiments; C.G. prepared figures; C.G. and A.B. drafted manuscript; C.G., J.S., and A.B. edited and revised manuscript; C.G., J.S., and A.B. approved final version of manuscript.

SUPPLEMENTAL DATA

Supplemental Table S1; all Supplemental Material is available at https://doi.org/10.6084/m9.figshare.14130020.

REFERENCES

1. **Bässler U.** The femur-tibia control system of stick insects - a model system for the study of the neural basis of joint control. *Brain Res Brain Res Rev* 18: 207–226, 1993. doi:10.1016/0165-0173(93)90002-H.
2. **Burrows M.** *The Neurobiology of an Insect Brain*. Oxford, UK: Oxford University Press, 1996.
3. **Deliagina TG**, **Zelenin PV**, **Orlovsky GN.** Physiological and circuit mechanisms of postural control. *Curr Opin Neurobiol* 22: 646–652, 2012. doi:10.1016/j.conb.2012.03.002.
4. **Grillner S**, **El Manira A.** Current principles of motor control, with special reference to vertebrate locomotion. *Physiol Rev* 100: 271–320, 2020. doi:10.1152/physrev.00015.2019.
5. **Jami L.** Golgi tendon organs in mammalian skeletal muscle: functional properties and central actions. *Physiol Rev* 72: 623–666, 1992. doi:10.1152/physrev.1992.72.3.623.
6. **Windhorst U.** Muscle proprioceptive feedback and spinal networks. *Brain Res Bull* 73: 155–202, 2007. doi:10.1016/j.brainresbull.2007.03.010.
7. **Büschges A**, **Gruhn M.** Mechanosensory feedback in walking: from joint control to locomotor patterns. In: *Insect Mechanics and Control*, edited by Casas J, Simpson SJ. San Diego, CA: Academic Press, 2007, p. 193–230. Advances in Insect Physiology 34. doi:10.1016/S0065-2806(07)34004-6.
8. **Field LH**, **Matheson T.** Chordotonal organs of insects. In: *Advances in Insect Physiology*, edited by Evans PD**.** San Diego, CA: Academic Press, 1998, vol. 27, p. 1–228.
9. **Tuthill JC**, **Wilson RI.** Mechanosensation and adaptive motor control in insects. *Curr Biol* 26: R1022–R1038, 2016. doi:10.1016/j.cub.2016.06.070.
10. **Zill S**, **Schmitz J**, **Büschges A.** Load sensing and control of posture and locomotion. *Arthropod Struc Develop* 33: 273–286, 2004. doi:10.1016/j.asd.2004.05.005.
11. **Zill SN**, **Moran DT.** The exoskeleton and insect proprioception. I. Responses of tibial campaniform sensilla to external and muscle-generated forces in the American cockroach, *Periplaneta americana*. *J Exp Biol* 91: 1–24, 1981. doi:10.1242/jeb.91.1.1.
12. **Büschges A**, **Wolf H.** Nonspiking local interneurons in insect leg motor control I. Common layout and species-specific response properties of femur-tibia joint control pathways in stick insect and iocust. *J Neurophysiol* 73: 1843–1860, 1995. doi:10.1152/jn.1995.73.5.1843.
13. **Büschges A.** Nonspiking pathways in a joint-control loop of the stick insect *Carausius morosus*. *J Exp Biol* 151: 133–160, 1990. doi:10.1242/jeb.151.1.133.
14. **Laurent GJ**, **Burrows M.** Direct excitation of nonspiking local interneurones by exteroceptors underlies tactile reflexes in the locust. *J Comp Physiol A* 162: 563–572, 1988. doi:10.1007/BF01342631.
15. **Schmitz J**, **Stein W.** Convergence of load and movement information onto leg motoneurons in insects. *J Neurobiol* 42: 424–436, 2000. doi:10.1002/(SICI)1097-4695(200003)42:4<424::AID-NEU4>3.0.CO;2-0.
16. **Burrows M.** Parallel processing of proprioceptive signals by spiking local interneurons and motor neurons in the locust. *J Neurosci* 7: 1064–1080, 1987. doi:10.1523/JNEUROSCI.07-04-01064.1987.
17. **Burrows M**, **Pflüger JH.** Positive feedback loops from proprioceptors involved in leg movements of the locust. *J Comp Physiol A* 163: 425–440, 1988. doi:10.1007/BF00604897.
18. **Bässler U**, **Büschges A.** Pattern generation for stick insect walking movements—multisensory control of a locomotor program. *Brain Res Rev* 27: 65–88, 1998. doi:10.1016/s0165-0173(98)00006-x.
19. **Edwards DH**, **Prilutsky BI.** Sensory feedback in the control of posture and locomotion. In: *Neurobiology of Motor Control: Fundamental Concepts and New Directions*, edited by Hooper SL, Büschges A. Hoboken, NJ: Wiley, 2017, p**.** 263–304.
20. **Sauer AE**, **Driesang RB**, **Büschges A**, **Bässler U.** Information processing in the femur-tibia control loop of stick insects 1. The response characteristics of two nonspiking interneurons results from parallel

excitatory and inhibitory inputs. *J Comp Physiol A* 177: 145–158, 1995. doi:10.1007/BF00225095.
21. **Burrows M**, **Laurent G**, **Field LH.** Proprioceptive inputs to nonspiking local interneurons contribute to local reflexes of a locust hindleg. *J Neurosci* 8: 3085–3093, 1988. doi:10.1523/JNEUROSCI.08-08-03085.1988.
22. **Sauer AE**, **Driesang RB**, **Büschges A**, **Bässler U.** Distributed processing on the basis of parallel and antagonistic pathways simulation of the femur-tibia control system in the stick insect. *J Comput Neurosci* 3: 179–198, 1996. doi:10.1007/BF00161131.
23. **Büschges A.** Processing of sensory input from the femoral chordotonal organ by spiking interneurones of stick insects. *J Exp Biol* 144: 81–111, 1989. doi:10.1242/jeb.144.1.81.
24. **Büschges A**, **Schmitz J.** Nonspiking pathways antagonize the resistance reflex in the thoraco-coxal joint of stick insects. *J Neurobiol* 22: 224–237, 1991. doi:10.1002/neu.480220303.
25. **Büschges A.** The physiology of sensory cells in the ventral scoloparium of the stick insect femoral chordotonal organ. *J Exp Biol* 189: 285–292, 1994.
26. **Hofmann T**, **Koch UT**, **Bässler U.** Physiology of the femoral chordotonal organ in the stick insect, *Cuniculina impigra*. *J Exp Biol* 114: 207–223, 1985. doi:10.1242/jeb.114.1.207.
27. **Stein W**, **Sauer AE.** Modulation of sensorimotor pathways associated with gain changes in a posture-control network of an insect. *J Comp Physiol* 183: 489–501, 1998. doi:10.1007/s003590050274.
28. **Stein W**, **Straub O**, **Ausborn J**, **Mader W**, **Wolf H.** Motor pattern selection by combinatorial code of interneuronal pathways. *J Comput Neurosci* 25: 543–561, 2008. doi:10.1007/s10827-008-0093-7.
29. **Kistemaker DA**, **Van Soest AJ**, **Wong JD**, **Kurtzer I**, **Gribble PL.** Control of position and movement is simplified by combined muscle spindle and Golgi tendon organ feedback. *J Neurophysiol* 109: 1126–1139, 2013. doi:10.1152/jn.00751.2012.
30. **Dinges GF**, **Chockley AS**, **Bockemühl T**, **Ito K**, **Blanke A**, **Büschges A.** Location and arrangement of campaniform sensilla in *Drosophila* melanogaster. *J Comp Neurol* 529: 905–925, 2021. doi:10.1002/cne.24987.
31. **Hofmann T**, **Bässler U.** Anatomy and physiology of trochanteral campaniform sensilla in the stick insect, *Cuniculina impigra*. *Physiol Entomol* 7: 413–426, 1982. doi:10.1111/j.1365-3032.1982.tb00317.x.
32. **Zill SN**, **Moran DT**, **Varela FG.** The exoskeleton and insect proprioception. II. Reflex effects of tibial campaniform sensilla in the American cockroach, *Periplaneta americana*. *J Exp Biol* 94: 43–55, 1981. doi:10.1242/jeb.94.1.43.
33. **Zill SN**, **Büschges A**, **Schmitz J.** Encoding of force increases and decreases by tibial campaniform sensilla in the stick insect, Carausius morosus. *J Comp Physiol* 197: 851–867, 2011. doi:10.1007/s00359-011-0647-4.
34. **Zill SN**, **Chaudhry S**, **Büschges A**, **Schmitz J.** Directional specificity and encoding of muscle forces and loads by stick insect tibial campaniform sensilla, including receptors with round cuticular caps. *Arthropod Struct Develop* 42: 455–467, 2013. doi:10.1016/j.asd.2013.10.001.
35. **Akay T**, **Bässler U**, **Gerharz P**, **Büschges A.** The role of sensory signals from the insect coxa-trochanteral joint in controlling motor activity of the femur-tibia joint. *J Neurophysiol* 85: 594–604, 2001. doi:10.1152/jn.2001.85.2.594.
36. **Akay T**, **Büschges A.** Load signals assist the generation of movement-dependent reflex reversal in the femur-tibia joint of stick insects. *J Neurophysiol* 96: 3532–3537, 2006. doi:10.1152/jn.00625.2006.
37. **Akay T**, **Haehn S**, **Schmitz J**, **Büschges A.** Signals from load sensors underlie interjoint coordination during stepping movements of the stick insect leg. *J Neurophysiol* 92: 42–51, 2004. doi:10.1152/jn.01271.2003.
38. **Höltje M**, **Hustert R.** Rapid mechano-sensory pathways code leg impact and elicit very rapid reflexes in insects. *J Exp Biol* 206: 2715–2724, 2003. doi:10.1242/jeb.00492.
39. **Zill SN**, **Schmitz J**, **Chaudhry S**, **Büschges A.** Force encoding in stick insect legs delineates a reference frame for motor control. *J Neurophysiol* 108: 1453–1472, 2012. doi:10.1152/jn.00274.2012.
40. **Haberkorn A**, **Gruhn M**, **Zill SN**, **Büschges A.** Identification of the origin of force-feedback signals influencing motor neurons of the thoraco-coxal joint in an insect. *J Comp Physiol A Neuroethol Sens Neural Behav Physiol* 205: 253–270, 2019. doi:10.1007/s00359-019-01334-4.
41. **Marquardt F.** Beiträge zur Anatomie der Muskulatur und der peripheren Nerven von Carausius (Dixippus) morosus. *Zool Jb Abt Anat Ont Tiere* 66: 63–128, 1940.
42. **Driesang RB**, **Büschges A.** The neural basis of catalepsy in the stick insect. *J Comp Physiol A* 173: 445–454, 1993. doi:10.1007/BF0019351.
43. **Weidler D**, **Diecke F.** The role of cations in conduction in the central nervous system of the herbivorous insect *Carausius Morosus*. *Z Verg Physiologie* 64: 372–399, 1969. doi:10.1007/BF00340433.
44. **Dörr H**, **Heß D**, **Gramoll S.** Interstitial voltage and potassium concentration in the mesothoracic ganglion of a stick insect at rest and during neuronal activation. *J Insect Physiol* 42: 967–974, 1996. doi:10.1016/0022-1910(96)00042-X.
45. **Schmitz J**, **Büschges A**, **Delcomyn F.** An improved electrode design for en passant recording from small nerves. *Comp Biochem Physiol A Comp Physiol* 91: 769–772, 1988. doi:10.1016/0300-9629(88)90963-2.
46. **Weiland G**, **Koch UT.** Sensory feedback during active movements of stick insects. *J Exp Biol* 133: 137–156, 1987. doi:10.1242/jeb.133.1.137.
47. **Hengstenberg R.** Spike responses of 'non-spiking' visual interneurone. *Nature* 270, 1977. doi:10.1038/270338a0.
48. **Berg E**, **Hooper SL**, **Schmidt J**, **Büschges A.** A leg-local neural mechanism mediates the decision to search in stick insects. *Curr Biol* 25: 2012–2017, 2015. doi:10.1016/j.cub.2015.06.017.
49. **Schmitz J.** Load-compensating reactions in the proximal leg joints of stick insects during standing and walking. *J Exp Biol* 183: 15–33, 1993. doi:10.1242/jeb.183.1.15.
50. **Goldammer J**, **Büschges A**, **Motoneurons SJ.** DUM cells, and sensory neurons in an insect thoracic ganglion: a tracing study in the stick insect *Carausius morosus*. *J Comp Neurol* 520: 230–257, 2012. doi:10.1002/cne.22676.
51. **Beenhakker MP**, **Kirby MS**, **Nusbaum MP.** Mechanosensory gating of proprioceptor input to modulatory projection neurons. *J Neurosci* 27: 14308–14316, 2007. doi:10.1523/JNEUROSCI.4404-07.2007.
52. **Keller CH**, **Heilgenberg H.** From distributed sensory processing to discrete motor representations in the diencephalon of the electric fish, *Eigenmannia*. *J Comp Physiol A* 165: 565–576, 1989. doi:10.1007/BF00614499.
53. **Lockery SR**, **Kristan WB, Jr.** Distributed processing of sensory information in the leech**.** II. Identification of interneurons contributing to the local bending reflex. *J Neurosci* 10: 1816–1829, 1990. doi:10.1523/JNEUROSCI.10-06-01816.1990.
54. **Spors H**, **Albeanu DF**, **Murthy VN**, **Rinberg D**, **Uchida N**, **Wachowiak M**, **Friedrich RW.** Illuminating vertebrate olfactory processing. *J Neurosci* 32: 14102–14108, 2012. doi:10.1523/JNEUROSCI.3328-12.2012.
55. **Siegler MVS.** Local interneurones and local interactions in arthropods. *J Exp Biol* 112: 253–281, 1984. doi:10.1242/jeb.112.1.253.
56. **Akay T.** *The role of sensory signals for interjoint coordination in stick insect legs* (PhD thesis). Cologne, Germany: Mathematisch-Naturwissenschaftliche Fakultät, University of Cologne, 2002.
57. **Berg E.** *Adaptive motor control: neuronal mechanisms underlying (targeted) searching movements* (PhD thesis). Cologne, Germany: Mathematisch-Naturwissenschaftliche Fakultät, University of Cologne, 2014.
58. **Combes D**, **Meyrand P**, **Simmers J.** Dynamic restructuring of a rhythmic motor program by a single mechanoreceptor neuron in lobster. *J Neurosci* 19: 3620–3628, 1999. doi:10.1523/JNEUROSCI.19-09-03620.1999.
59. **De Serres SJ**, **Yang JF**, **Patrick SK.** Mechanism for reflex reversal during walking in human tibialis anterior muscle revealed by single motor unit recording. *J Physiol* 488: 249–258, 1995. doi:10.1113/jphysiol.1995.sp020963.
60. **Schomburg ED**, **Behrends HB.** Phasic control of the transmission in the excitatory and inhibitory reflex pathways from cutaneous afferents to α-motoneurones during fictive locomotion in cats. *Neurosci Lett* 8: 277–282, 1978. doi:10.1016/0304-3940(78)90136-2.
61. **Driesang RB**, **Büschges A.** Physiological changes in central neuronal pathways contributing to the generation of a reflex reversal. *J Comp Physiol* 179: 45–57, 1996. doi:10.1007/BF00193433.

62. **Büschges A**, **Sauer AE**, **Bassler U.** Flexibility of a proprioceptive feedback system results from its "parliamentary" (distributed) organization. In: *Prerational Intelligence: Adaptive Behavior and Intelligent Systems Without Symbols and Logic*, edited by Cruse H, Dean J, Ritter H. Dordrecht: Springer, 2000, p. 267–286. doi:10.1007/978-94-010-0870-9_19.
63. **Sauer AE**, **Büschges A**, **Stein W.** Role of presynaptic inputs to proprioceptive afferents in tuning sensorimotor pathways of an insect joint control network. *J Neurobiol* 32: 359–376, 1997. doi:10.1002/(SICI)1097-4695(199704)32:4<359::AID-NEU1>3.0.CO;2-5.
64. **Wittenberg G**, **Kristan WB, Jr.** Analysis and modeling of the multisegmental coordination of shortening behavior in the medicinal leech I. Motor output pattern. *J Neurophysiol* 68: 1683–1692, 1992. doi:10.1152/jn.1992.68.5.1683.
65. **Wittenberg G**, **Kristan WB Jr.** Analysis and modeling of the multisegmental coordination of shortening behavior in the medicinal leech II. Role of identified interneurons. *J Neurophysiol* 68: 1693–1707, 1992. doi:10.1152/jn.1992.68.5.1693.
66. **Rudomin P**, **Schmidt RF.** Presynaptic inhibition in the vertebrate spinal cord revisited. *Exp Brain Res* 129: 1–37, 1999. doi:10.1007/s002210050933.
67. **Stein W**, **Schmitz J.** Multimodal convergence of presynaptic afferent inhibition in insect proprioceptors. *J Neurophysiol* 82: 512–514, 1999. doi:10.1152/jn.1999.82.1.512.
68. **Czarkowska J**, **Jankowska E**, **Sybirska E.** Common interneurones in reflex pathways from group Ia and Ib afferents of knee flexors and extensors in the cat. *J Physiol* 310: 367–380, 1981. doi:10.1113/jphysiol.1981.sp013555.
69. **Tuthill JC**, **Wilson RI.** Parallel transformation of tactile signals in central circuits of Drosophila. *Cell* 164: 1046–1059, 2016. doi:10.1016/j.cell.2016.01.014.
70. **Agrawal S**, **Dickinson ES**, **Sustar A**, **Gurung P**, **Shepherd D**, **Truman JW**, **Tuthill JC.** Central processing of leg proprioception in Drosophila. *eLife* 9: e60299, 2020. doi:10.7554/eLife.60299.
71. **Jankowska E**, **McCrea DA.** Shared reflex pathways from Ib tendon organ afferents and Ia muscle spindle afferents in the cat. *J Physiol* 338: 99–111, 1983. doi:10.1113/jphysiol.1983.sp014663.
72. **Follmann R**, **Goldsmith CJ**, **Stein W.** Multimodal sensory information is represented by a combinatorial code in a sensorimotor system. *PLoS Biol* 16: e2004527, 2018. doi:10.1371/journal.pbio.2004527.
73. **Jankowska E.** Spinal interneurons. In: *Neuroscience in the 21st Century*, edited by Pfaff DW. New York: Springer, 2013, p. 1189–1224. doi:10.1007/978-1-4939-3474-4_34.
74. **Büschges A**, **Kittmann R**, **Schmitz J.** Identified nonspiking interneurons in leg reflexes and during walking in the stick insect. *J Comp Physiol* 174: 685–700, 1994. doi:10.1007/BF00192718.
75. **Laurent G**, **Burrows M.** Intersegmental interneurons can control the gain of reflexes in adjacent segments of the locust by their action of nonspiking local interneurons. *J Neurosci* 9: 3030–3039, 1989. doi:10.1523/JNEUROSCI.09-09-03030.1989.
76. **Schmitz J**, **Büschges A**, **Kittmann R.** Intracellular recordings from nonspiking interneurons in a semiintact, tethered walking insect. *J Neurobiol* 22: 907–921, 1991. doi:10.1002/neu.480220904.
77. **von Uckermann G**, **Büschges A.** Premotor interneurons in the local control of stepping motor output for the stick insect single middle leg. *J Neurophysiol* 102: 1956–1975, 2009. doi:10.1152/jn.00312.2009.
78. **Kittmann R**, **Schmitz J**, **Büschges A.** Premotor interneurons in generation of adaptive leg reflexes and voluntary movements in stick insects. *J Neurobiol* 31: 512–531, 1996. doi:10.1002/(SICI)1097-4695(199612)31:4<512::AID-NEU10>3.0.CO;2-F.
79. **Wolf H**, **Büschges A.** Nonspiking local interneurons in insect leg motor control II. Role of nonspiking local interneurons in the control of leg swing during walking. *J Neurophysiol* 73: 1861–1875, 1995. doi:10.1152/jn.1995.73.5.1861.
80. **Zill SN**, **Chaudhry S**, **Büschges A**, **Schmitz J.** Force feedback reinforces muscle synergies in insect legs. *Arthropod Struct Dev* 44: 541–553, 2015. doi:10.1016/j.asd.2015.07.001.
81. **Zill SN**, **Dallmann CJ**, **Büschges A**, **Chaudhry S**, **Schmitz J.** Force dynamics and synergist muscle activation in stick insects: the effects of using joint torques as mechanical stimuli. *J Neurophysiol* 120: 1807–1823, 2018. doi:10.1152/jn.00371.2018.
82. **Stolz T**, **Diesner M**, **Neupert S**, **Hess ME**, **Delgado-Betancourt E**, **Pflüger HJ**, **Schmidt J.** Descending octopaminergic neurons modulate sensory-evoked activity of thoracic motor neurons in stick insects. *J Neurophysiol* 122: 2388–2413, 2019. doi:10.1152/jn.00196.2019.

3 Timing of Multimodal Proprioceptive Feedback

3.1 Temporal Differences of Load & Movement Signal Integration in the Sensorimotor Network of the Insect Leg

Gebehart, C., Büschges, A.

In Chapter 3, the timing of proprioceptive signals and of the resulting responses in interneurons, MNs, and muscle fibers is determined and compared between the two sensory modalities load and movement. Signal transmission times and latencies establish distinct short- and long-latency responses in neurons postsynaptic to sensory afferents. The data is used to infer anatomical and functional network connectivity and to determine a timeline of multimodal proprioceptive integration in the sensorimotor network of an insect leg.

Sensory afferents, NSIs, and MNs were stained for morphological characterization. Exemplary stainings of recorded neurons are shown in Figure 2.4 and Supplementary Figure 2.1.

3.2 Author Contributions

Conceived & designed experiments:

Corinna Gebehart, Ansgar Büschges

Performed experiments, analyzed data & prepared figures:

Corinna Gebehart

Interpreted experimental results:

Corinna Gebehart, Ansgar Büschges

Drafted manuscript:

Corinna Gebehart

Edited & revised manuscript:

Corinna Gebehart, Ansgar Büschges

3.3 Abstract

Animals navigating through complex environments are faced with a torrent of sensory inputs, including proprioceptive feedback about their body's movement and perceived forces and load. The nervous system is faced with the task of integrating these sensory inputs, and signal integration does not only depend on spatially, but also on temporally coinciding signals. It is unclear how sensorimotor networks time the arrival of signals from multimodal, spatially distant sense organs, and whether the processing of sensory signals from different sense organs has distinct time courses. We measured signal transmission times and response latencies along the sensorimotor pathways controlling movements of the stick insect leg using intra- and extracellular recordings. Sensory signals from load-sensing CS (tiCS, tr/fCS) had longer transmission times to the premotor network than movement signals from the fCO. We identified the connectivity pattern of sensory signals from tiCS, tr/fCS, and the fCO to identified local premotor NSIs and MNs by distinguishing between short- and long-latency responses to sensory stimuli. Functional connectivity of NSIs, i.e. whether they were 1st or higher order neurons in the sensory processing cascade, depended on the specifics of the sensory input. The timeline of sensorimotor processing of simultaneously elicited tiCS and fCO signals showed an early phase of movement signal processing, and a delayed phase of load integration. The temporal shift between load and movement processing persisted into the motor output of the network. Initial responses of MNs and muscle force were solely based on movement feedback, and load effects manifested with a temporal delay. The results show a consistent temporal shift in the processing of two distinct sensory modalities, load and movement, that persists throughout the sensorimotor network and is able to affect motor output. The impact of sensory signal timing on sensory processing and signal integration establishes its relevance for motor control, and for understanding sensory network computation and function.

3.4 Introduction

Motor control, as well as most, if not all, other neural processing, critically depends on the integration of inputs from multiple sources, including distant neuronal networks, or distinct sense organs. Neuronal signal integration in this sense will be defined by spatial and temporal summation, meaning *where*, in which neurons, are signals integrated, and *when* are signals combined in these networks. Taken together, spatial and temporal summation shape the amplitude and time course of signals, and thus, a network's processing and output. In recent years, time and effort of motor control research in various model organisms and different regions of the nervous system have been invested to identify and examine neuronal points of convergence, e.g. in reticulospinal pathways in monkeys (Fisher et al., 2021), interlimb coordination in crayfish (Smarandache-Wellmann et al., 2014), the feeding connectome of *Drosophila melanogaster* (Miroschnikow et al., 2018), or sensory convergence in motor and interneurons of the stick insect walking system (Schmitz and Stein, 2000; Gebehart et al., 2021 (Chapter 2)). With the increasing availability of connectomes and EM datasets, our knowledge on *where* neuronal signals converge is likely to expand rapidly (e.g. Scheffer et al., 2020; Phelps et al., 2021). Increasingly detailed information on morphological connectivity necessitates in-depth studies about the functional relevance of individual, specific connections, including temporal aspects of signal integration. We therefore decided to make use of the size of the stick insect, *Carausius morosus,* which results in signal transmission times and velocities on time scales that are measurable and easily within the temporal resolution of electrophysiological techniques. Combined with the vast background of knowledge on locomotor networks in large insects (for reviews, see Burrows, 1996; Bässler and Büschges, 1998; Büschges et al., 2008), this allowed us to compare temporal aspects of premotor processing between multiple proprioceptive sense organs.

Proprioception, an organism's sense of self-motion and body position, is essential for skilled movements and fine-tuning of ongoing muscle activity, as well as for postural control and stabilization (reviews in Bässler, 1993; Burrows, 1996; Deliagina et al., 2012; Grillner and El Manira, 2020). The sense of proprioception arises from the concerted action of different types of sensory structures, especially load and movements sensors, which are providing distinct information to the nervous system. The diverse sensory signals converge in local networks to establish the comprehensive representation of sensory context that is used to shape and adapt motor output to self-generated feedback and external perturbations (Kistemaker et al., 2013). Although based on anatomically different sense organs, proprioception shares many common principles between vertebrates and invertebrates (Tuthill and Azim, 2018). Movement sensors, i.e. muscle spindles in vertebrates and chordotonal organs in insects, monitoring joint position and velocity, and load or strain sensors, i.e. Golgi tendon organs and CS, respectively, send signals from the limbs to local premotor networks in the spinal cord or ventral nerve

cord (Zill and Moran, 1981a; Field and Matheson, 1998; Duysens et al., 2000; Zill et al., 2004; Büschges and Gruhn, 2007; Windhorst, 2007; Tuthill and Wilson, 2016a). The information is subsequently processed to adjust the motor output, e.g. by initializing a resistance reflex to maintain leg posture or by updating the control of an ongoing active movement. In both cases, i.e. sudden external perturbation and ongoing movement, the sensory input is changing on very short time scales. External perturbations cause the sensory signaling to the network to jump from no velocity, fixed position, and constant load to an abrupt increase in sensory activity caused by the transient increase in the rate of change of the sensory input (Hofmann and Bässler, 1982; Büschges, 1994). During active movements, for example, the stance phase of walking, the sensory flow to local networks is constant, but not consistent, i.e. it varies in strength and information content as joints move and forces change when the leg exerts forces on the ground to propel the body forward (Dallmann et al., 2016).

In insects, the constant flow of sensory information can be transmitted to MNs directly via monosynaptic connections from sensory afferents to MNs, or indirectly via polysynaptic pathways that include one or more intercalated spiking and nonspiking local interneurons (Burrows, 1996). Assuming longer transmission times from more distally located sense organs (Hustert et al., 1981), an intuitive hypothesis, which will be tested in this study, is that the sensory information that is most relevant in a given physiological context will be transmitted along the shortest pathway. The shortest pathway in this case being from the most proximal sense organ monosynaptically onto the MN or the processing network. The parallel transmission across multiple synapses and processing within any number of interneurons of the premotor network will necessarily require more time. In a previous study, load signals from the distal tibial and the more proximal trochanterofemoral CS (tiCS, tr/fCS), and movement feedback from the fCO was found to be distributed onto a single set of local premotor NSIs, which control movements of the FTi leg joint (Siegler, 1981; Büschges, 1990; Büschges and Wolf, 1995; Sauer et al., 1996; Gebehart et al., 2021 (Chapter 2)). Local NSIs are individually identifiable in the stick insect and it is therefore possible to pinpoint with a high degree of precision *where* load and movement signals are summed in the premotor network of the insect leg. The question therefore arises *when* this information actually converges and whether monosynaptic parallel pathways from sensory afferents to MNs circumvent time-consuming network processing.

Temporal summation, as we are approaching it in this study, can be subdivided into two aspects: 1) The number, and order, of neurons a signal passes through before being summed, and 2) the absolute signal latency that is imposed by transmission distances in unmyelinated invertebrate neurons, but which can also be affected by other aspects such as axon diameter (Hodgkin, 1954; Hartline and Colman, 2007). The number of neurons, and thereby computations, that a signal has to traverse to reach the converging neuron might alter its content. This means that the later in the chain of

connectivity a signal is merged with another, the more possibilities there are in the upstream neurons to preprocess, shape, and contextualize the information. The connectivity of networks that process sensory inputs is a determining factor for their function. Clear examples of this are lateral inhibition improving spatial discrimination in vision (review in Thoreson and Mangel, 2012), and the neuronal delay line and coincidence detection in cricket song pattern recognition (Hedwig and Sarmiento-Ponce, 2017). In this study, we addressed the question of neuronal connectivity by using transmission times and signal latencies to infer mono- and polysynaptic connections from sensory afferents onto NSIs and MNs. We tested the connectivity within the well-studied control loop of the FTi joint, i.e. fCO, tiCS, NSIs, and the ExtTi MNs, and use tr/fCS and the RetCx MNs of the more proximal thorax-coxa joint as a reference (Bässler, 1993). Individual NSIs and MNs received load and movement signals via a web of mono- and polysynaptic connections. We show how the signaling cascade through the NSI network during concurrent sensory inputs changed depending on the sensory context, i.e. depending on the sensory afferents transmitting information in a given situation. The concept of flexible functional network connectivity was supported by reciprocal excitation between a pair of NSIs identified by a paired double intracellular recording.

The absolute timing of a signal, i.e. how long it takes for sensory signals from multiple sense organs at different locations on the leg to reach and pass through the network, will predetermine its impact on network activity and, thereby, on motor coordination, force production, and even action selection (Sponberg and Daniel, 2012; von Reyn et al., 2014; Putney et al., 2019). We hypothesized that, should signal transmission times differ between sensory modalities, this would be reflected in the time course of the resistance reflex to simultaneously elicited bimodal stimuli.

In this study, we compare the absolute transmission times of load and movement feedback to and within the local network and find a marked disparity in which movement signals consistently outpaced load feedback. This pattern was already established during sensory transmission to the local networks, holding true even for the more proximally located tr/fCS, and was reflected by delayed effects of load on movement resistance reflexes in the ExtTi MNs and the resulting isometric muscle force. These findings will be essential in our understanding of how proprioceptive signals, and their timing, shape time- and phase-dependent behaviors like walking.

3.5 Materials & Methods

3.5.1 Animals

Adult female stick insects, *Carausius morosus*, were reared in a 12 h light / dark cycle at 23-27 °C and 50 % humidity in the parthenogenetic colony at the University of Cologne, and fed with blackberry leaves. Experiments were performed at room temperature (20-24 °C) in inactive animals (distinction

between behavioral states reviewed in Bässler, 1993). Animal dissection, electrophysiological recordings, and mechanical stimulation paradigms followed the procedures described in a previous study (Gebehart et al., 2021 (Chapter 2)).

3.5.2 Dissection

The right mesothoracic leg was left intact, all other legs were removed. The two most proximal leg joints were immobilized at right angles with light curing glue (3M ESPE Sinfony, Neuss, Germany) and a minuten pin inserted into the ventral trochanter (Haberkorn et al., 2019). Animals were positioned dorsal side up. To stimulate tiCS, the FTi joint was additionally set to 90-110 ° and glued to the platform.

The mesothoracic ganglion was exposed, all lateral mesothoracic nerves except nervus cruris (ncr), nl3, and nl5 were cut or squeezed (nomenclature according to Marquardt, 1940), and the ganglion was pinned with cactus spines on a wax-coated steel platform (cf. e.g. Büschges, 1990; Driesang and Büschges, 1993). Pronase E crystals (VWR, Darmstadt, Germany) were applied directly to the ganglion sheath for 45 s before rinsing with extracellular saline (178.54 mM NaCl, 17.61 mM KCl, 7.51 mM $CaCl_2$, 25 mM $MgCl_2$, 10 mM Hepes buffer, set to pH 7.2 with NaOH (Weidler and Diecke, 1969)).

3.5.3 Electrophysiological Recordings

Intracellular activity from neuropilar arborizations of NSIs, sensory afferents, and MNs in the ipsilateral hemiganglion was recorded with sharp microelectrodes (resistance 25-35 MΩ, borosilicate glass capillaries 8GB100TF-8P, Science Products, Hofheim, Germany, micropipette puller P-1000, Sutter Instruments, Novato, CA, USA) with chlorinated silver wire and intracellular saline (1 M KAc, 0.1 M KCl, 5 % neurobiotin tracer (Vector Laboratories, Burlingame, CA, USA)). Interstitial potentials were compensated (5 - 20 mV; Dörr et al., 1996), current injection was controlled digitally (MS501 stimulator, Electronics Workshop Animal Physiology, University of Cologne, Germany). For the paired double intracellular recording of two NSIs, the equipment was mirrored to a second intracellular recording electrode containing a different dye (3 % tetramethylrhodamine dextran, 3,000 MW, Invitrogen). Recording procedure was the same as in single electrode recordings. Both intracellular electrodes were inserted into the ganglion before each electrode was lowered into an individual neuron.

Motor activity was recorded extracellularly with hook electrodes (Schmitz et al., 1988) from nl3 or F2 (ExtTi MNs) and nl5 (RetCx MNs), and sensory signals from ncr proximal (1 mm) or distal (7 – 10 mm) to the ganglion.

Electric signals were amplified (intracellular: gain x20, high-cut filter 3 kHz, SEC-06 preamplifier, SEC-10LX single electrode clamp amplifier, npi, Tamm, Germany; extracellular: gain x2000, low-cut filter 0.3 kHz, high-cut 2.5 kHz, notch filter 50 Hz, MA101 preamplifier & MA102 differential amplifier,

Electronics Workshop, University of Cologne), digitized and stored (sampling rate 12.5 kHz (extracellular signals), 6.25 kHz (intracellular signals), ADC Micro1401 mkI, Spike2 v7.16, CED, Cambridge, UK).

3.5.4 Mechanical Sensory Stimulation

A metal probe pushed the trochanterofemur into a posterior or anterior, or the tibia into a dorsal or ventral direction by 50 µm with ramp-and-hold stimuli to activate tr/fCS or tiCS, respectively (see also Zill et al., 2013; Haberkorn et al., 2019; Gebehart et al., 2021 (Chapter 2)). Ramp duration was 0.1 s with a hold duration of 1 s if not indicated otherwise. The onset of the stimulus corresponds to loading, returning to the initial baseline to unloading of the leg.

In experiments with tiCS stimulation, the dorsal femur was cut and the fCO receptor apodeme was clamped and elongated / relaxed to imitate flexion / extension movements, respectively, using ramp-and-hold stimuli. Ramp duration was 0.2 s, with a hold duration of 1 s. Ramp amplitude was 300 µm, corresponding to a 60 ° tibial flexion, rising stimuli indicate increasing mimicked flexion (Weiland and Koch, 1987). fCO clamp, tr/fCS, and tiCS stimulators were controlled using Spike2 (CED) or a digital stimulator (MS501) and driven by custom-build linear motors (lowpass filter 1 kHz, VCM Controller/Power Amplifier, Electronics Workshop, University of Cologne).

In experiments with tr/fCS stimulation and for sensory recordings in Figure 3.1 A and B the tibia was not immobilized. tiCS were ablated with a heated metal probe before tr/fCS stimulation, and the fCO was stimulated by ramp-and-hold flexion of the tibia with a forked metal probe controlled by a rotational stepper motor (Mach3 software, v7.13, CNC Steuerung Bocholt, Germany). This stimulation paradigm constrained the fCO stimulus parameters to an angle of 50 °, velocity of stimulus ramps was 300 °/s, approximating 0.2 s ramp duration; hold duration was 1 s. Minimum interval between CS and / or fCO stimuli was 2.6 s. For fCO signal latency analysis other than Figure 3.1 A and B, only experiments with fCO clamp, but not tibial movement, stimuli were analyzed.

3.5.5 Isometric Muscle Forces

To determine the timing of ExtTi muscle force in response to exclusive or combined fCO and tiCS stimulation, isometric muscle force was measured. A window was cut into the most distal femur, the ExtTi muscle tendon and the cuticle surrounding its attachment into the FTi joint were excised and placed on a hook shaped from a minuten pin. The hook was attached to the lever arm of a force transducer (Aurora 300 B dual-mode lever system; Aurora Scientific Inc., Ontario, Canada, resolution 0.3 mN). Isometric muscle length was maintained by adjusting the transducer's force to exceed ExtTi muscle forces. Force baseline values were defined as force measured while the minuten hook rested on the FTi joint, but without the muscle tendon attached. Data was digitized, stored, and analyzed with Spike2 software (sampling rate 6.25 kHz, ADC Micro1401 mkI, CED).

3.5.6 Neuron Identification

For the identification of individual NSIs, their effect on ExtTi MNs activity during de- and hyperpolarizing current injection, responses to fCO and CS stimuli, and morphologies were compared to established characteristics (Büschges, 1990; Sauer et al., 1996; Gebehart et al., 2021 (Chapter 2)). Recorded neurons were classified as nonspiking if no action potentials occurred at any time during the experiment or could be elicited by sensory and tactile stimuli, current injection, or when the animal was actively moving (Hengstenberg, 1977; Büschges, 1990). The identity of MNs, NSIs, and sensory afferents was verified by intracellular staining with iontophoretic neurobiotin tracer injection, following the same procedure as described in Gebehart et al. 2021 (Chapter 2, cf. Berg et al., 2015).

3.5.7 Data Analysis

Latencies were calculated from waveform averages of 5-10 consecutive stimuli if not indicated otherwise, using Spike2 software (CED). Latencies were defined as time differences from stimulus begin to onset of the initial neural response. Only latencies of responses with unequivocal identification of response onset were included. Conduction times from sense organ to distal and proximal ncr (A*, A', Fig. 3.1) were inferred from extracellular recordings, all other latencies are based on intracellular data. Conduction velocity of tiCS signals was calculated from signal time difference and distance between proximal and distal ncr electrodes. To test for correlation between tiCS action potentials recorded from the distal ncr and intracellular changes of NSI membrane potential, both signal traces were triggered on tiCS action potentials and averaged across 5 consecutive stimuli (Fig. 3.2 A-D). For identification of short- and long-latency connections, latencies were normalized by subtracting the maximal duration for signal transmission from each sense organ to the neuropilar arborizations of the respective sensory afferent. Specifically, the standard deviation and average latency to recording site B in Fig. 3.2 E were subtracted from response latencies of the recorded neurons. Action potential frequencies in Figure 3.4 were calculated over the duration of the entire simultaneous load and movement stimulus, and over the initial 50 ms of stimulation. These frequencies were normalized to frequencies elicited by exclusive fCO stimulation in the same animal. Throughout the manuscript, N refers to the number of animals, n to the number of stimulus runs per animal. If not indicated otherwise in the figure legends, each stimulus run consisted of 5 – 10 consecutive stimuli. N, n, averages, standard deviation, and original data for all figures are included in Supplementary Tables 3.1 and 3.2. Figures were created with MATLAB (R2018b, Mathworks), Spike2 (CED), and Adobe Illustrator CS6 (v16, Adobe Systems).

3.6 Results

Proprioceptive feedback from load and movement sensors in and on the leg plays a critical role in generating and controlling the motor output of the leg muscle control system both in standing and during active leg movements. The fact that these signals are processed within a distributed network of local premotor NSIs raises the question to which extent temporal characteristics of conduction and processing play a role in the integration of movement and load feedback. In the following, we will present data on latencies and relative timing of sensory signals from individual movement and load sense organs to the membrane of premotor NSIs and MNs to unravel connectivity between sensory neurons and postsynaptic neurons. Using absolute timing of sensory responses in sensory afferents, NSIs, and MNs, we demonstrate the timeline of load and movement signal processing. We show that temporal differences between load and movement processing affect the resulting motor output, thereby establishing behavioral relevance.

3.6.1 Signal Transmission Times from Load & Movement Sense Organs to the Local Premotor Network

The sense organs providing information about leg loading and movement are located on and within the leg and are spatially separated (Fig. 3.1). The spatial distribution results in different distances from the sensory spike initiation zone to the central nervous system for individual sense organs. In the comparably large stick insect, these differences amount to 11 mm (the length of the trochanterofemur) between tiCS and the fCO, while tr/fCS and the fCO are located at about the same distance from the local networks (approx. 2 mm). We therefore asked whether these differences in location have functional effects on transmission times.

The axons of fCO, tiCS, and tr/fCS afferents enter the ganglion via the ncr, with tiCS afferents joining the ncr more distally than fCO and tr/fCS afferents. The fCO and tiCS are activated when the tibia is flexed by an external force (Fig. 3.1 Ai). Extracellular electrodes on the distal ncr (Fig. 3.1 Aii, A*) record only tiCS signals, while both fCO and tiCS signals traverse the proximal ncr (A'). Latencies from stimulus onset to the recorded signals in the ncr were longer for tiCS in the distal ncr than for fCO signals in the proximal ncr (Fig. 3.1 Bi). The effect was consistent (A*: 9.1 ± 0.5 ms, A': 4.3 ± 0.3 ms, Fig. 3.1 Bii) and suggest that the transmission times for tiCS signals through the proximal ncr and into the local premotor networks will be even longer. The number of experiments and stimulus runs for all analyses are given in Supplementary Table 3.1 (Fig.s 3.1-3.4) and Supplementary Table 3.2 (Fig. 3.2 E).

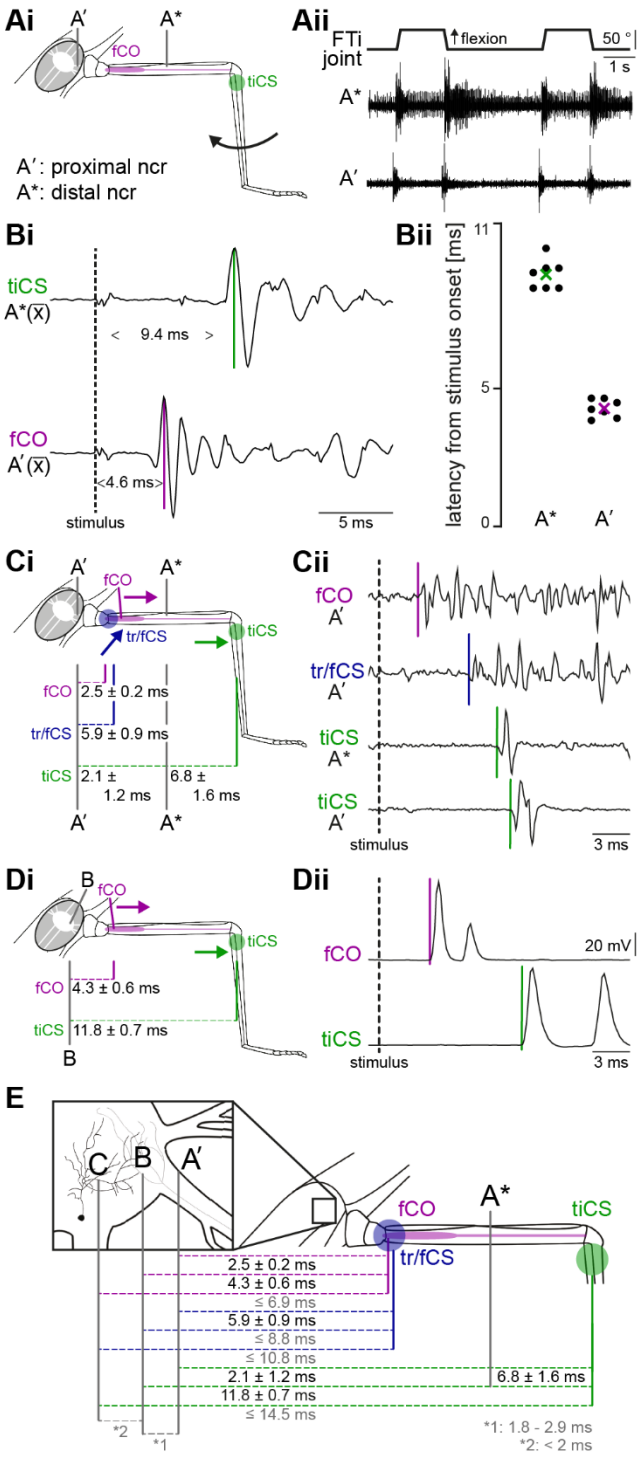

Figure 3.1: Transmission times of fCO (magenta), tr/fCS (blue), and tiCS (green) signals to the local premotor network. **A**: Signal transmission of fCO and tiCS signals during passive flexion of the tibia, mimicking a natural stimulus. Sensory signals were recorded from the proximal (A') and distal (A*) ncr. **i**: Position of sense organs (fCO, tiCS), extracellular recording electrodes (A', A*), and stimulus direction. **ii**: Flexion movement of the tibia elicited strong responses at both recording positions on the ncr. **B**: fCO and tiCS signal latencies during a natural stimulus as shown in **Ai**. **i**: Latency of tiCS (A*) and fCO (A') signals following stimulus onset. Exemplary waveform average ($\bar{x}$) of ncr signals. **ii**: Longer transmission times of tiCS signals (A*) compared to fCO signals (A') were consistent. **C**: Signal transmission to A* (tiCS) and A' (fCO, tr/fCS, tiCS) during sensory stimuli targeting single sense organs. **i**: Position of sense organs (fCO, tr/fCS, tiCS), extracellular recording electrodes (A', A*), stimulation directions, and signal latencies. **ii**: Transmission times to the ncr differed between sense organs. **D**: Signal transmission to neuropilar arborizations of sensory afferents (fCO, tiCS) during the respective sensory stimuli. **i**: Position of sense organs (fCO, tiCS), intracellular recording electrode (B), stimulation directions, and signal latencies. **ii**: Transmission times from tiCS to the neuropil were longer than from the fCO, consistent with **C**. **E**: Sensory signal transmission times between middle leg sense organs and the mesothoracic ganglion; data summarized from **C** & **D**, including synaptic transmission time to the first postsynaptic neuron (C). *1: signal conduction time from ncr to neuropilar arborizations of sensory afferents (fCO: 1.8 ms, tiCS: 2.9 ms); *2: signal conduction time across a synapse, assuming a monosynaptic connection (< 2 ms, Burrows and Siegler, 1978).

Figure 3.1 (*continued*): Black: experimental data, grey: estimated values. All panels: Latencies: mean ± SD; dashed vertical lines: stimulus onset; arrows indicate stimulus directions; **Aii**, **Cii**, **Dii**: exemplary raw data traces. For detailed data, standard deviation, and N, see Suppl. Table 3.1.

The situation in Figure 3.1 Ai resembles a natural stimulus, but the unspecific stimulation paradigm might obscure responses of individual sense organs. We therefore applied mechanical stimuli exclusively targeting either the fCO, tiCS, or tr/fCS, while the other two respective sense organs were not stimulated or ablated (Fig. 3.1 Ci). tr/fCS were included because they provide information about the same modality as tiCS while being spatially close to the fCO. To allow for precise fCO stimulation (see Chapter 3.5), the electrode needed to be positioned slightly more distally. This resulted in shorter latencies from stimulus onset to the recorded tiCS afferent signals (A*: 6.8 ± 1.6 ms, Fig. 3.1 Ci, cf. Fig. 3.1 B). tiCS signals in the recording of the distal ncr were used to identify the same spikes in the proximal ncr. This added another 2.1 ± 1.2 ms to the transmission time for tiCS signals into the ganglion (Fig. 3.1 Ci), resulting in an approximate total of 8.9 ms. From these experiments we were also able to determine the conduction velocity of tiCS signals to be 2.24 ± 0.31 m/s (N = 6), which is in good accordance with previous reports from the locust (2.3 ms; Burrows and Pflüger, 1988).

Surprisingly, although tr/fCS are located close to the fCO, their transmission time was markedly longer (fCO: 2.5 ± 0.2 ms, tr/fCS: 5.9 ± 0.9 ms, Fig. 3.1 Ci), while tr/fCS signals were only 3 ms faster than the total transmission time for the much more distal tiCS. Taken together, this resulted in a signal cascade in which fCO signals were the fastest to pass the proximal ncr and thus to reach the premotor networks, followed by tr/fCS and lastly by tiCS (Fig. 3.1 Cii). This was reflected in intracellular recordings from the neuropilar arborizations of tiCS and fCO afferents within the ganglion, where signal latencies for both sense organs were longer, but the temporal offset between them remained (fCO: 4.3 ± 0.6 ms, tiCS 11.8 ± 0.7 ms, Fig. 3.1 D). For the following analyses, we assumed a latency similar to tiCS, i.e. 2.9 ms, for the short distance from the proximal ncr into neuropilar tr/fCS afferent arborizations. Adding 5.9 ms latency from stimulus onset to the tr/fCS signals in the proximal ncr, we expect tr/fCS signals to reach the afferent arborizations 8.8 ms after stimulus onset. Transmission times from all three sense organs to the recording positions in the ncr, the neuropilar arborizations of the sensory afferents, and the estimated total latency to a monosynaptically connected neuron are summarized in Figure 3.1 E. Latency from each sense organ to the first postsynaptic neuron was estimated by summation of mean latencies to sensory afferents, the standard deviation, and 2 ms for synaptic transmission, respectively (Burrows and Siegler, 1978). Based on these estimates, sensory signals will reach the first postsynaptic neuron in the local network after 6.9 ms (fCO), 10.8 ms (tr/fCS), and 14.5 ms (tiCS) following stimulus onset at the latest (Fig. 3.1 E).

In summary, latency differences appeared to be no simple correlate of the distance between sense organ and the central nervous system, as transmission times from tr/fCS, whose location is near the fCO, were markedly longer than from the fCO and not as much faster than tiCS as would be expected given the difference in distance from the ganglion of approximately 11 mm.

3.6.2 Signal Transmission Times from Movement & Load Sensory Afferents to Nonspiking Interneurons & Motor Neurons

Transmission times from sense organs to the segmental ganglion and the local postsynaptic neurons showed marked differences for load and movement sensors (Fig. 3.1). A second potential source for time delays arises from intra-ganglionic network connectivity between sensory afferents, interneurons, and the output stage of the motor system, i.e. MNs. The more synapses between sensory input and MNs, the longer the latency between the two will be. Previous studies on the locust have found mono- and polysynaptic connections between tiCS and unidentified NSIs (Burrows and Pflüger, 1988; Laurent and Burrows, 1988), leading to short and long latencies of sensory responses in MNs, respectively. When focusing on the same sense organ (tiCS) we found a similar situation in the stick insect, i.e. differences in transmission times between sensory neurons and NSIs, by using time-locked events between extracellular tiCS spikes and intracellular changes in NSI membrane potential (Fig. 3.2 A-C).

Identification of short- and long-latency connections between sensory afferents and their postsynaptic partners based on time-locked events requires unambiguous identification of sensory action potentials in extracellular ncr recordings (for classification of mono- and polysynaptic pathways, see Chapter 3.7). The signal-to-noise ratio of tiCS signals in the distal ncr is sufficiently high to enable threshold-based triggering on single tiCS spikes (Fig. 3.2 A-Di). Averaging extracellular tiCS and intracellular neuron activity at the time of tiCS spikes resulted in distinct single tiCS action potential shapes (Fig. 3.2 A-Dii). A short-latency connection between a tiCS afferent and a postsynaptic neuron should result in a time-locked and sharply defined change in membrane potential occurring within a short time window, as was observed for NSI E3 (Fig. 3.2 A). A time-locked, distinct change in membrane potential with a long latency indicates an indirect, polysynaptic connection (see Chapter 3.7). The latter is likely mediated by a single intercalated neuron which relays tiCS action potentials one-to-one to the NSI, as shown for NSI I4 (Fig. 3.2 B). Gradual changes in membrane potential without a distinct, time-locked event such as found in NSI I3 indicate long-latency, indirect connectivity (Fig. 3.2 C). A lack of synaptic inputs from short- and long-latency pathways is exemplified by a RetCx MN that showed only a weak response to tiCS stimulation (Fig. 3.2 D).

Expanding the analysis of sensory signal transmission times to include tr/fCS and the fCO required an alternative approach. Triggering on individual sensory action potentials in ncr recordings is not feasible for fCO and tr/fCS signals, as the signal-to-noise ratio in the proximal ncr recordings allows to

distinguish the onset of the overall sensory response, but not to identify single action potentials from a given type of sensory neuron. It is, however, possible to detect the onset of the response to sensory stimuli in intracellular recordings of NSIs and MNs and, by comparison with stimulus onset, to determine signal latencies. We used this fact to determine the latencies of tr/fCS and fCO responses in postsynaptic NSIs and MNs, and to increase our sample size of latencies with regard to tiCS inputs.

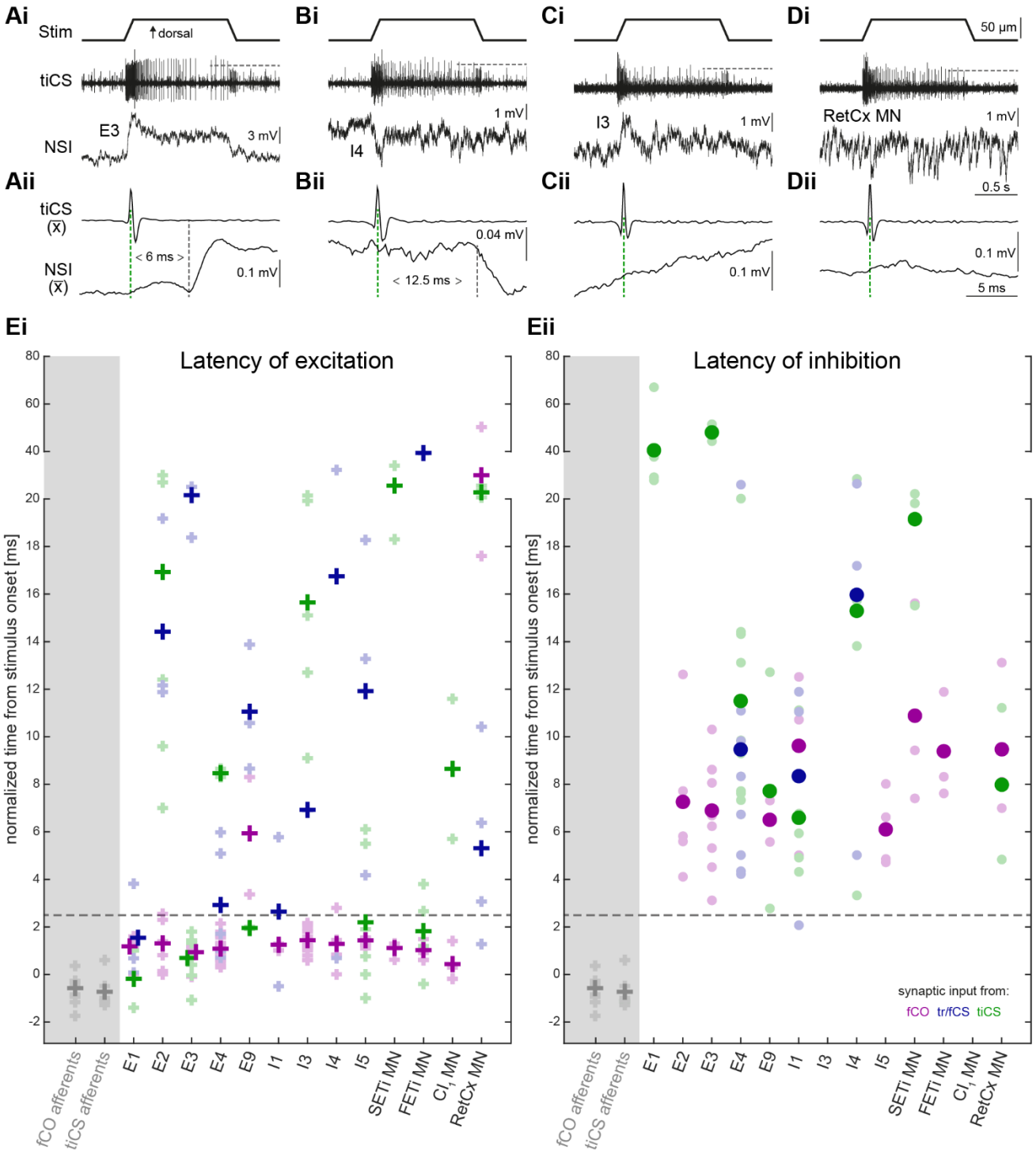

Figure 3.2

Figure 3.2 *(previous page)*: Connectivity from sensory afferents onto NSIs and MNs. **A-D**: Identification of short- and long-latency connections between tiCS afferents, identified NSIs and a RetCx MN using time-locked events. Data from tiCS and NSIs / RetCx MN recordings (**i**) were averaged ($\bar{x}$) over 5 consecutive stimuli and triggered on tiCS spikes (**ii**, trigger threshold dotted horizontal line in **i**). Distinct time-locked, short-latency events were indicative of direct connections (6 ms, **A**, E3). Long latencies with (12.5 ms, **B**, I4) or without (**C**, I3) distinct time-locked events suggest intercalated interneurons. No time-locked event occurred in the RetCx MN (**D**). **i**: exemplary data traces of tiCS (extracellular) and NSI / MN (intracellular) recordings; **ii**: averaged tiCS (top) and NSI / MN (bottom) traces. **E**: Sensory signal transmission latencies to sensory afferents, NSIs, and MNs, normalized to conduction times from the respective sense organ to the local network (cf. Fig. 3.1 E (B)). Latencies of excitatory (**i**) and inhibitory (**ii**) intracellular responses in NSIs and MNs to fCO (magenta), tr/fCS (blue), tiCS (green) signals. Bold symbols: average across responses in one neuron type to individual sensory stimuli; faded symbols: each data point (average of 5-10 stimuli) represents one animal. Fast inhibition in I1 is an outlier. For details on normalization, see Chapters 3.5 and 3.6.2. For detailed data, see Suppl. Table 3.2.

We used signal latencies, distinguishing between short-latency and long-latency responses, as a proxy for network connectivity. The shorter the signal latency between stimulus onset and neuronal response, the more likely is a direct connection between sensory afferent and the recorded neuron, as signal transmission along neurites and across synapses takes time (Fig. 3.2 E). We used the same population of NSIs and MNs presented in Gebehart et al. (2021, Chapter 2) and included not only the elements of the FTi joint control loop, i.e. fCO, tiCS, and NSIs, but also tr/fCS and RetCx MNs as reference.

To compare transmission times between different sense organs, we normalized intracellularly measured latencies to the maximal time by which the signal will have been transmitted to the ipsilateral neuropil of the mesothoracic ganglion (cf. Fig. 3.1 E (B), for details on latency normalization, see Chapter 3.5). This provided us with a common baseline for all sensory signals; negative latencies result from using maximal latencies for normalization. Accounting for synaptic transmission and distance between input synapse and recording electrode, we set the limit for potentially monosynaptic connections to 2.5 ms in normalized latencies (Fig. 3.2 E, dashed line; Burrows and Siegler, 1978; see Chapter 3.7). We distinguished between excitatory and inhibitory effects on intracellularly recorded NSIs and MNs induced by fCO (magenta), tr/fCS (blue), and tiCS (green) stimulation (Fig. 3.2 E). Normalized latencies of signals recorded from intra-ganglionic neuropilar arborizations of fCO and tiCS afferents are shown as reference. Sensory afferent responses were all excitatory and had short latencies, being directly transmitted from the periphery, and represent the entry of the sensory signal into the local network.

All recorded NSIs except for those of type E9 received short-latency inputs from fCO afferents (Fig. 3.2 Ei). Short-latency transmission from tiCS or tr/fCS to NSIs did not overlap between the recorded types of neurons, except for NSI E1, which received short-latency inputs from all three sense organs. tiCS signals were transmitted with short latencies to NSIs E1, E3, E9, and I5, tr/fCS signals to E1, E4, I1, and I4, whereas all CS inputs to NSIs E2 and I3 had long latencies. Average values show a clear grouping of short-latency responses below the defined threshold for potential monosynaptic connections, and of long-latency responses above it (Fig. 3.2 Ei, dashed line). Note that average values mask the possibility of multiple signaling pathways from one sense organ to the same postsynaptic neuron. Averages for tr/fCS responses in E4 and I1, and for tiCS responses in I5 were close to threshold, and tr/fCS responses in I4 showed clearly distinct short- or long-latency responses, indicating two distinct signaling pathways to the same type of neuron (see also Suppl. Table 3.2). Polysynaptic excitation was more common for CS than fCO signals and found in all NSIs, with latencies up to 39.4 ms (Fig. 3.2 E, I4). All inhibitory signals had long latencies (Fig. 3.2 Eii). NSIs were inhibited by fCO, tiCS, or tr/fCS signals in varying combinations, apart from I3, which was not inhibited following onset of any stimulation.

We identified the latency pattern from sense organs onto the ExtTi MNs SETi, FETi, and CI_1, as well as RetCx MNs to search for potential differences in the connectivity between CS and MNs of the same and adjacent joints (Fig. 3.2 E). Whereas all ExtTi MNs received short-latency excitation from the fCO, only FETi was excited by short-latency tiCS inputs. tiCS-elicited excitation of SETi was mediated by long-latency connections. While fCO and tiCS responses in RetCx MNs consistently had long latencies, tr/fCS latencies were more diverse, potentially indicating diverse connectivity to individual RetCx MNs (Fig. 3.2 E).

3.6.3 Functional Connectivity between Sense Organs & Premotor Nonspiking Interneurons in Different Sensory Contexts

Distributed multimodal sensory processing within the same network of premotor interneurons (Gebehart et al., 2021 (Chapter 2)) raises the question whether functional coordination of sensory afferent signals, their synaptic inputs to the studied NSI network, and the resulting effects on ExtTi MNs are based on a fixed network connectivity, or whether signal processing pathways change depending on the sensory context. Sensory context depends on the behavior of the animal and individual leg movements and is determined by the activity of individual sense organs at any given time. Responses of the premotor NSIs depend on the type of sensory feedback and can support or oppose ongoing motor activity, such as stimulus-elicited resistance reflexes (Büschges, 1990; Gebehart et al., 2021 (Chapter 2)), and are mediated by a pattern of short- and long-latency connections from sensory afferents (Fig. 3.2). Focusing on the FTi joint control premotor network and the contributing neural

components, i.e. sensory neurons of the fCO, the tiCS, and the premotor NSIs, allowed us to reduce the complexity to four simple sensory settings. These are combinations of tibial flexion and extension, leading to fCO elongation or relaxation signaling, and activation of tiCS G6A (ventral stimulation) or G6B (dorsal stimulation) elicited by forces exerted on the tibia. The sense organs would be activated by a passive flexion or extension of the tibia while the leg does not have ground contact (Fig. 3.3. Ai, iv), and a passive flexion or extension while the leg has ground contact (ii, iii), respectively. NSIs were categorized as being 1st or higher order depending on whether sensory input in the given context was relayed via short- or long-latency influences (Fig. 3.3 A). Since at least one NSI could be sorted into each category of 1st and higher order recipient of tiCS and fCO inputs in all possible combinations of the aforementioned sensory signals, the group of NSIs analyzed present a representative sample of the entire NSI network.

In each of the four sensory contexts (Fig. 3.3 Ai-iv), NSIs that were higher order processing neurons for both movement and load stimuli, i.e. which received long-latency sensory inputs from both sense organs, are supporting the movement response in ExtTi MNs (Driesang and Büschges, 1996; Sauer et al., 1996; Gebehart et al., 2021 (Chapter 2)). One of these supporting NSIs in every sensory setting additionally supported the respective load response (Fig. 3.3 A, bold type, bottom right quarters). Depending on the sensory context, most NSIs changed their position in the hierarchy of sensory signal processing. For example, E1 received short-latency excitation upon fCO elongation and tiCS G6A activation, and was thus classified as a 1st order NSI for these sensory signals, i.e. responding to signals that had not been processed by another upstream interneuron (Fig. 3.3 Ai). E1 became a higher order neuron, i.e. receiving signals at longer latencies, when tiCS G6B were stimulated instead (Fig. 3.3 Aii). We found a set of NSIs, i.e. I3, I4, and E4, that did not change their functional connectivity. These NSIs, referred to as stable NSIs, received synaptic inputs of the same latency category in any sensory context. The stable NSIs were 1st order NSIs for fCO signals and higher order for tiCS signals (Fig. 3.3 Ai-iv). For all other NSIs, functional hierarchy, i.e. position in the sensory processing cascade, depended on, and changed with, the context of sensory feedback.

Intracellular double recording of an exemplary pair of NSIs included in this study, i.e. E2 and E4, revealed recurrent connectivity (Fig. 3.3 B). E2 was depolarized by current injection into E4 and vice versa (Fig. 3.3 Bi, iii), and the effects were increased when the respective postsynaptic NSI was hyperpolarized (Fig. 3.3 Bii, iv). E4 was a stable NSI, whereas E2 received sensory inputs of similar (Fig. 3.3 Ai, ii) or different latencies (Fig. 3.3 Aiii, iv) as E4, depending on the sensory context. Recurrent connectivity between NSIs support the hypothesis of a flexible functional connectivity that depends on the context of sensory feedback.

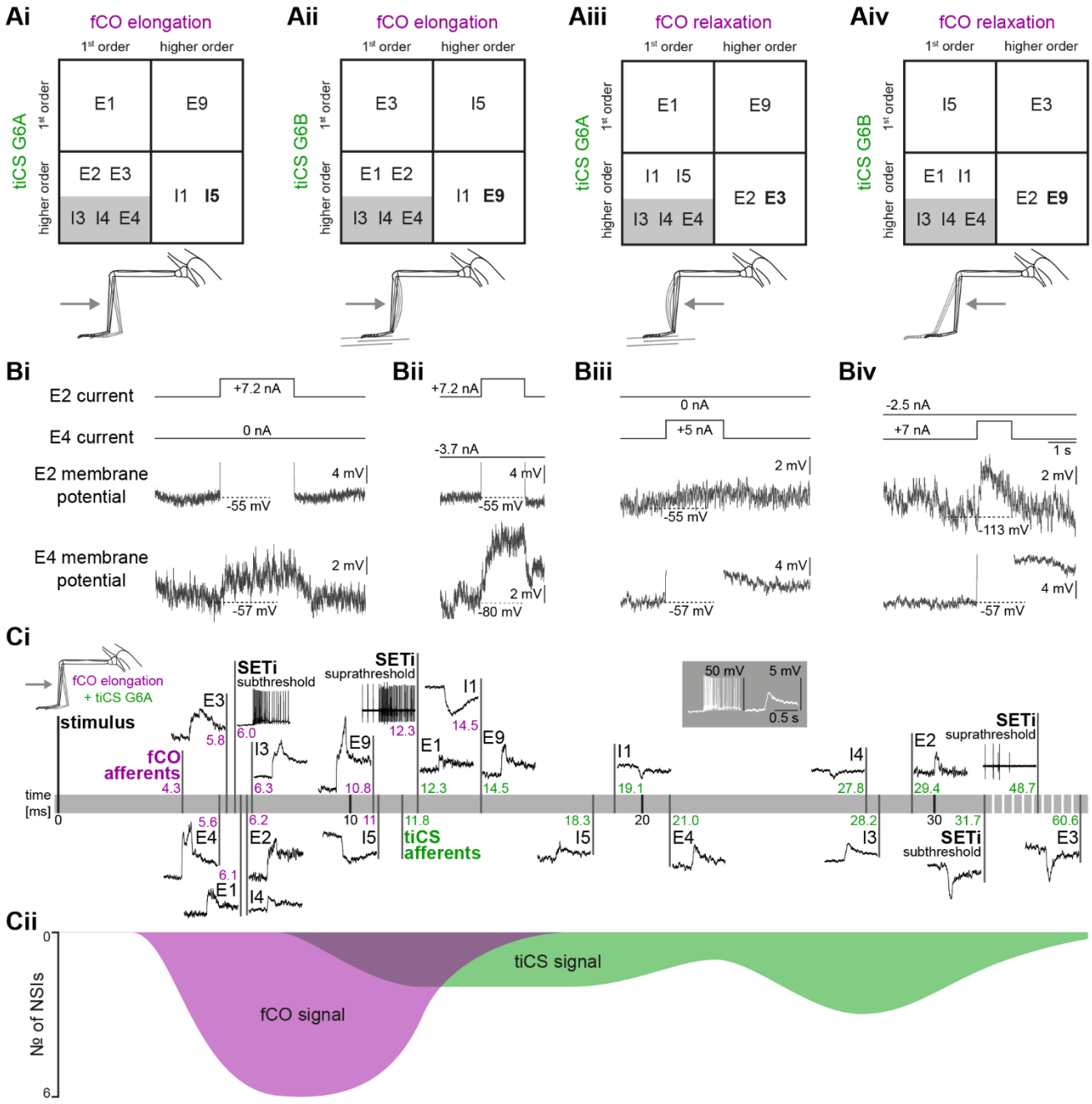

Figure 3.3: Functional hierarchy of NSI processing and sensory integration. **A**: Functional NSI processing connectivity depended on multisensory context. NSIs sorted by short- (1st order) and long-latency (higher order) signal transmission during fCO elongation (**i**, **ii**) or relaxation (**iii**, **iv**) and tiCS G6A (ventral bending, **i**, **iii**) or G6B activation (dorsal bending, **ii**, **iv**). Position of NSIs, i.e. functional connectivity, changed with the sensory context, with the exception of I3, I4 and E4 (grey box). Independent of sensory context, all NSIs that were higher order for both sensory modalities were supporting the respective fCO stimulus-evoked motor output (**i**-**iv**, bottom right quarter). Of those NSI, one in each sensory context was additionally supporting tiCS-evoked motor output (bold). **B**: Recurrent connection between 2 exemplary NSIs.

Figure 3.3 (*continued*): Double intracellular recording of NSIs E2 and E4, positive current was injected into E2, while no (**i**) or negative current (**ii**) was injected into E4, and vice versa for the opposite synaptic direction (**iii**, **iv**). Resting membrane potential indicated by dashed line, upper limits of membrane potential of the current-injected NSI cut off. **C**: Timeline of multimodal sensory integration in the local network. **i**: Absolute latencies of responses in fCO and tiCS afferents, NSIs, and SETi MN to fCO elongation and tiCS G6A activation, grey box: scale bars for neuron responses. **ii**: Graphical representation of the number of NSIs being activated by a transient stimulus in 5 ms bins. fCO signal latencies (magenta) were shorter than tiCS latencies (green) in sensory afferents and NSIs, and the movement-evoked motor response in SETi started before NSIs responded to load signals. Stimulus in **B** corresponds to a forced flexion of the tibia in the resting animal when the leg is suspended in midair (cf. **Ai** & Fig. 3.1 Ai). Data in **C** depicts mean latencies, for detailed data, standard deviation, and number of experiments, see Suppl. Table 3.1. Data was recorded in separate experiments (For more details on NSI response shapes see Büschges, 1990; Sauer et al., 1996; Gebehart et al., 2021 (Chapter 2)).

3.6.4 Absolute Response Timing Delineates a Hierarchy of Sensory Modalities in the Local Network

Normalizing latencies of signals from different sense organs is necessary to delineate and compare a timeline of the processing for multiple types of sense organs and NSIs (Fig. 3.3 A). Normalizing, as was done in Figure 3.2 to establish network connectivity, creates an artificial situation in which all sensory signals reach the central nervous system simultaneously, by deliberately neglecting differences in transmission times from the sense organs in the periphery to the premotor network. To investigate the functional consequences of the timing of sensory signal processing in a behaviorally relevant context, absolute latencies of sensory stimulus-evoked signals in sensory afferents, NSIs, and MNs have to be compared. For this we chose the sensory context of simultaneous elongation of the fCO and activation of tiCS G6A. This sensory context likely mimics a perturbation of the leg suspended in midair, causing a forced flexion of the tibia (cf. Fig. 3.1 Ai, 3.3 Ai, Zill et al., 2011). Aligning the responses of separately recorded neurons to fCO elongation and tiCS G6A activation due to ventral bending of the immobile, resisting tibia along a single timeline depicts the cascade of neural activity in the local network following perturbation (Fig. 3.3 C). fCO afferent signals were the first to reach the neuropil (4.3 ms, cf. Fig. 3.1 D), eliciting the initial wave of changes in NSI membrane potential (Fig. 3.3 C, magenta). tiCS afferent signal transmission through the length of the trochanterofemur was markedly longer (11.8 ms, cf. Fig. 3.1 D). The tiCS signal thus entered the neuropil after the subthreshold response in the ExtTi MN SETi to the fCO stimulus had begun and only 0.5 ms before the MNs suprathreshold response (6.0 ms, 12.3 ms, Fig. 3.3 Ci). The timing of responses in NSIs to load feedback spans a wide range, the earliest starting at 14.5 ms (E9), others initiated as late as 60.6 ms (E3), and

consistently, tiCS G6A inhibition of SETi firing had strikingly long latencies (31.7 ms subthreshold, 48.7 ms suprathreshold, Fig. 3.3 Ci).

The absolute timing of responses in NSIs and the SETi MN to load and movement feedback revealed a staggered processing of multimodal sensory signals in the local network. Movement signals from the fCO arrived and were processed early after stimulus onset, while load signals were processed later and over a wider time range (Fig. 3.3 Cii).

3.6.5 Delayed Effects of Load on Movement-Elicited Resistance Reflexes

The timeline of multimodal sensory processing in the premotor network established in Figures 3.1 and 3.3 demonstrates temporal differences in the processing of load and movement feedback in the range of a few milliseconds. We asked whether this is sufficient to affect motor output and behavior, or if temporal differences would be smoothed and filtered by MN activity and muscle properties. ExtTi MN and muscle responses were analyzed and compared during exclusive fCO, and simultaneous fCO and tiCS stimuli (Fig. 3.4).

Timing and sign of the motor response in the SETi MN, i.e. a fast, fCO elongation-elicited frequency increase and a slow, tiCS G6A-based frequency decrease, predict a time course of the motor response in situations when both signals are elicited concurrently. Absolute latencies and sensory signal transmission times suggest a resistance reflex in the resting animal whose initial response is unaffected by load feedback (Fig. 3.1, 3.3). The effect of tiCS activation should alter SETi MN frequency and ExtTi muscle force in response to fCO stimuli with a temporal delay. We tested these predictions experimentally (Fig. 3.4). An elongation of the fCO combined with a dorsal stimulus targeting tiCS G6B (Fig. 3.4 A) corresponds to the situation demonstrated in Figure 3.3 Aii; elongation combined with ventral stimuli targeting G6A (Fig. 3.4 B-F) corresponds to Figure 3.3 Ai and C. For analysis of SETi MN frequency, load was applied by a ramp stimulus with no hold phase to avoid adaptation to load signals during the hold phase of the movement stimulus (Fig. 3.4 A-C). Activation of tiCS G6B, elicited by dorsally directed bending of the tibia, i.e. a forced extension, increases ExtTi MN frequency in comparison to exclusive movement stimuli (Fig. 3.4 A, Zill et al., 2011). A forced flexion of the tibia by ventrally directed bending activates G6A and decrease ExtTi MN frequency (Fig. 4 Bii, Cii, Zill et al., 2011). Consequently, during the fCO-evoked resistance reflex, the frequency of the excitatory ExtTi MNs SETi and FETi was in- or decreased respectively in the presence of load ($f_{stimulus}$: 1.13 ± 0.19, 0.67 ± 0.15, normalized to $f_{stimulus}$ in i, Fig. 3.4 A, B). In the initial 50 ms of the resistance reflex, however, the frequency was essentially unaltered in both load conditions, albeit slight shifts were observed ($f_{50\ ms}$: 1.05 ± 0.35, 0.93 ± 0.19, normalized to $f_{50\ ms}$ in i, Fig. 3.4 A, B). Similar observations were made in an intracellular recording of the SETi MN (Fig. 3.4 C), where load elicited a delayed hyperpolarization of the membrane potential (Fig. 3.4 Cii, arrow).

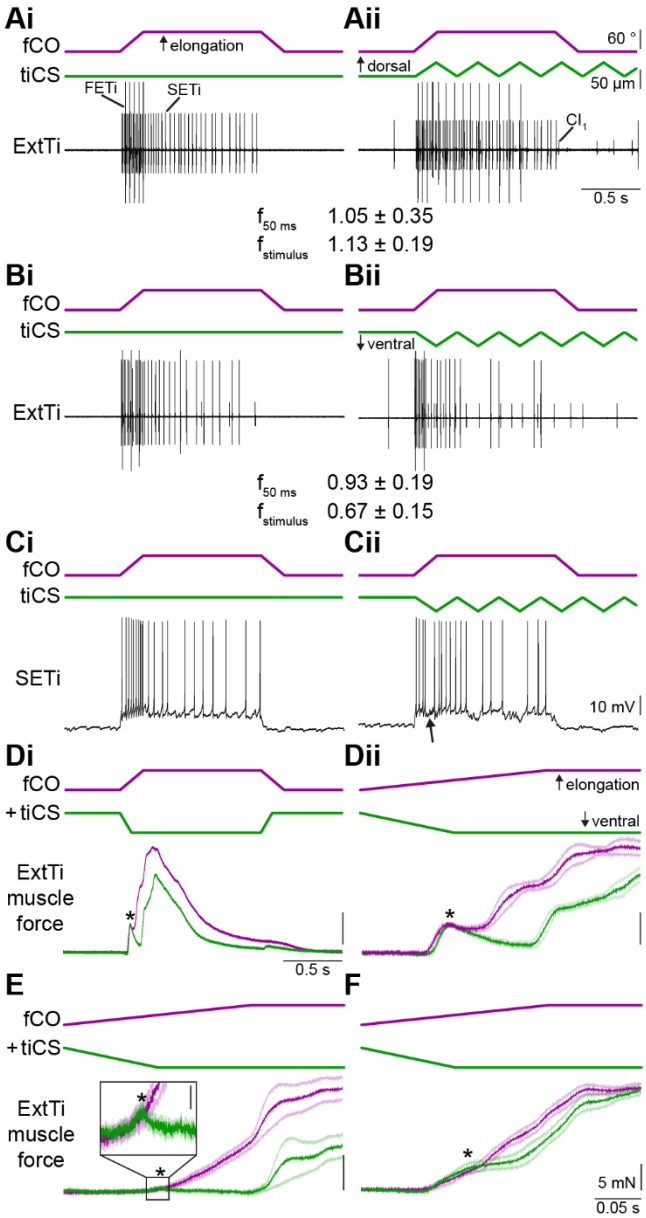

Figure 3.4: Delayed effects of load feedback on movement-elicited resistance reflexes. Exclusive fCO stimulation caused a reflex activation of ExtTi MNs (**Ai**, **Bi**, **Ci**). Excitatory ExtTi MN (SETi, FETi) frequency during the course of the fCO stimulus was increased when tiCS G6B were stimulated simultaneously ($f_{stimulus}$, dorsal stimulation, **Aii**). Concurrently, the frequency was decreased by tiCS G6A stimulation (ventral stimulation, **Bii**). The effect was smaller in the initial 50 ms following ramp onset in both loading conditions ($f_{50\ ms}$). **C**: Delayed effects of load in an intracellular SETi MN recording (arrow: onset of load-evoked inhibition). **Di**: Simultaneous stimulation of tiCS G6A (green) delayed and altered ExtTi muscle force responses to fCO stimuli (magenta). **Dii**: The effect of tiCS stimulation was delayed and interrupted the ongoing fCO-elicited response; enlarged view of **Di**. **E** & **F**: Timing of fCO response onset in muscle force varied between animals, but tiCS response delay was consistent. Inset in **E**: enlarged view. Asterisk: time points at which load began to alter force trajectories (D: 29.9 ms following fCO-evoked response onset, E: 25.2 ms, F: 44.5 ms). Force traces in D-F are waveform averages of 5 consecutive stimuli in individual animals; Di, E, F: horizontal scale as in F, vertical scale: 5 mN; faded traces: standard deviation. For detailed data, see Suppl. Table 3.1.

In the ExtTi muscle, simultaneous stimulation of fCO and tiCS G6A with ramp-and-hold stimuli led to markedly slower and, typically, lower isometric force development in the ExtTi muscle than fCO stimuli alone (Fig. 3.4 Di). The difference in the force trajectories between fCO stimuli with and without load occurred with a delay of 29.8 ms (Fig. 3.4 D-F). Simultaneous occurrence of load signals disrupted movement stimulus-evoked isometric force development in the ExtTi muscle, highlighting the behavioral relevance of sensory signal timing.

3.7 Discussion

The integration of converging multimodal sensory feedback depends not only on spatial, but also on temporal summation. In this study, we analyzed the timing of proprioceptive sensory signals along their sensorimotor pathways in the local network controlling stick insect leg movements. We measured signal transmission times from peripheral sense organs of the same (tiCS / tr/fCS) and between different proprioceptive modalities (load / movement) to the premotor network. We identified short- and long-latency pathways from sense organs to local premotor NSIs and MNs of the FTi joint control loop and the more proximal thorax-coxa joint, providing the connectivity pattern underlying multimodal sensory integration of load and movement feedback in the stick insect local network. The functional connectivity of the premotor network, i.e. the NSI pathways along which signals were processed, changed with the sensory context. The timeline of premotor NSI processing and motor output within the local network constituted a hierarchy of sensory modalities in which movement signals consistently outpaced load feedback, which will be discussed in the following. Functional relevance for network processing and motor output was established by demonstrating the effects of delayed load signaling on the reflex responses of ExtTi MNs and muscle force.

Signal timing in NSIs and MNs determines how signals will be integrated and, ultimately, affect motor control. Knowledge about functional network connectivity is an essential step for understanding circuit function, and the path that a signal takes through the network, i.e. the chain of neurons or computational units along which it is transmitted, will determine how it is shaped and how it will affect the system's output. We will also discuss the behavioral relevance of, relative to each other, fast movement and delayed load signal processing.

3.7.1 Connectivity of Load & Movement Signal Integration in the Local Premotor Network

In the stick insect, load and movement signals are distributed into one set of local premotor NSIs (Gebehart et al., 2021 (Chapter 2)). We extend this view by showing that although both modalities are distributed to all recorded NSIs, distribution is not equal with regard to the latency of NSI responses to sensory inputs, and therefore, network connectivity (Fig. 3.2). Short latencies are indicative of direct, monosynaptic connections between the respective sensory neuron and the postsynaptic neuron, long-latency inputs suggest intercalated interneurons and polysynaptic connections (Berry and Pentreath, 1976). CS and fCO afferents are cholinergic, a transmitter considered to be predominantly excitatory in invertebrates (Florey, 1963; Lutz and Tyrer, 1988). Inhibitory effects on postsynaptic neurons, therefore, will be mediated by polysynaptic pathways. Consistently, all inhibitory responses in NSIs and MNs had long latencies, and were thus concluded to be polysynaptic (Fig. 3.2 Eii). The results were independently confirmed by time-locked event-based connectivity identification of tiCS afferents to NSIs E3, I4, and I3, and a RetCx MN (Fig. 3.2 A -D).

Movement signals from the fCO were transmitted directly to all but one type of NSIs (Fig. 3.5). fCO-evoked response latencies were in the range that was previously described for some of the NSI types analyzed in this study (Sauer et al., 1995, 1996). tiCS and tr/fCS, respectively, targeted only a subset of the recorded NSIs via monosynaptic connections (Fig. 3.5). Monosynaptic connections from the fCO (stick insect) and CS (locust) to unidentified NSIs have been reported (Burrows and Siegler, 1976; Burrows and Pflüger, 1988; Sauer et al., 1995). Interestingly, there was little overlap between the monosynaptically targeted neurons of the two sets of CS (tiCS / tr/fCS, Fig. 3.5). Only NSI E1 was monosynaptically excited by afferents from all three sense organs, which might be the source of the strong phasic excitation E1 receives during the stance phase of walking (von Uckermann and Büschges, 2009).

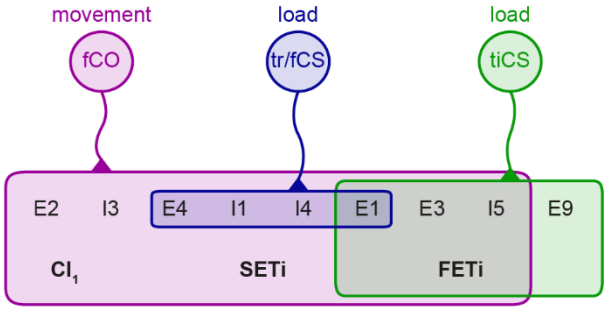

Figure 3.5: Monosynaptic targets of fCO, tr/fCS, and tiCS afferents in the FTi joint control loop. Afferents of the fCO (magenta), tr/fCS (blue), and tiCS (green) formed excitatory monosynaptic, i.e. short-latency, connections with overlapping subsets of NSIs and ExtTi MNs (bold). Most NSIs received direct input from fCO afferents, whereas the monosynaptic receptive fields of tr/fCS and tiCS where smaller. Only NSIs of type E1 were monosynaptically targeted by afferents from all three sense organs. The three ExtTi MNs received direct inputs from fCO afferents, FETi was additionally directly targeted by tiCS afferents.

The pattern of fast, monosynaptic connections from the fCO onto NSIs and MNs, and to a large extent slower, polysynaptic inputs from CS indicates that movement signals might be used for fast initial priming of network action. Load afferents targeted only specific NSIs directly; their main effects were delayed by polysynaptic transmission. Load signals are thus well suited to A) be subject to modulation by intercalated interneurons, and B) to modify and sculpt an ongoing movement response.

3.7.2 Distinct Innervation of Fast & Slow Motor Neurons by Load Afferents

In the locust, load and movement afferents directly target individual MNs via monosynaptic connections (Burrows, 1987a; Burrows and Pflüger, 1988). We found specificity in monosynaptic connections for individual joint control loops, i.e. fCO and tiCS afferents, if at all, directly targeted ExtTi but not RetCx MNs, and vice versa for tr/fCS. ExtTi MNs control movement of the tibia, whose movements and strains are monitored by the fCO and tiCS (Fig. 3.5, Zill et al., 2011; Gebehart et al., 2021 (Chapter 2)). RetCx MNs, by contrast, control movement of the coxa, the strains of which are monitored by tr/fCS (Schmitz, 1993; Akay et al., 2004). Therefore, monosynaptic connectivity between sensory afferents and MNs was joint-specific, whereas the premotor NSI network integrated direct synaptic inputs from all three sense organs.

tiCS afferent showed distinct connectivity to individual ExtTi MNs (Fig. 3.5). We found monosynaptic connections only to the FETi MN, but not to SETi. This corresponds to the situation in the locust hindleg and the fast tibia flexor in *Drosophila melanogaster* (Burrows and Pflüger, 1988; Phelps et al., 2021). We did not distinguish between individual RetCx MNs, but latencies indicated a similar subdivision into short- and long- latency connections. The consistent distinction across insect species of different sizes and specialized behaviors, i.e. flying and high-speed running in *Drosophila melanogaster*, flying and jumping in locusts, walking and twig mimesis in stick insects, indicates that direct connections from load afferents to fast leg muscle MNs could be a general characteristic with functional relevance for insect motor networks and represent species-specific specialization.

3.7.3 The Functional Hierarchy of Multimodal Sensory Integration

Polysynaptic pathways from load afferents to the premotor network constitute a source for modality-specific processing time differences. Another crucial aspect of temporal summation are absolute transmission times from sense organs to the premotor network. Movement signals from the fCO were transmitted to the network faster than load signals (Fig. 3.1). Adding to the delays from polysynaptic pathways, this causes concurrently elicited movement and load signals to reach premotor NSIs with a temporal shift in which load signals are delayed in comparison to movement feedback (Fig. 3.3). The delays constitute a functional hierarchy of sensory integration in which movement outpaces load processing, visible at the level of the motor output (Fig. 3.4). This corresponds to the results of a modeling study in which long delays in positive force feedback stabilized movement control of the mammalian limb (Prochazka et al., 1997).

Note that movement signals being faster than load feedback is not simply an inevitable property emerging from the distal location of tiCS on the leg. tr/fCS are spatially close to the fCO, but temporally their effects were comparable to tiCS, as was observed in this and a previous study on femoral CS (Akay and Büschges, 2006). Independent of the location on the leg at which load is perceived, and even considering that strain is transmitted along the cuticle to the most proximal tr/fCS faster than tiCS neuronal transmission (Höltje and Hustert, 2003), signal transmission of movement feedback will be faster and the initial motor response will be based on movement signals. The delay was not circumvented by monosynaptic connections from sensory afferents to MNs, since no short-latency connections from CS to SETi were found and load inputs to FETi are usually not sufficient to evoke supra-threshold responses (Gebehart et al., 2021 (Chapter 2)).

Under natural conditions, movement and load stimuli rarely occur separately. Based on the functional hierarchy between sensory modalities we present in this study, the initial motor response to a perturbation will be based on movement signals alone. The later arrival, and broader time range, of load signals is well suited to tune ongoing activity and put a fast movement response into a sensory context,

e.g. by dampening a resistance reflex to a persistent forced flexion to avoid damage to the cuticle (Fig. 3.4 B, C). In a stick insect in the bushes, a passing external perturbation, e.g. a wind-blown leaf, causing tibial flexion of a leg suspended in midair will elicit only weak load feedback, while the movement signals about tibial bending will elicit a resistance reflex. If the perturbation is mediated by a persistent force, e.g. a solid branch, load feedback will not alter the early initial movement-evoked reflex response. It will, however, dampen the ongoing response, so that forces too large to be overcome by the stick insect leg are not resisted futilely to the point of breaking (Zill et al., 1981).

Fast movement feedback contextualized by load signals will likely also have implications for walking and the transitions between stance and swing phases. Load feedback has been suggested as a cue for the transition from swing to stance, and, via CS signaling unloading, for swing initiation (Newland and Emptage, 1996; Noah et al., 2001; Akay et al., 2004; Akay et al., 2007). In insects, the relevance of gravity for leg movements is negligible in comparison to passive muscle forces and the activity of the antagonistic muscle (Hooper et al., 2009). It is therefore necessary to consider the onset of muscle activity, not kinematic changes, for analyzing the effects of sensory signals on phase transitions (discussed in Rosenbaum et al., 2010). Activity of stance phase muscles, however is initiated *before* or very briefly after touchdown of the leg, leaving not enough time for load sensors signaling ground contact to assist in the transition of muscle activity. Interestingly, when the levator trochanteris induces unloading, other swing muscles are activated with a latency of 40 ms (Rosenbaum et al., 2010). Admitting for the time from levator muscle EMG activity to force development and actual movement (Hooper et al., 2007), this fits very well into the range of CS latencies we report here. Surprisingly consistent, given the differences in muscle size and signal conduction velocities between invertebrates and vertebrates, cats show a difference in the muscle activity of the stepping pattern when stepping into an unexpected hole only 30 ms after ground contact should have occurred, indicating that this would have been the time at which the effects of load signaling would normally take place (Gorassini et al., 1994).

Taken together, these findings lead to the conclusion that signals about leg loading and unloading during touchdown and liftoff, respectively, can support ongoing muscle activity during stance and activation of muscles during the initiation of swing phase. The precise cues mediating the initiation of muscle activity, however, are more likely to originate from movement sensors. Our results are supported by studies on the timing of muscle activation during stepping phase transitions (Rosenbaum et al., 2010; Schmitz et al., 2015). The long delays of some load signals, (e.g. 60.6 ms, E3, Fig. 3.3 C) might even serve as a form of extreme short-term memory or delay line (cf. Hedwig and Sarmiento-Ponce, 2017) for comparing past load signals with more recently experienced movement feedback.

3.7.4 The Functional Connectivity of Premotor Interneuron Processing

In vertebrates and invertebrates alike, studies have shown the transmission of proprioceptive signals to distinct populations of interneurons or MNs (Siegler and Burrows, 1983; Tuthill and Wilson, 2016b; Imai and Yoshida, 2018). Interneurons may, however, process the same type of sensory information transmitted along different pathways, i.e. intra-populational connectivity might vary. Inherent in the concept of distinct, distributed pathways involving different (numbers of) neurons is the assumption that the same sensory signal will be subjected to different computations before reaching individual elements of the network. A signal may therefore be distributed onto a population of interneurons, but distinguishing between mono- and polysynaptically pathways is crucial for the interpretation of a signal as being either preprocessed, and shaped by network activity, or as direct, and comparably unbiased by the neuronal properties and the context of the surrounding neuronal activity. Note that we are not considering presynaptic inhibition here, which will act on both cases (Clarac and Cattaert, 1996). We emphasized this distinction by categorizing local premotor NSIs as 1st or higher order neurons and establishing a functional hierarchy of premotor NSIs for a given sensory context (Fig. 3.3 A). According to this classification, unlike higher order NSIs, a 1st order NSI receives monosynaptic, thus relatively raw and unprocessed, signals from sensory afferents.

The functional connectivity of most NSIs, i.e. whether they were 1st or higher order neurons, changed with the sensory context. Sensory context refers to the precise subsets of sensory afferents being active: tiCS G6A or 6B, fCO afferents signaling elongation or relaxation. Altered functional connectivity has consequences for how a signal is shaped by the premotor network: The earlier in the processing cascade a signal passes through a given NSI, the more effect its influences on signal shape, sign, and information content, will have on downstream processing units. Future studies may reveal how the individual properties of a given NSI, and its position within the processing hierarchy, tune downstream signal processing, and what consequences sensory context-dependent functional connectivity has for motor output and behavior.

A noteworthy exception from the flexible positioning of NSIs within the processing hierarchy were the stable NSIs I3, I4, and E4, whose position was not altered, independent of the sensory context. Interestingly, these NSIs share other characteristics. They coordinate movements around several joints via postsynaptic effects on multiple MNs pools, not only the FTi joint (Büschges, 1990; Büschges et al., 1994; Büschges, 1995; Sauer et al., 1996; Gebehart et al., 2021 (Chapter 2)). E4 and I4, besides the sensory allrounder E1, and potentially I1, belonged to the NSIs monosynaptically targeted by tr/fCS, which integrate load acting on the entire leg (Fig. 3.2, discussed in Höltje and Hustert, 2003; Akay et al., 2004; Zill et al., 2012). No direct connection was found from tr/fCS to I3, but this might be due to a lower sampling number. The similarities between sensory connectivity to and downstream MN targets

of the stable NSIs, in addition to their fixed position in the functional hierarchy, and the fact that E4 and I4 play crucial roles in walking and searching behaviors, respectively (Büschges, 1995; Berg et al., 2015), might indicate that these NSIs play specific roles in the premotor network, e.g. by being involved in higher level processing and the recruitment of muscle synergies (see also Zill et al., 2015), as opposed to other NSIs putatively serving mainly as signal integrators for single leg joints.

The functional role of these NSIs, especially the only recently characterized I3, will have to be subject to further investigations. Furthermore, synaptic connections between NSIs, as they were found here and in a previous study, suggest the existence of layers within the NSI network, which in the past has been considered as a single computational layer within the network (Burrows, 1979; Burrows, 1996). Resolving this problem will necessitate more information about the interconnectivity between individual NSIs, which will also shed light on the details of 1st order NSIs "priming" higher order NSIs (and their processing) for the sensory input to come. Load and movement stimuli will have to be combined to investigate the interaction of concurrent sensory signals in the NSIs, and how delayed load signals affect movement signal transmission. Finally, it will have to be examined whether the hierarchy of sensory modalities scales with the size of the insect. To identify common principles, it will be necessary to determine whether signal transmission times and delays play the same role in the nervous systems of 8 cm long *Carausius morosus* as in those of 30 cm long *Ctenomorpha gargantua* (Hasenpusch and Brock, 2006) or 0.3 cm long *Drosophila melanogaster*.

4 Gain Control in Multimodal Proprioceptive Processing

4.1 Gain Control in Sensorimotor Processing – Nonlinear Integration of Load & Movement Proprioceptive Feedback in the Premotor Network of an Insect Leg

Gebehart, C., Büschges, A.

In Chapter 4, the interaction of multimodal proprioceptive signals from load (tiCS) and movement (fCO) sense organs is analyzed. The findings of Chapters 2 and 3, specifically the spatial summation of load and movement signals that occurs with a temporal delay, led to the hypothesis of ongoing movement signal processing being tuned by delayed load feedback. This hypothesis was tested in Chapter 4, and the effects of load feedback on movement signal processing are traced throughout the network, from presynaptic sensory afferent interactions via nonlinear summation in local NSIs to changes in the gain of the motor output. The study thereby establishes a local mechanism for context-dependent multi-modal proprioceptive processing.

Sensory afferents, NSIs, and MNs were stained for morphological characterization. Exemplary stainings of recorded neurons are shown in Figure 2.4 and Supplementary Figure 2.1.

4.2 Author Contributions

Conceived & designed experiments:

Corinna Gebehart, Ansgar Büschges

Performed experiments, analyzed data & prepared figures:

Corinna Gebehart

Interpreted experimental results:

Corinna Gebehart, Ansgar Büschges

Drafted, edited & revised manuscript:

Corinna Gebehart

4.3 Abstract

An animal's sense of proprioception emerges from the integration of multiple sensory modalities. To enable appropriate motor responses to multimodal, externally or internally generated, sensory signals, the local network controlling leg movement must combine feedback from distinct sensory structures. In the stick insect, two main proprioceptive senses, i.e. load (tiCS) and movement (fCO), are integrated within a network of premotor NSIs to shape motor output. In this study, the interaction of fCO and tiCS signals was traced from the sensory afferents, through the premotor network, to the motor output and resulting muscle forces. The aim was to determine whether, and how, movement signal processing is altered in the presence of load. Movement signal gain was reduced at the earliest neuronal stage by presynaptic inhibition. tiCS stimulation elicited primary afferent depolarizations (PADs) and reduced action potential amplitude in fCO afferents. In the postsynaptic antagonistic network of premotor NSIs, combined sensory feedback was summed nonlinearly, with load altering the gain of movement signal responses. Notably, the gain of NSIs opposing the resistance reflex of the SETi MN in response to fCO elongation was increased. Consistently, SETi MN gain in response to movement stimuli was decreased in the presence of load. The effects on individual ExtTi MNs were movement parameter- and neuron-specific. Changes in sensorimotor gain were dependent on presynaptic inhibition; the dependence of movement signal gain on the presence of load signals in the SETi MN was abolished by pharmacologically blocking presynaptic inhibition. The effects of sensorimotor gain control mediated by presynaptic inhibition are shown at the sensory, interneuronal, and motor output level of the network. The results thereby demonstrate a mechanism by which a local premotor network can implement context-dependent proprioceptive processing based on the presence, or absence, of specific sensory feedback. The findings broaden our understanding of how the nervous system integrates multiple sensory modalities to create an internal representation of the state and position of the body and its limbs in space.

4.4 Introduction

All biological, and indeed also non-biological, neural networks face the task of combining signals from distinct input sources, to process them, and, ultimately, to generate an appropriate output. In motor control, e.g. locomotor networks, the input includes signals from central networks, from other regions of the nervous system, and sensory signals about self-generated feedback (proprioception) and the external world (exteroception; Bidaye et al., 2018; Grillner, 2021). In legged animals, the various signals are combined, integrated, and contextualized by premotor networks to coordinate walking, but also to generate and maintain posture against gravity and other external perturbations (Burrows, 1996; Deliagina et al., 2012; Grillner and El Manira, 2020).

To prevent this barrage of signals from various sources from flooding the network with information that is not relevant in the given context, signal gain needs to be controlled. Abolishing gain control destabilizes motor systems and leads to motor oscillations, as was shown in goal-directed reaching in mice (Fink et al., 2014). Multiple functions for gain control in sensorimotor systems have been discussed, including, though not limited to, stabilization of MN activity, gating of self-generated feedback, and increased precision of online motor control by strengthening of relevant feedback (Azim and Seki, 2019).

Controlling the gain of sensory feedback by either increasing its influences or dampening them, results in optimized network performance and a more precise motor output (McComas, 2016). However, what can be counted as optimized performance of a motor network strongly depends on the context in which the resulting motor output will occur. Gain control therefore needs to be context-dependent and specific. Consequently, presynaptic modulation of sensory afferent activity depends on the behavioral context, for example, locomotion, in the premotor networks of vertebrates (Koch et al., 2017), and invertebrates (Wolf and Burrows, 1995).

Sensory signals that are crucial for skilled walking and posture control originate from load and movements sensors in the limbs, i.e. Golgi tendon organs and muscle spindles, respectively, in vertebrates (Jami, 1992; Windhorst, 2007; Santuz et al., 2019; Grillner, 2021), and CS and chordotonal organs in insects (Field and Matheson, 1998; Zill et al., 2004; Tuthill and Wilson, 2016a; Bidaye et al., 2018). The role of these proprioceptive sense organs, in vertebrates and insects alike, is to provide the local motor networks in the spinal or ventral nerve cord with information about joint movement and position (muscle spindles & chordotonal organs), and about forces acting on the limbs, e.g., imposed by body weight, resisted muscle forces, or external perturbations (Golgi tendon organs & CS; Pearson, 1995a).

Conceptually, load and movement signals are considered separate sensory modalities. Under most natural circumstances, however, they are likely to occur simultaneously. A clear example is the stance

phase of walking, when the leg pushes against the ground to propel the body in the direction of walking, but simultaneous activation also occurs when an external perturbation exerts pressure onto an originally stationary limb (Schmitz, 1993; Zill et al., 2004; Büschges et al., 2008). Signal integration and multimodal processing require the premotor networks to consider movement *in the context* of load feedback, and vice versa.

Load and movement sensory feedback are combined by local networks. A recent study on the premotor network of the stick insect leg found signals from the fCO (movement) and distinct groups of CS on the leg (load) to be integrated by a single distributed network of local premotor NSIs (Gebehart et al., 2021 (Chapter 2)). In the same motor system, load and movement signals have been shown to interact at the level of the motor output. Specifically, the strength of movement reflexes is altered in the presence of load (Schmitz and Stein, 2000; Gebehart et al., 2021 (Chapter 2)). Load feedback additionally alters the likelihood of occurrence of reflex reversals, a dramatic shift in sensory processing in which the resistance reflex in a resting animal is switched to an assistance reflex during active movements (Akay and Büschges, 2006). Reflex reversal occurs in various species (e.g. Forssberg et al., 1975 (cat); Bässler, 1976 (stick insect); De Serres et al., 1995 (human)). Detailed studies on the stick insect leg motor system revealed that it involves changes in sensory processing in multiple elements of the motor network (Driesang and Büschges, 1996; Hellekes et al., 2012). The fact that load signals shift the network balance towards an active reaction is indicative of a more complex integration of load and movement feedback than simple signal summation. This is supported by a study that found presynaptic inhibition of fCO (movement) afferents mediated by stimulation of tr/fCS (load) (Stein and Schmitz, 1999).

Based on the existing knowledge about multimodal proprioceptive integration in local networks, including presynaptic inhibition between multimodal sensory afferents, and the function of presynaptic inhibition as a mediator for sensory gain control in motor systems, we investigated and traced the interplay of load and movement signals throughout the accessible and well-studied premotor network of the stick insect leg (reviews in Bässler and Büschges, 1998; Büschges et al., 2008; Fink et al., 2014; Azim and Seki, 2019). We hypothesized that load signals are used by the local premotor network to infer the context of simultaneously occurring movement feedback, and to adapt the latter's processing.

Using the stick insect FTi joint control loop, we specifically asked whether load feedback from tiCS can change the gain of movement reflexes induced by fCO stimulation. We traced the interaction of these load and movement signals from the earliest neuronal stage, i.e. presynaptic sensory inhibition, via nonlinear summation and neuron-specific gain control in the downstream network of NSIs, to the motor output of ExtTi MNs and muscle force. We show that motor output gain was movement parameter-

and MN-dependent. Pharmacologically blocking presynaptic inhibition established a causal link between the effects at in- and output sites of the network. By tracing multimodal signal interaction along the entire processing pathway, i.e. sensory afferents, interneurons, and MNs, our study provides a mechanism by which a small, local network can implement context-dependent processing of proprioceptive feedback.

4.5 Materials & Methods

4.5.1 Animals

Experiments were conducted on adult female stick insects, *Carausius morosus*, from the parthenogenetic colony at the University of Cologne. The colony is kept at 22 – 24 °C, 50 % humidity, 12 h light / dark cycle, and fed with blackberry leaves.

4.5.2 Dissection

Animals were dissected as described in a previous study (Gebehart et al., 2021 (Chapter 2)). In short, all legs except for the right mesothoracic leg were removed; the thorax-coxa, coxa-trochanter, and FTi joints were immobilized at 90 ° angles using light curing glue (3M ESPE Sinfony, Neuss, Germany) and a minuten pin inserted into the ventral trochanter. The animal was pinned to a platform, the distal femur glued to the edge with the tibia protruding from the platform. The mesothoracic ganglion was exposed by a dorsal midline incision; all lateral nerves except for the ipsilateral ncr and nl3 were squeezed (nomenclature according to Marquardt, 1940).

For intracellular recordings, the ganglion was pinned with cactus spines on a wax-coated steel platform (cf. Büschges, 1990; Driesang and Büschges, 1993). The ganglion sheath was softened with Pronase E crystals (VWR, Darmstadt, Germany). The body cavity was rinsed and filled with extracellular saline (178.54 mM NaCl, 17.61 mM KCl, 7.51 mM $CaCl_2$, 25 mM $MgCl_2$, 10 mM HEPES buffer, set to pH 7.2 with NaOH, Weidler and Diecke, 1969). All experiments were performed in inactive, resting animals (as defined in Bässler, 1993).

4.5.3 Electrophysiological Recordings

Intracellular sharp microelectrodes (35-45 MΩ) were made from borosilicate glass capillaries (8GB100TF-8P, Science Products, Hofheim, Germany) using a micropipette puller (P-1000, Sutter Instruments, Novato, CA, USA) and contained a chlorinated silver wire. Electrodes were filled with intracellular saline (1M KAc, 0.1 M KCl). 5 % neurobiotin tracer was added for morphological neuron identification (for staining and fixation procedure, see Berg et al., 2015; Gebehart et al., 2021 (Chapter 2)).

Intracellular signals were recorded from arborizations of NSIs and MNs in the medio-dorsal neuropil of the ipsilateral hemiganglion, and from arborizations of sensory afferents at the point where the ncr

enters the ganglion. Intracellular signals were compensated for interstitial potential (5-20 mV, Dörr et al., 1996), and amplified (gain x20, highcut filter 3 kHz, SEC-06 preamplifier, SEC-10LX single electrode clamp amplifier, npi, Tamm, Germany). Extracellular signals of ExtTi MNs were recorded with a hook electrode from nerve F2 within the femur (Schmitz et al., 1988), and amplified (gain x2000, lowcut filter 0.3 kHz, highcut 2.5 kHz, notch filter 50 Hz, MA101 preamplifier & MA102 differential amplifier, Electronics Workshop, University of Cologne). All signals were digitized and stored with Spike2 software (sampling rate 12.5 kHz for extracellular, 6.25 kHz for intracellular signals, ADC Micro1401 mkI, Spike2 v7.16, CED, Cambridge, UK).

4.5.4 Mechanical Sensory Stimulation

The fCO was stimulated by opening the dorsal proximal femur, clamping, and moving the receptor apodeme (cf. Hofmann et al., 1985; Büschges, 1989). Receptor elongation mimics tibial flexion (upward deflection of stimulus trace in the following figures), vice versa for receptor elongation. Ramp-and-hold fCO stimuli in experiments where stimulation amplitude was altered had a consistent ramp velocity of 300 °/s. Ramp-and-hold fCO stimuli where stimulation velocity was altered had a consistent hold amplitude of 60 °, corresponding to 300 µm elongation of the receptor apodeme (Weiland and Koch, 1987).

tiCS were stimulated by a metal probe that pushed the proximal tibia into a ventral or dorsal direction by 50 µm in all stimulus paradigms, activating G6A or G6B, respectively (Zill et al., 2013). In the following figures, an upward deflection of the stimulus trace denotes an increase in load, a downward deflection the return to control condition without load stimulus. Ramp-and-hold tiCS stimuli had rise and fall times of 0.1 s each, with a hold phase of 1 s in between. Triangle tiCS stimulus rise or fall ramp duration was 0.17 s without a hold component to avoid adaptation and was used as a continuous stimulation in experiments with fCO stimuli of increasing amplitudes or velocities. The order of exclusive movement and combined load and movement stimuli was varied to exclude adaptational effects.

Sinusoidal waveform stimuli of the fCO and tiCS had a frequency of 0.7 Hz, a maximum amplitude of 60 ° or 50 µm, respectively, and consisted of 15 continuous cycles. Intervals between all types of stimuli were at least 2.6 s long. The time within stimulation paradigms between different stimulus velocities or amplitudes was at least 10 s during which neither tiCS nor the fCO were stimulated. Mechanical stimulators were controlled by Spike2 or a digital stimulator (MS501) and moved by custom-built linear motors (lowpass filter 1 kHz, VCM Controller/Power Amplifier, Electronics Workshop, University of Cologne).

4.5.5 Muscle Force Measurement

ExtTi isometric muscle contraction force was measured with a force transducer (ALS, Aurora 300 B dual-mode lever system; Aurora Scientific Inc., Ontario, Canada, resolution 0.3 mN), digitized, and stored (sampling rate 6.25 kHz, ADC Micro1401 mkl, Spike2, CED). ALS force level was set above the maximum muscle force to maintain constant muscle length. The most distal, dorsal part of the femur was cut open. The cuticular attachment site of the ExtTi muscle tendon was detached from its insertion in the FTi joint and fixated with a hook-shaped minuten pin that was attached to the ALS lever arm. Force offset was determined with the pin in position before the muscle tendon was attached. Stimulus runs with FETi MN activity were excluded from analysis.

4.5.6 Pharmacology

To block presynaptic inhibition, the ganglion was superfused with the noncompetitive $GABA_A$ (γ-aminobutyric acid A) receptor antagonist picrotoxin (PTX, Sigma-Aldrich, cf. Sauer et al., 1997). Starting concentration was 0.03 mM, incomplete removal of extracellular saline from the body cavity prior to drug application led to further dilution. An increase in ExtTi MN frequency was used as an indicator for the effect of PTX. Stimulations were started when MN frequency had reached a constant level, approx. 10 min following drug application. Both stimulus paradigms, i.e. movement stimuli with or without simultaneous load stimulation, were analyzed before and after application of PTX and compared within each condition. PTX effects on the gain of velocity dependence were not tested. PTX abolishes velocity dependence in the system, potentially because blocking presynaptic inhibition causes the gain of velocity information in the system to saturate (cf. Sauer et al., 1997; Stein et al., 2006).

4.5.7 Neuron Identification

Local premotor NSIs were identified as nonspiking if no action potentials were elicited by current injection, tactile or sensory stimulation, and by subthreshold effects on MNs (Hengstenberg, 1977). Individual types of NSIs were identified based on their excitatory or inhibitory effects on ExtTi MNs, and their responses to fCO ramp-and-hold stimuli (Büschges, 1990; Sauer et al., 1995). Sensory afferents were identified by their responses to sensory stimuli. Current injection into the neuropilar arborizations of these neurons fails to alter their action potential frequency. ExtTi MNs were identified by the time-locked relationship between intracellularly and extracellularly recorded action potentials. Identities of the different types of neurons were verified by their morphology.

4.5.8 Data Analysis

Activation of tiCS subgroups G6A and B by ventral and dorsal tibial bending, respectively, has differential effects on the firing rate of ExtTi MNs, i.e. inhibition by G6A and excitation by G6B (Zill et al., 2011). The subgroups showed no differential effects on the gain of NSIs and ExtTi MNs, therefore results were

pooled. For linear summation of NSI responses to sinusoidal stimuli, the offset of 15 sweeps of responses to exclusive fCO and tiCS stimulation was removed and response traces to fCO and tiCS stimuli were summed. Changes in gain were tested by incremental increases of fCO ramp-and-hold stimulus amplitude or velocity with or without concurrent triangle stimuli to tiCS.

The initial ramp-and-hold fCO stimulus of each tested amplitude or velocity started simultaneously with the triangle tiCS stimulus, which, in experiments with intracellularly measured changes in membrane potential, consistently led to outliers and was thus discarded. Only responses to the following 4 ramp-and-hold stimuli were included in these analyses. This effect was not observed in experiments were extracellularly measured action potential frequencies were analyzed, thus all 5 ramp-and-hold stimuli were included.

Changes in membrane potential to increasing stimulus amplitudes were measured as the average change from resting potential during the hold phase of the fCO stimulus. For increasing stimulus velocities, depending on the overall response direction of the neuron, the maximum or minimum change from resting potential during the rising ramp of the fCO stimulus was analyzed. For analysis of action potential frequencies, we used the average frequency during the hold phase (increasing stimulus amplitude) or the rising ramp (increasing stimulus velocity). We did not distinguish between action potentials from the slow and fast ExtTi MNs (SETi, FETi) in analysis of extracellular activity, since suprathreshold responses of FETi to fCO ramp-and-hold stimuli were much sparser than those of SETi, thus the bulk of the effect will be based on SETi activity, with FETi having little to no effect on the analyses. Within one recording, only stimulus runs with similar baseline levels of MN firing frequencies were compared. Action potentials of the CI_1 MN were extracted from extracellular F2 recordings by spike sorting. CI_1 is not reliably active during the hold phase of ramp-and-hold stimuli, thus only its velocity-dependence during ramps could be analyzed.

We chose linear fits for our data, as they yield a more intuitive read-out of the slope, i.e. gain, of a curve than sigmoidal curves, although the latter is typically more realistic for most physiological data. The parameters tested were chosen because they lie well within the dynamical range of the FTi control loop, and thus in the linear range of the sigmoidal curve (Weiland and Koch, 1987). Linear fits are thus a sufficiently precise estimation for the purposes of this study and will, at worst, underestimate any effects reported here. In Figure 4.3, only data from linear fits whose R^2 value is equal or greater than 0.6 were included. In all figures, N refers to the number of animals, n to the number of stimulus runs. For each recording, the data of no more than one stimulus run of increasing amplitude and velocity, respectively, were included in the analysis. Significance was tested with paired t-tests, significance levels: * 0.05, ** 0.01, *** 0.001. All analyses were done in Matlab (R2020a, Mathworks).

4.6 Results

4.6.1 Local Sensorimotor Pathways for Load & Movement Signal Processing

Load feedback provided by tiCS and movement feedback from the fCO constitute two major sources of proprioceptive information in the FTi control loop. Besides monosynaptic connections from sensory afferents to MNs, signals are transmitted from sensory afferents to local premotor NSIs, which in turn have excitatory or inhibitory effects on the SETi MN (Fig. 4.1; Büschges, 1990; Burrows, 1996; Gebehart et al., 2021 (Chapter 2)). Some NSIs additionally affect the fast ExtTi MN (FETi), or the CI_1 MN. If load or movement stimuli are presented individually, sensory afferent and MN firing frequency and NSI membrane potential are accurate neuronal representations of stimulus shape and distinct parameters such as velocity or amplitude. Sensory afferents of tiCS G6A and G6B and the fCO, and their downstream neuronal partners were able to follow ramp-and-hold, continuously changing sinusoidal waveform, or triangle stimuli (Fig. 4.1).

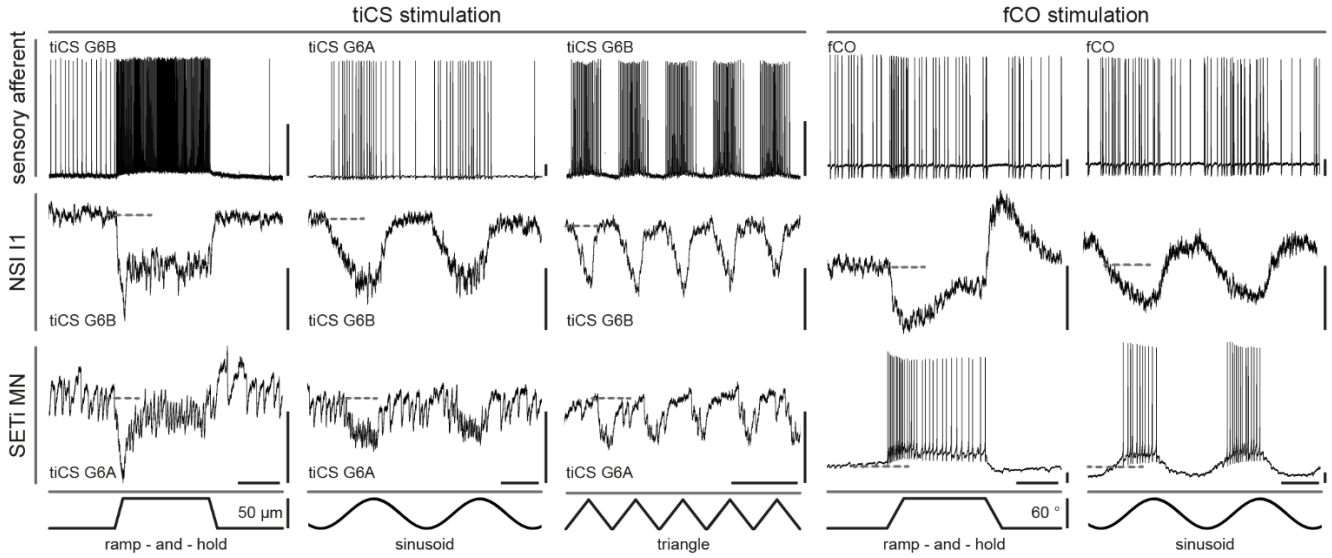

Figure 4.1: Local sensorimotor pathways for load (tiCS) and movement (fCO) signal processing. Intracellular responses of fCO, tiCS G6A, and tiCS G6B sensory afferents (1st row), an exemplary NSI (I1, 2nd row), and the SETi MN (3rd row) to distinct mechanical simulation of tiCS (1st – 3rd column) and the fCO (4th & 5th column). tiCS subgroups were stimulated by ventral (G6A) or dorsal (G6B) bending of the tibia; stimulated subgroups are indicated in the respective panels. 1st row: indicated stimulated tiCS subgroup also denotes recorded afferent identity. Responses of G6A and G6B were qualitatively similar apart from opposing directional sensitivity. Bottom row, stimulus traces: upward deflection indicates fCO elongation (flexion), or increased ventral (G6A) or dorsal (G6B) tibial bending. Dashed line: NSI / MN resting membrane potential. Scale bar: 0.5 s / 5 mV. (For more details on the diversity of NSI responses to multimodal stimuli, see Gebehart et al., 2021, Chapter 2.)

4.6.2 Presynaptic Inhibition from Load onto Movement Sensory Afferents

Unlike the controlled experimental settings presented in Figure 4.1, proprioceptive feedback from load and movement sense organs rarely occurs separately under natural conditions. Temporal and spatial coincidence of signals in the premotor network could therefore lead to nonlinear interaction, i.e. signal processing and transmission of one modality being altered in the presence of the other. Presynaptic inhibition can be used by the nervous system to control the gain of sensory signals when they enter into the premotor network (Clarac and Cattaert, 1996; Rudomin and Schmidt, 1999; Fink et al., 2014). Gain refers to the slope of the stimulus-response curve, in other words, the ratio between signal input and output. Intracellular recordings from neuropilar arborizations of fCO afferents showed altered firing frequencies, PADs, and a reduced normalized action potential amplitude (0.985 ± 0.007, N = 5) when presented with movement stimuli (Fig. 4.2 A). The latter two are considered hallmarks of presynaptic inhibition, confirming previous findings on presynaptic interactions between fCO afferents themselves (Burrows and Matheson, 1994; Sauer et al., 1997). Stimulation of tiCS in the same recording did not alter firing frequencies in fCO afferents, but elicited PADs and caused a reduction in normalized fCO afferent action potential amplitude (0.986 ± 0.009, N = 5, Fig. 4.2 B). Presynaptic inhibition from load-sensing tiCS thus altered movement signal gain in fCO afferents via presynaptic afferent inhibition.

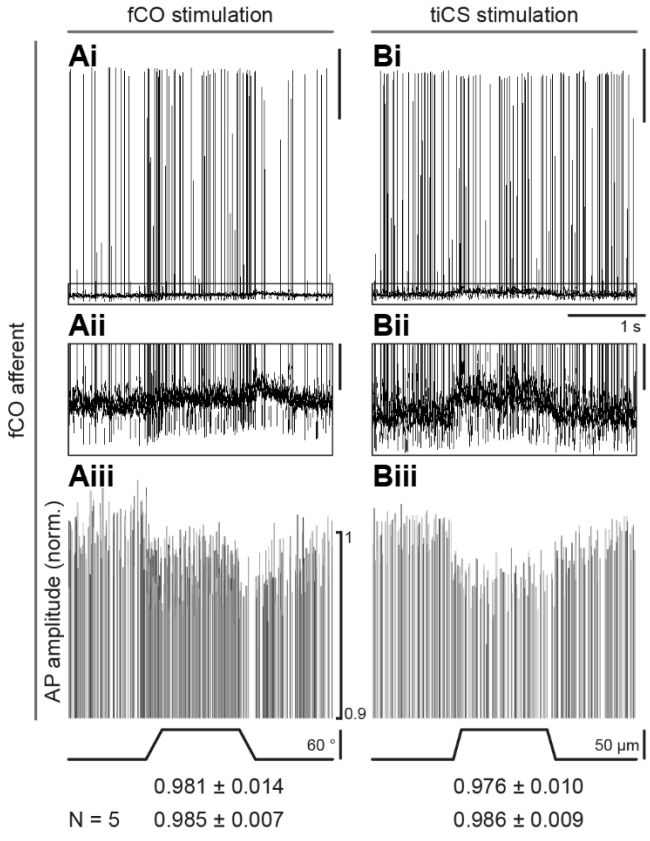

Figure 4.2: Presynaptic inhibition of movement (fCO) sensory afferents induced by movement (fCO) and load (tiCS) stimulation. Intracellular recording of a fCO sensory afferent during fCO (**A**) and tiCS (**B**) stimulation. fCO afferent action potential (AP) frequency was altered by fCO but not during tiCS stimulation (**i**). Both types of stimuli elicited PADs (**ii**, enlarged view of inset shown in **i**), and reduced AP size (**iii**). Data in **iii** normalized to the average AP amplitude in the 1 s interval previous to stimulation. All panels show data from the same fCO afferent, 5 sweeps of consecutive stimuli overlaid in each panel. Bottom rows: Effect size of AP amplitude reduction for this neuron (top) and for N = 5 (bottom, pooled results for G6A & G6B stimulation). Scale bar: 20 mV (**i**), 2 mV (**ii**), **iii** as given in **Aiii**, time scale in **Bi**.

4.6.3 Nonlinear Summation & Neuron-specific Gain Modulation in Nonspiking Interneurons

Sensory afferents of the fCO are mono- and polysynaptically connected with a population of individually identifiable local premotor NSIs that integrate both load and movement signals (Büschges, 1990; Sauer et al., 1996; Gebehart et al., 2021 (Chapter 2)). Presynaptic interactions between load and movement sensory afferents will therefore directly affect signal integration and processing in NSIs. Sinusoidal waveform stimulation targeting exclusively the fCO or tiCS elicited distinct responses in NSIs (Fig. 4.3 Ai-Ci, top row, cf. Fig. 4.1). Stimulation of both sense organs at the same time and with the same phase led to summed responses in NSIs. Summation of load and movement signals was nonlinear (Fig. 4.3 Ai-Ci bottom row, total N = 20), as would be expected by the interaction of both signals in the sensory afferents presynaptic to the NSIs (Fig. 4.2). Note that individual sinusoidal load stimuli did not elicit a response in the recording of NSI E2 (Fig. 4.3 Ai, top right), but responses to combined stimuli differed from those to exclusive movement stimulation.

To identify changes in sensory gain, or parameter dependence, we tested the NSIs' responses to movement stimuli of increasing amplitude (Fig. 4.3 Aii, Bii) or velocity (Fig. 4.3 Cii) in the presence and absence of triangle waveform load stimulation (cf. Fig. 4.1). Triangle stimuli were used to maintain an ongoing presence of load signaling within the network, and no effects of adaptation were found in control tiCS afferent intracellular recordings for the duration of the applied stimulus paradigms (n = 2, not shown). Individual NSIs show different degrees of amplitude and velocity dependence which, in the range applied in this study, can be approximated by a linear relationship between movement stimulus parameter and NSI membrane potential (Weiland et al., 1986; Büschges, 1990; Sauer et al., 1996). Figure 4.3 shows examples of NSIs in which the gain of movement signal responses, i.e. the slope of the linear curve fitted to the change in membrane potential, was increased (Aii), decreased (Bii), or even reversed (Cii) in the presence of load feedback. In some NSI recordings with clear movement stimulus amplitude dependence, the change in gain could be correlated with the waveform of the nonlinearly summed response. The same neuron that showed an increase in response gain (Fig. 4.3 Aii) also showed an increased amplitude in the summation experiment (Ai), while a decrease in gain in a different NSI coincided with a summation that was smaller than its constituent parts (Fig. 4.3 B). Movement signal gain was up- or downregulated depending on NSI type and movement parameter (Fig. 4.3 D, 1st column, N = 23).

All NSIs studied here either in- or decrease activity in the SETi MN. Load and movement signal processing in this network is distributed and antagonistic, meaning that each NSI's response to a given sensory stimulus either supports (+) or opposes (-) the ExtTi MNs' response to the same stimulus (Büschges, 1990; Sauer et al., 1996; Gebehart et al., 2021 (Chapter 2)). We categorized NSIs using this

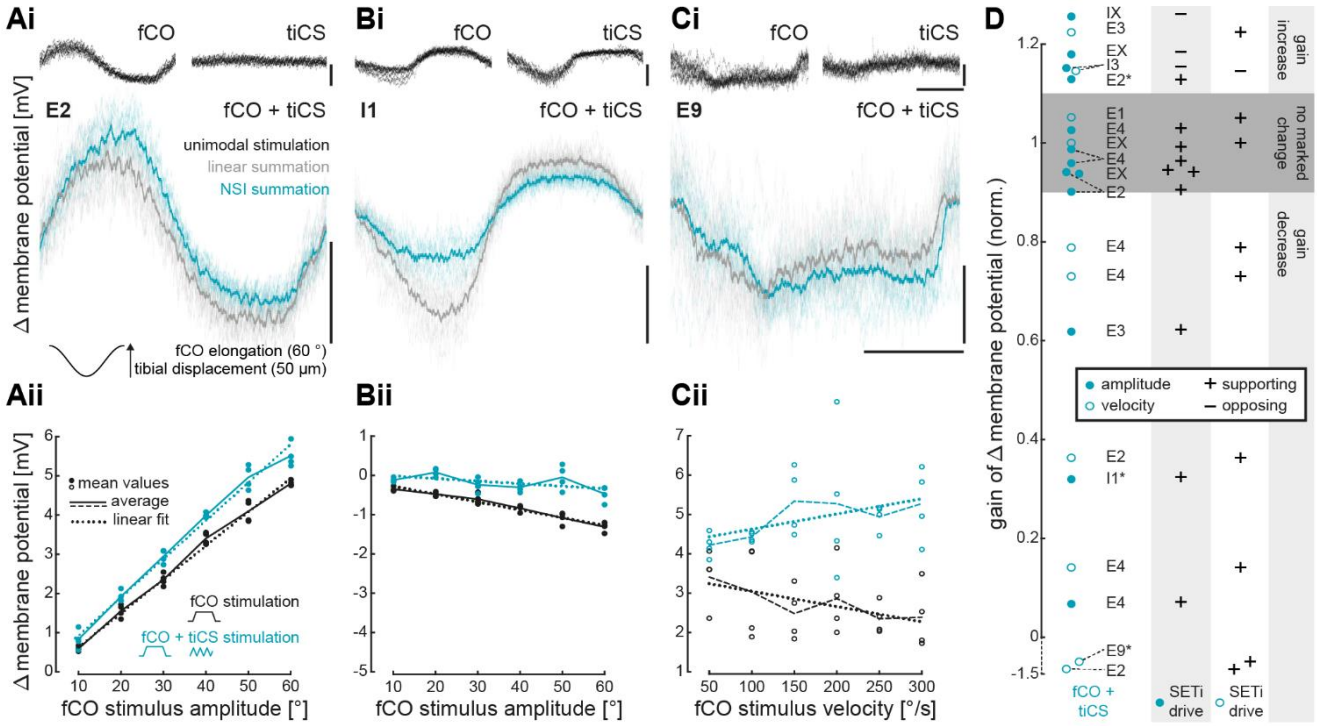

Figure 4.3: Nonlinear summation and neuron-specific gain modulation in NSIs. Load (tiCS) and movement (fCO) signals were summed nonlinearly in NSIs (**Ai-Ci**). Exemplary data from NSIs E2 (**A**), I1 (**B**), E9 (**C**). Top panels (black): NSI membrane potential, sinusoidal waveform stimulation of the fCO (left) or tiCS (right). Bottom panels: NSI membrane potential to combined sinusoidal waveform stimulation of the fCO and tiCS (blue), mathematical linear summation of response traces to individual stimuli (grey). Solid lines in bottom panels: average traces. 15 sweeps of consecutive stimuli overlaid in each panel. Stimulus trace in **Ai**. Scale bar: 5 mV / 0.5 s. In the same NSIs, membrane potential dependence to movement stimulus amplitude (**Aii**, **Bii**) and velocity (**Cii**) was increased (**Aii**), decreased (**Bii**) or reversed (**Cii**) in the presence of triangle waveform load stimuli (blue) when compared to exclusive movement ramp-and-hold stimuli (black). Changes in membrane potential to increasing movement stimulus parameters: average over hold phase of the ramp-and-hold movement stimulus (amplitude dependence) or peak value during rising stimulus ramp (velocity), for more details, see Chapter 4.5. Dots (amplitude) / circles (velocity): data from single ramp-and-hold stimuli; solid (amplitude) / dashed (velocity) line: average; dotted line: linear fit. **D**: Gain (slope of linear fits as depicted in **Aii**-**Cii**) of NSI movement parameter dependence in the presence of triangle load stimuli normalized to exclusive movement stimuli (1st column), and their classification as having a supporting (+) or opposing (-) drive onto the ExtTi SETi MN (2nd & 3rd column). NSIs were identified; EX / IX: inconclusive identification, excitatory (E) or inhibitory (I) effects on SETi. * NSIs in **D** that are depicted in **A-C**. Data was excluded if R^2 of the linear fit < 0.6. N (number of NSIs) = 12, no more than 1 data point per recording and movement parameter.

dichotomy, distinguishing between sensory gain changes affecting velocity or amplitude dependence (Fig. 4.3 D, 2nd & 3rd column). Sensory gain was increased in all opposing NSIs. This effect was strongly expressed in the set of NSIs whose gain of amplitude dependency was altered (increase: 3x (-), 1x (+); no change: 6x (+); decrease: 3x (+)), whereas there was no unidirectional effect on velocity dependence (increase: 1x (+), 1x (-); no change: 2x (+); decrease: 4x (+); note multiple recordings from same NSI types).

4.6.4 Parameter-Dependent & Neuron-specific Modulation of Motor Neuron Gain

The velocity and amplitude dependence, i.e. gain, to movement stimuli in NSIs that in- or decrease activity in ExtTi MNs was modulated in the presence of load (Fig. 4.3). Notably, the amplitude dependence in NSIs opposing SETi activation during the movement resistance reflex was upregulated (Fig. 4.3 D). To test the effects of sensory gain modulation on the motor output of the network we used the same stimulation paradigm as described for NSIs in Figure 4.3 Aii – Cii. Movement stimulus amplitude or velocity was incrementally increased and ExtTi MN response gain was compared in the presence and absence of load signals (Fig. 4.4). The gain of action potential frequency of the excitatory ExtTi MNs (eExtTi MNs, i.e. SETi & FETi) in response to movement stimuli of increasing amplitude was significantly decreased in the presence of load (Fig. 4.4 Ai, N = 1, Fig. 4.4 D, 1st column, blue, N = 22, $p = 4.8 \times 10^{-6}$), consistent with the increase of amplitude dependence in SETi-opposing NSIs (Fig. 4.3 D). This effect was dependent on presynaptic inhibition, as it was abolished by the application of PTX (Fig. 4.4 Aii, N = 1, Fig. 4.4 D, 1st column, grey, N = 6, p = 0.14). The $GABA_A$ antagonist PTX blocks presynaptic inhibition while other inhibitory connections in the network are unaffected in the stick insect premotor network (Sauer et al., 1997).

SETi MN activity constitutes the majority of eExtTi action potentials during a movement reflex response, whereas FETi MN action potential numbers, especially at lower stimulus amplitudes and velocities, lie in the lower single-digit range. The effect on frequency gain in Figure 4.4 A and D in eExtTi MNs will thus be mediated by SETi MN. Intracellularly measured membrane potential changes in FETi MN did not show the same decrease in gain, but rather a tendency towards an increase in amplitude dependent sensorimotor gain in the presence of load that was significant only for higher fCO amplitudes, but not for lower amplitudes, thus indicating a change in gain (Fig. 4.4 B, N = 1, $p = 7.5 \times 10^{-4}$, $N_{total} = 2$). Velocity dependence was not consistently up- or downregulated across NSIs (Fig. 4.3 D), and, accordingly, velocity dependent gain in eExtTi MNs was not significantly modulated into either direction in the presence of load (Fig. 4.4 D, 2nd column, N = 14, p = 0.09). The gain of movement stimuli of increasing velocities in the inhibitory ExtTi MN, CI_1, however, was significantly increased (Fig. 4.4 C, N = 1, Fig. 4.4 D, 3rd column, N = 9, $p = 1.1 \times 10^{-2}$). Consistent with the change in eExtTi action potential frequency, the amplitude dependence of isometric ExtTi muscle force in response to movement stimuli

without FETi MN activation was decreased in the presence of load (Fig. 4.4 E, N = 3 / 4).

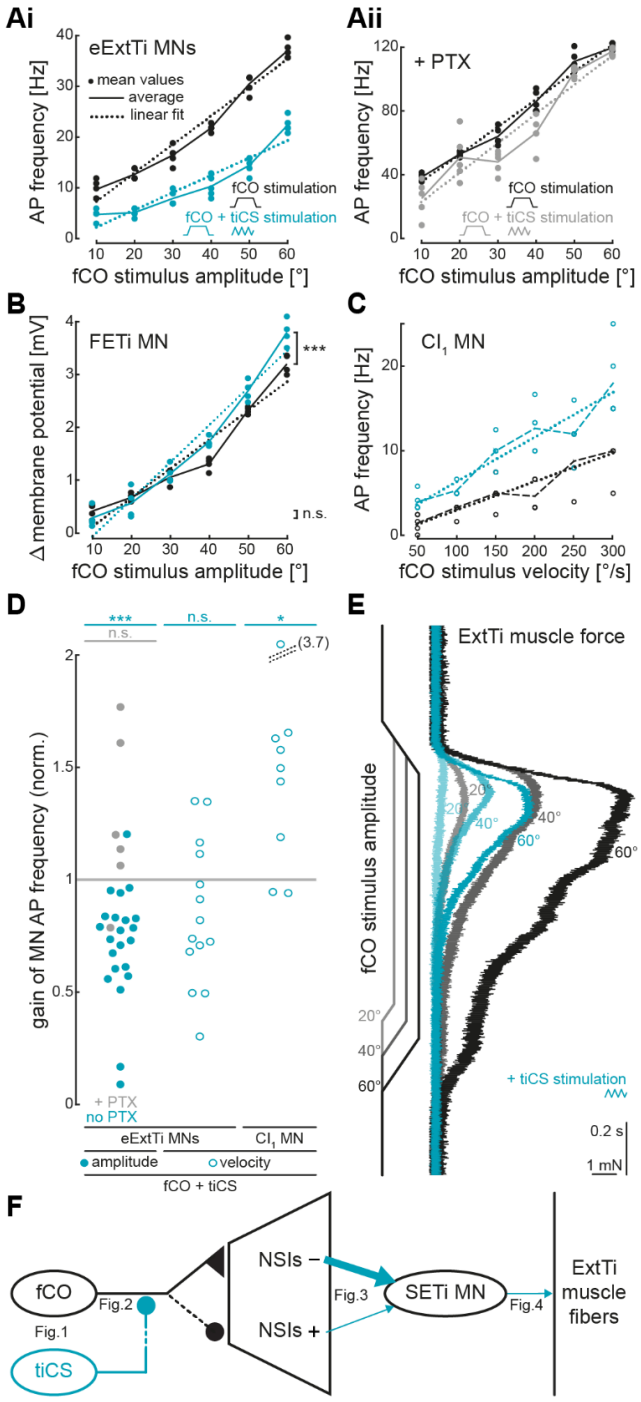

Figure 4.4: Parameter-dependent and neuron-specific modulation of motor output gain. **A**: Amplitude dependence in eExtTi MNs, measured as action potential (AP) frequency, was decreased in the presence of triangle waveform load stimuli (**Ai**, blue) in comparison to exclusive ramp-and-hold movement stimulation (black). The effect was abolished when presynaptic inhibition was blocked with PTX (**Aii**). **B**: Gain of changes in membrane potential in the FETi MN was increased; responses differed significantly at high (60 °), but not low (10 °) movement stimulus amplitudes. **C**: Velocity dependence, measured as AP frequency, was increased in the CI_1 MN. **A**, **B**, and **C**: Data from single animals, dots (amplitude) / circles (velocity): data from single ramp-and-hold stimuli; average: over hold phase of the ramp-and-hold movement stimulus (amplitude dependence) or peak value / average frequency during rising stimulus ramp (velocity), for more details, see Chapter 4.5. Solid (amplitude) / dashed (velocity) line: average; dotted line: linear fit. Color code as in **A**. **D**: AP frequency gain (slope of linear fits as depicted in **A**-**C**) of amplitude (1st column) and velocity dependence (2nd & 3rd column) in eExtTi MNs (1st & 2nd column) and CI_1 MN (3rd column), slope of combined load and movement stimuli normalized to exclusive movement stimuli. Dots (amplitude) / circles (velocity): data from single animals. Grey: PTX trials. **E**: Amplitude dependence of isometric ExtTi muscle force was decreased during triangle waveform load stimuli (blue) in comparison to exclusive ramp-and-hold movement stimuli (black). **F**: Schematic pathways along which load signals affected movement signal gain. Dashed line: polysynaptic pathway; triangle / circle: excitatory / inhibitory synapse; + / -: supporting / opposing NSI.

In summary, the effects of sensory load signals on the gain of movement-signal responses in ExtTi MNs were movement parameter- and MN dependent. Amplitude dependence was upregulated in the FETi MN and, consistent with the enhancing effects of load on amplitude gain in SETi-antagonizing NSIs, downregulated in the SETi MN. Velocity dependence was not unidirectionally modulated in eExtTi MNs, but was increased in the inhibitory MN targeting the same muscle.

4.7 Discussion

Understanding the complexity of motor systems requires information about signal interactions, such as gain control in sensorimotor processing. In many model systems, targeting of specific neurons and tractability of signals impose limitations on our current possibilities to retrieve this information. In the stick insect, each individual element of the neural network can be recorded from, and sensory signals can be precisely controlled with mechanical stimuli using a naturalistic parameter space. We traced interactions between proprioceptive load (tiCS) and movement (fCO) sensory signals and the resulting gain control through the FTi joint control network (Fig. 4.4 F). Signals interacted via presynaptic inhibition from load onto movement sensory afferents. In their, in part monosynaptically connected, downstream targets, the network of NSIs, this led to nonlinear signal summation and differential sensory gain modulation. Specifically, the movement amplitude dependence of NSIs opposing the reflex response in the SETi MN was upregulated in the presence of load. Consistently, we found a decrease in the amplitude dependence, i.e. sensory gain, in SETi, and the resulting isometric ExtTi muscle force, thereby establishing a behavioral relevance. The effects on individual ExtTi MNs varied for distinct movement signal parameters and were dependent on presynaptic inhibition, as the effects were abolished when the latter was pharmacologically blocked. Taken together, the results clearly demonstrate how load feedback specifically tunes individual movement signal pathways, thereby contextualizing movement signal processing.

4.7.1 Proprioceptive Integration in Local Premotor Nonspiking Interneurons

The network of local premotor NSIs processes movement and load sensory feedback by way of distributed, antagonistic processing (Büschges, 1990; Sauer et al., 1996; Bässler and Büschges, 1998; Gebehart et al., 2021 (Chapter 2)). Shifting the weighting between individual pathways of the distributed network has been suggested as a mechanism for controlling MN gain, especially in the context of reflex reversal and active behavior (Bässler, 1993; Pearson, 1993; Büschges and Wolf, 1996; Driesang and Büschges, 1996; Hess and Büschges, 1997; Kittmann, 1997). Controlling the gain of sensory signals in distributed networks is necessary to use the same network for different tasks and to endow behavioral flexibility. Distributed processing is a crucial component of the mechanism presented in this study; it permits the system to fine-tune individual pathways of the network and thus modulate distinct motor channels in different sensory contexts using the same set of NSIs.

Load and movement signals are processed along antagonistic pathways, i.e. the activity of single NSIs can support or oppose an ongoing motor output (Büschges, 1990; Gebehart et al., 2021 (Chapter 2)). In this study, we present for the first time a mechanism that could shape a distributed, antagonistic network into a dedicated network. In the presence of load, movement amplitude dependence was specifically increased in those NSIs which oppose the reflex activation of SETi. Consistently, SETi amplitude dependence was decreased in the presence of load and the gain of muscle force decreases. While this is most likely not the only way in which NSI network activity can be tuned, it provides a first step to a more detailed understanding of flexible, distributed sensory processing.

4.7.2 Sensorimotor Gain Control

Presynaptic inhibition is a ubiquitous mechanism for controlling sensorimotor gain (Clarac and Cattaert, 1996; Rudomin and Schmidt, 1999; Torkkeli and Panek, 2002), and is the focus of studies on active behaviors in model systems ranging from the monkey (Confais et al., 2017), to the locust (Wolf and Burrows, 1995). It is essential for stable motor output and to prevent oscillations (Fink et al., 2014), to avoid sensory habituation and saturation (Krasne and Bryan, 1973; Burrows and Matheson, 1994), and to ensure proper coordination during walking (Koch et al., 2017). Here we studied the effects of presynaptic afferent inhibition on movement signal gain control in the quiescent animal. In the absence of active behavior, we demonstrate a local circuit mechanism for multimodal sensorimotor gain control that is based on the presynaptic interaction of distinct sensory afferents.

By controlling the gain of sensory signals in a motor network, the impact of these signals on downstream processing circuits is up- or downregulated. Modulation depends on signal type, i.e. information content, their relevance for the current behavioral context, or the necessity to stabilize the system and prevent signal overload (Azim and Seki, 2019). Using detailed insights into the differential fine-tuning of individual interneuronal and MN pathways, we suggest a mechanism by which a small locomotor network can implement contextualized sensorimotor control. Movement signal processing and response gain of the motor output for joint control in the stick insect was dependent on the presence, or absence, of load feedback. Thereby, movement sensorimotor gain control was dependent on the proprioceptive context, i.e. the presence, or absence, of load. This is of especial relevance in the context of proprioception as a multimodal sense, where load and movement will frequently occur simultaneously.

4.7.3 Functional Relevance for the Control of Leg & Joint Movement

Our results clearly show that to understand motor control and leg movement, we need to consider movement signals in the context of load, and vice versa. The gain of movement amplitude and velocity was differentially modulated in the motor system and its outputs, i.e. ExtTi MNs. In the presence of load, SETi MN movement amplitude dependence was decreased, its velocity dependence was not

consistently altered, whereas FETi MN amplitude and CI_1 MN velocity dependence were increased. From a general perspective, downregulation of SETi activity and upregulation of CI_1 and FETi is can be used to support fast leg movements by reducing slow ExtTi muscle fiber activation and recruiting fast muscle fibers (Bässler et al., 1996). CI_1 activation reduces tonic slow fiber activity, thus supporting a fast movement. Our experiments were performed in resting, inactive animals, and muscle forces were measured in the absence of FETi activity. The situation might differ for active behaviors, for example, by increasing the weak effects on FETi response gain. An indication that the situation might be similar between inactive and active animals is found in the reflex reversal, when the response to a sensory stimulus switches from a resistance reflex in an inactive animal to an assistance reflex in the active animal (e.g. Forssberg et al., 1975; Bässler, 1976; De Serres et al., 1995; Pearson, 1995b). In the stick insect, the balance of the reflex reversal is shifted towards the active reaction by load stimuli, and the first part of the active response, similar to our data, involves a decrease in SETi and an increase in CI_1 activity (Bässler, 1986; Akay and Büschges, 2006). In the context of the results presented here, this supports the hypothesis that load controls the gain of movement signal processing and thereby shifts the network balance towards reflex reversal and an active reaction.

In the presence of load, SETi velocity dependence was unaffected, while its gain in CI_1 was upregulated. In stick insects, velocity dependence is a critical premise for catalepsy, a major component of twig mimesis. Velocity dependence is a prerequisite for the nervous system to accomplish the tight control over reflexes and muscle activity that enables the extremely slow movements. The latter, in response to external perturbation of the leg, return the limb to its original position at velocities that are too slow for predators to detect (Bässler and Foth, 1982; Bässler et al., 1982; Bässler, 1983b; Driesang and Büschges, 1993). By reducing the amplitude dependent component of SETi's response without affecting its velocity dependence, the relative weighting of the velocity component in the SETi response is increased. In combination with an increased velocity dependence in CI_1, gain control mediated by load signals could support the generation of velocity dependent, slow movements seen in catalepsy. Sensorimotor gain control could thereby support the low pass filter characteristics of the muscle fibers (Bässler, 1983b). Interesting to see would be a comparison with the sensorimotor gain control in the locust, as these animals do not perform twig mimesis and do not show the same degree of velocity dependence (Büschges and Wolf, 1995).

Apart from catalepsy, reducing the response strength of MNs to increasing stimulus parameters could provide a general mechanism by which a leg motor system might prevent damage to its effectors if the resisted external force is too strong. Consistently, the role of tiCS has been discussed to lie primarily in the tuning of muscle activity in the ExtTi and its antagonist when activation of these muscles leads to an increased load on the tibia (Cocatre-Zilgien and Delcomyn, 1999).

Until recently, functional schemata of load and movement signal pathways were considered as mainly separate, equivalent pathways that act on the same MNs. In a previous publication, we could show that load and movement signals are processed within the same network of NSIs (Gebehart et al., 2021 (Chapter 2)). In the present study, we combined sensory signals from distinct sense organs of different modalities and trace their interaction through the network, from the inputs of the sensory afferents via the processing in the interneuronal network to the output of the MNs. Our results show that load tuned movement processing pathways, thus contextualizing movement information in the local network. Taking advantage of the accessibility of the network in the stick insect, we provide a mechanism that applies gain control of sensory feedback processing to implement context-dependency. Proprioceptive feedback from distinct load and movement sensors, as well as the other neuronal mechanisms described here, are also found in other locomotor systems that face similar tasks as the stick insect. In a study on the integration of touch and proprioceptive signals in the ventral nerve cord of *Drosophila melanogaster*, Tuthill and Wilson discussed the putative contextualization of sensory signals by load and movement feedback, which we have demonstrated here (Tuthill and Wilson, 2016b). Future studies will have to show whether the contextualization of sensory signals by means of sensorimotor gain control is a general mechanism of motor networks.

Büschges and Wolf suggested four putative mechanisms for sensory gain control in the motor system of an insect leg, i.e. presynaptic inhibition, changes in weighting of parallel pathways, changes at the MN membrane, and altered sensitivity of sensory afferents (Büschges and Wolf, 1996). Our results demonstrate that the first two options might be considered as part of the same mechanism in which presynaptic inhibition alters the gain of parallel pathways, thereby shifting the balance of antagonistic pathways. The last two possibilities are thought to be potentially mediated by neuromodulators. These play an important role in sensorimotor processing and leg muscle control (Stolz et al., 2019; Liessem et al., 2021), and might present a complimentary mechanism to the neuronal interactions we investigated here.

5 Perspectives: Lateral Connectivity in the Sensorimotor Network

The following Chapters 5.1 - *Presynaptic Interactions between Proprioceptive Sensory Afferents*, and 5.2 - *Lateral Connectivity & Rhythmicity in the Network of Nonspiking Interneurons* provide perspectives for future lines of research on the lateral connectivity within the sensorimotor network. They are based on data that is not part of the manuscripts of Chapters 2, 3, and 4, and no contributions from persons other than yours truly, the author of this dissertation, are included.

In Chapter 5.1, lateral connections mediating presynaptic interactions between sensory afferents of the fCO and tiCS were examined in detail. A new mechanism for presynaptic signal gain control was identified that results in disinhibition, i.e. release from presynaptic inhibition, in specific fCO afferents upon tiCS stimulation. This upregulation of sensory signal gain was found only in fCO afferents whose signals contain unidirectional information about tibial movement, and was sensitive to PTX. Additionally, presynaptic inhibition was found from fCO to tiCS afferents, and between tiCS afferents of the same and different subgroups, i.e. G6A and G6B.

The results on lateral connections within the premotor network of local NSIs will be described in Chapter 5.2. Paired double intracellular recordings revealed reciprocal excitation between all recorded pairs of NSIs. In the absence of external stimuli, individual pairs showed correlated, in some cases rhythmically correlated, fluctuations of their membrane potential. The membrane potential of specific types of NSIs showed rhythmic oscillations at a frequency that was, with few exceptions, consistent across oscillating NSI types and recordings. The data suggest a previously undetected mechanism for network synchronization that might increase coupling strength within the NSI network.

5.1 Presynaptic Interactions between Proprioceptive Sensory Afferents

5.1.1 Introduction

In Chapter 2 it was shown that proprioceptive feedback from load and movement sensors is integrated by local premotor NSIs. As the data provided in Chapter 4 and the study by Stein and Schmitz demonstrate, these signals already interact at an earlier neuronal stage, i.e. via presynaptic afferent inhibition (Stein and Schmitz, 1999). This necessitates investigations on the degree of preprocessing that proprioceptive signals are subjected to before they can be integrated into the premotor network. If "raw" signals from sense organs are filtered and altered by presynaptic mechanisms, this will impact the information that postsynaptic networks may use to control movement. In Chapter 5.1, I will therefore focus on the lateral connectivity between sensory afferents of the fCO and tiCS, and provide data that might provide the basis and a perspective for future investigations.

Presynaptic inhibition is neither a novel concept, nor is it restricted to invertebrates or insects. It was discovered almost at the same time in vertebrates (Frank and Fuortes, 1957 as cited in Clarac and Cattaert, 1996; review in Rudomin and Schmidt, 1999), and in crayfish (Dudel and Kuffler, 1961; review in Clarac and Cattaert, 1996). In the insect leg, fCO afferents have been found to be the target of presynaptic inhibition originating from afferents of the same sense organ (Burrows and Matheson, 1994; Sauer et al., 1997), or from CS afferents (Stein and Schmitz, 1999, Chapter 4). The following Chapter 5.1 will extend the view of presynaptic effects of CS onto fCO afferents to include also facilitatory effects, and provide an overview of the presynaptic effects occurring in CS afferents themselves.

The mechanisms underlying presynaptic inhibition may differ between systems. However, studies on crayfish are complemented by data from locusts and stick insects and thereby provide a coherent picture on arthropod presynaptic inhibition, some aspects of which are also found in vertebrate systems (reviews in Clarac and Cattaert, 1996; Rudomin and Schmidt, 1999; Torkkeli and Panek, 2002): Presynaptic inhibition is mediated by inputs from GABAergic interneurons to the neuropilar branches of sensory afferents (Burrows and Matheson, 1994; Clarac and Cattaert, 1996). The inputs are sensitive to the $GABA_A$ antagonist PTX (e.g. Burrows and Laurent, 1993; Sauer et al., 1997), and result in the opening of chloride channels (discussed in Clarac and Cattaert, 1996; Torkkeli and Panek, 2002). Due to a concentration gradient of chloride in sensory afferents that differs from other parts of the nervous system, chloride ions flow out of the neuron, causing a PAD (cf. Clarac and Cattaert, 1996). The equilibrium potential of chloride at the afferent membrane thus causes a depolarization, which has nevertheless inhibitory effects. The conductance increase induced by the opening of chloride channels acts as a shunting mechanism that reduces the amplitude of action potentials passing through this part of the neuronal membrane. Because presynaptic inhibition primarily occurs near the ends of neuropilar afferent branches where electrical transmission becomes passive, the action potential amplitude

cannot be recovered and leads to a decrease in transmitter released at the afferent synapse (Clarac and Cattaert, 1996; Cattaert and El Manira, 1999; Cattaert et al., 2001).

In the following study, I will provide data and initial findings that might guide future investigations on the lateral connectivity of multimodal sensory afferents. The presynaptic effects of tiCS onto fCO afferents will be characterized in detail, and a new type of presynaptic interaction will be described. Specifically, not all presynaptic effects in fCO afferents are inhibitory, leading to the hypothesis that the machinery of presynaptic inhibition is harnessed for the upregulation of afferent information by a form of disinhibition, i.e. a release from tonic presynaptic inhibition. The specific presynaptic actions of tiCS afferents onto fCO afferents with different sensitivities to tibial position, movement velocity, and acceleration will be analyzed (cf. Büschges, 1994). Additionally, the reverse situation will be examined, i.e. whether fCO afferents in turn mediate presynaptic inhibition onto tiCS afferents, and whether tiCS afferents themselves interact at the presynaptic level. Previous studies, including the results presented in this dissertation, have focused on fCO afferents as the target of presynaptic inhibition, mediated, for example, by either sensory afferents of the same (Burrows and Matheson, 1994; Sauer et al., 1997) or different sense organs, e.g. tr/fCS and hairplates (Stein and Schmitz, 1999), and tiCS (Chapters 4). Apart from the study by Stein and Schmitz, which indicates the presence of presynaptic inhibition from hairplates to CS, presynaptic effects on proprioceptive afferents of the insect leg other than the fCO have received little attention (Stein and Schmitz, 1999). This raises the question whether presynaptic interactions are comparable between proprioceptive afferents of the fCO and CS, or whether this type of sensory processing is asymmetrical and mainly occurs in the fCO.

5.1.2 Materials & Methods

The experiments and analyses were performed according to the same procedures described in detail in Chapter 4. Neural activity was recorded intracellularly from neuropilar arborizations of sensory afferents from tiCS G6A and G6B and the fCO. Mechanical stimuli were used to activate sense organs. Note that changes in action potential amplitude could only be analyzed in sensory afferents with tonic resting activity or during their preferred stimulus. Where indicated, bath application of 0.03 mM PTX (Sigma) was used to block presynaptic inhibition.

To observe changes in the input resistance of the neuronal membrane, short pulses of negative current were injected via the intracellular electrode (pulse duration 0.05 s, frequency 10 Hz). Pulses were controlled using a digital stimulator (MS501). The amount of current injected into the neuron was adapted in each recording to evoke changes in membrane potential of approximately 5 mV, to avoid activation of active membrane conductances. In the examples presented in the following, current pulse amplitude was set to -0.4 nA. According to Ohm's law (potential equals resistance times current, $V = R * I$), the changes in membrane potential evoked by the negative current pulses will be positively correlated

with the membrane's input resistance. The latter depends on the number of transmembrane channels that are open at the time of the current injection. The larger the number of channels that are open at a given moment, the smaller the input resistance and the smaller the change in membrane potential evoked by the same amount of current.

5.1.3 Results

Presynaptic inhibition between sensory afferents is an important aspect of sensorimotor gain control (Clarac and Cattaert, 1996; Azim and Seki, 2019). A mechanism by which presynaptic inhibition could alter premotor processing and the motor output of the FTi joint control loop dependent on the sensory context was described in the previous Chapter 4. These results raised questions about the complexity of presynaptic afferent interactions, including the putative presence of reciprocal effects between afferents carrying load (tiCS) and movement (fCO) information, and the specific identity, i.e. parameter sensitivity, of the targeted afferents. During these experiments emerged another observation, i.e. that classical, in the following called PAD type, presynaptic inhibition is not the only regulatory mechanism of sensory afferent activity in this system.

5.1.3.1 Presynaptic Inputs to Neuropilar Arborizations of Femoral Chordotonal Organ Afferents

Presynaptic inhibition has been described to occur between fCO afferents themselves (Burrows and Matheson, 1994; Sauer et al., 1997), and from tr/fCS and tiCS onto fCO afferents (Chapter 4, Stein and Schmitz, 1999, for morphology of neuropilar fCO arborizations, see Suppl. Fig. 2.1). These effects between fCO afferents and from tiCS onto fCO afferents were also found and analyzed in detail in the following experiments, and corresponded to descriptions of the "classical", or regular, PAD type effects. Stimulation of the fCO (Fig. 5.1 A) or tiCS (Fig. 5.1 B) induced a depolarization of the fCO afferent membrane potential (Fig. 5.1 Ai, ii, Bi, ii) that was increased by hyperpolarizing the neuron with a tonic injection of negative current (Fig. 5.1 Aiii, Biii). Simultaneously, the membrane input resistance was decreased (Fig. 5.1 Aiv, Biv), as could be observed by the decreased amplitude of changes in membrane potential evoked by negative current pulses (for details on measurements of input resistance, see Chapter 5.1.2). In combination, these results indicate that ion channels were opened during the applied sensory stimulus, resulting in an inward current that depolarized the cell. Hyperpolarizing the membrane increased the deviation from the equilibrium potential of the underlying ionic current and thereby increased the amplitude of the PAD.

The stimulus-induced PADs decreased the amplitude of concurrent action potentials in the fCO afferent, thereby characterizing it as presynaptic inhibition (Fig. Av, Bv). Presynaptic inhibition of this "regular" PAD type between fCO afferents was found in 27 out of 28 recordings, whereas only in 8 out of 27 fCO afferent recordings the regular PAD type effects were observed upon tiCS stimulation (cf. Table 5.1). Note that, if not indicated otherwise, stimulations targeting tiCS G6A and G6B were pooled.

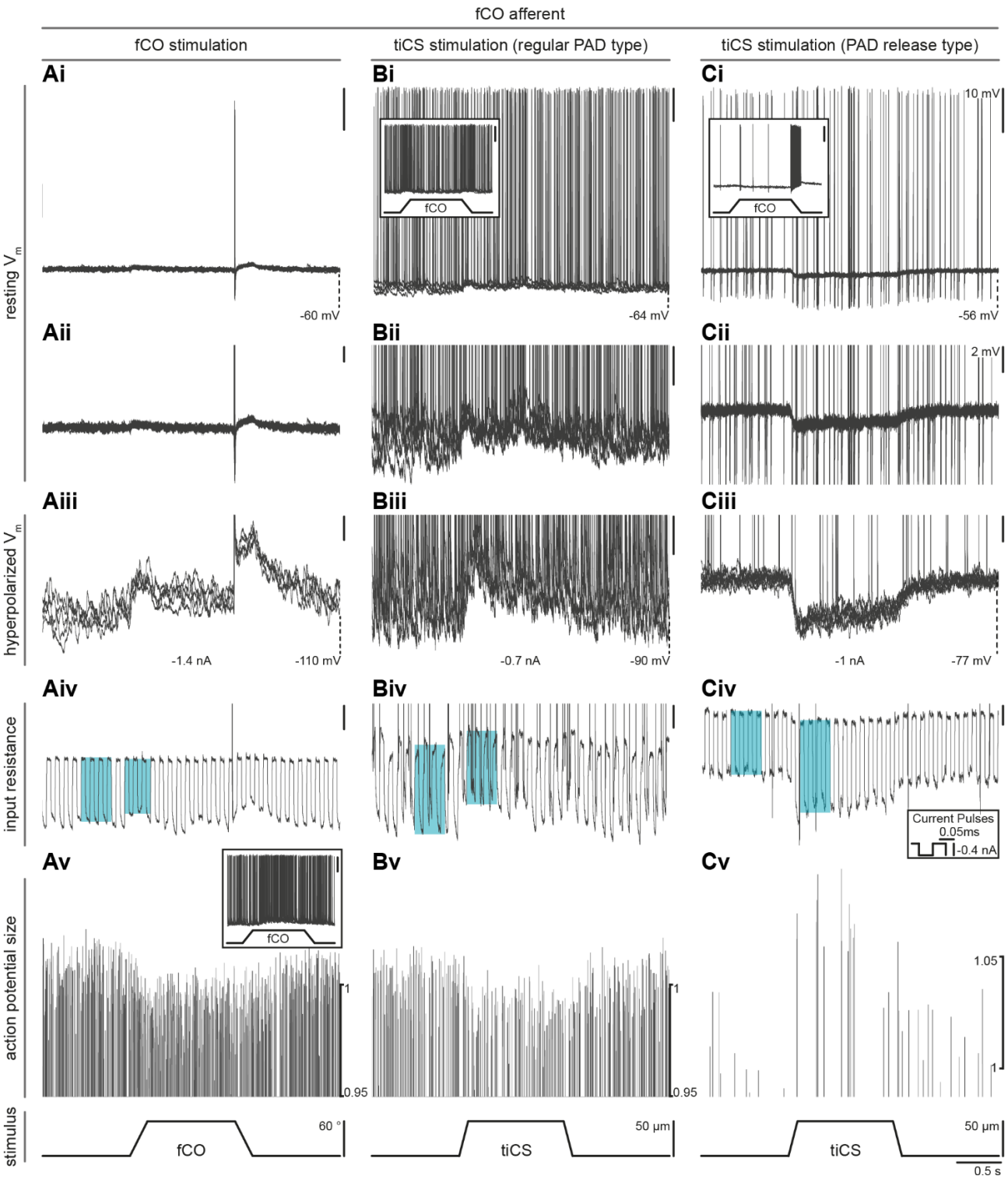

Figure 5.1: Presynaptic inputs to neuropilar arborizations of fCO afferents. Presynaptic effects of fCO (**A**), and tiCS (**B**, **C**) stimulation on fCO afferent activity. **A**: Presynaptic inhibition in an fCO afferent resulting from activation of the same sense organ. **B**: "Regular", i.e. as previously described, PAD type response in an fCO afferent upon tiCS stimulation. **C**: PAD release type response in an fCO afferent upon tiCS stimulation. **A**, **B**, and **C** depict recordings from the same fCO afferent, respectively. Exception: **Av**, **Biv**, corresponding afferent response to fCO stimulation in inset in **Av**. **i**: fCO afferent stimulus response, insets

Figure 5.1 (continued): in **B** & **C** show the respective afferent's response to fCO stimulation. **ii**: Changes in membrane potential upon tiCS stimulation, enlarged view of **i**. **iii**: Stimulus-induced changes in membrane potential while the membrane potential was hyperpolarized by injecting negative current. **iv**: Stimulus-induced changes in afferent membrane input resistance, inferred by injecting negative current pulses (see inset in **C**) and monitoring the amplitude of the resulting changes in membrane potential before and during the sensory stimulus (for details, see text). **v**: Changes in action potential amplitude induced by sensory stimuli, normalized to average amplitude in 1 s interval previous to stimulation. Scale 10 mV (**i**), 2 mV (**ii**-**iv**). Membrane potential (V_m) indicated (**i**, **iii**). Bottom row: Stimulus traces. All panels except **iv**: 5-10 sweeps of consecutive stimuli. For another example of regular PAD type responses, see Fig. 4.2.

Differing total numbers of afferent recordings are due to experimental constraints that prevented all types of sensory stimuli to be tested in every single recording.

Aside from the regular PAD type effects on fCO afferents, in very few fCO afferents no effect of tiCS stimulation was visible (N = 2 / 27). In the majority (N = 17 / 27), the membrane potential of the fCO afferent was hyperpolarized, i.e. its membrane potential was decreased, in response to a stimulation of the tiCS (Fig. 5.1 Ci). The hyperpolarization was not mediated by an outward current induced by the opening of ion channels. This was concluded as the amplitude of the hyperpolarization increased when the afferent membrane potential was further hyperpolarized (Fig. 5.1 Cii, N = 4 / 5, no visible change in N = 1 / 5). Additionally, the membrane input resistance was increased during tiCS stimulation (Fig. 5.1 Civ, N = 6 / 6). This indicates the closing of ion channels, i.e. a decreased conductance across the membrane, which leads to larger changes in membrane potential upon negative current pulse injection. It was therefore hypothesized that the hyperpolarization, which did not decrease when the afferent membrane was lowered and was accompanied by the closing of ion channels, represented a disinhibition, in other words a release from tonic presynaptic inhibition. This type of presynaptic input response in fCO afferents was therefore termed PAD release type. Strikingly, and supporting the hypothesis that this phenomenon constitutes the opposite of regular presynaptic inhibition, the amplitude of fCO afferent action potentials concurring with the tiCS stimulus was increased (Fig. 5.1 Cv, N = 4 / 4). Note that no fCO afferent was found to receive both types of presynaptic inputs, e.g. regular PAD type from tiCS G6A and PAD release type from G6B.

Presynaptic afferent inhibition can be blocked by the $GABA_A$ antagonist PTX while inhibitory connections within the premotor network remain unaffected (Sauer et al., 1997). Figure 5.2 depicts the PAD release type response in a fCO afferent before (A) and 10 min after (B) bath application of PTX (N = 1). PTX reduced the amplitude of the tiCS-stimulus induced hyperpolarization in the fCO afferent (Fig. 5.2 Ai, Bi). When presynaptic inhibition was blocked, no more changes in membrane input

resistance could be observed, i.e. the amplitude of changes in fCO afferent membrane potential elicited by negative current pulses did not differ with or without tiCS stimulation (Fig. 5.2 Aii, Bii). The overall membrane input resistance, independent of sensory stimuli, was increased after PTX application and the resting membrane potential was slightly decreased.

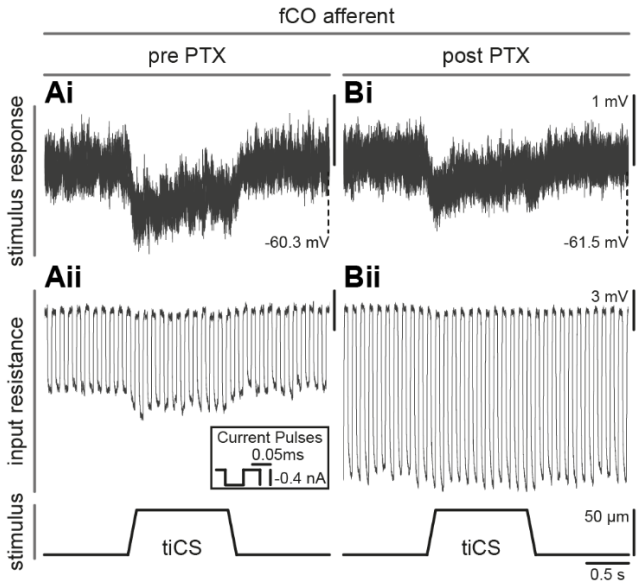

Figure 5.2: Effects of blocking presynaptic inhibition in a PAD release type fCO afferent. fCO afferent response to tiCS stimulation before (**A**) and 10 min after (**B**) bath application of the $GABA_A$ antagonist PTX. **i**: Stimulus-induced reduction in fCO afferent membrane potential, 5-10 sweeps of consecutive stimuli. **ii**: Change in input resistance upon tiCS stimulation, inferred by injecting negative current pulses (see inset in **A**) and monitoring the amplitude of the resulting changes in membrane potential before and during the sensory stimulus (for details, see text). Scale 1 mV (**i**), 3 mV (**ii**). Membrane potential indicated (**i**). Bottom row: Stimulus traces. All panels: same fCO afferent recording.

5.1.3.2 Specificity of Presynaptic Inputs to Femoral Chordotonal Organ Afferents with Different Parameter Sensitivities

Individual fCO parameters encode different parameters of a movement stimulus (Büschges, 1994; Field and Matheson, 1998; Mamiya et al., 2018). A single fCO afferent might alter the frequency of its action potentials to represent the velocity (V) or acceleration (A) of tibial movement, or tibial position (P) or vibration. Note that it was not possible to test for vibration sensitivity in this experimental setup. The movement parameter sensitivity of fCO afferents was characterized and sorted by their PAD response type to tiCS activation, i.e. regular PAD *versus* PAD release type *versus* no PAD (Fig. 5.3 A). Parameter sensitivities were separated into unidirectional and bidirectional velocity or acceleration responses, i.e. whether the fCO afferent responded only to stimuli in the direction of flexion or extension, or both, and into positive or negative position dependence, i.e. increased activity by more flexed or extended positions, respectively (Fig. 5.3 B).

The described sorting of fCO afferents revealed that the release from tonic presynaptic inhibition, the PAD release type responses, exclusively occurred in fCO afferents which were unidirectionally sensitive to velocity or acceleration (Fig. 5.3 A). Regular PAD type responses were found in unidirectional afferents with positive position sensitivity as well (N = 4), but bidirectionally velocity or acceleration

sensitive fCO afferents all received the regular PAD type inputs ($V_{bidirectional}$ P_- N = 2, $V_{bidirectional}$ N = 1, $A_{bidirectional}$ N = 1). In contrast, all fCO afferents with PAD release type inputs were unidirectionally sensitive to velocity ($V_{unidirectional}$ P_+ N = 10, $V_{unidirectional}$ N = 1), or acceleration ($A_{unidirectional}$ N = 2), or a combination thereof ($V_{unidirectional}$ $A_{unidirectional}$ N = 4).

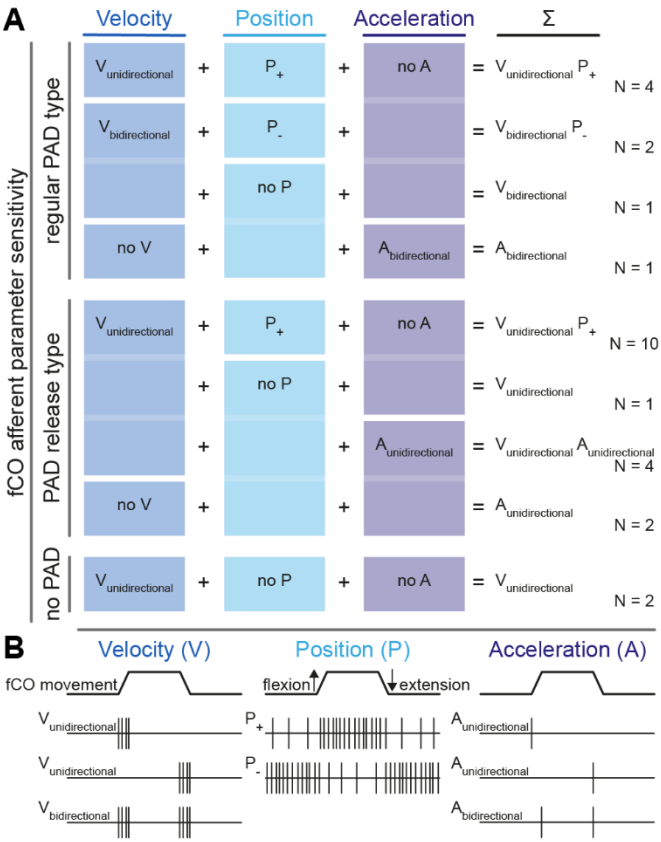

Figure 5.3: Specificity of presynaptic inputs to fCO afferents with different parameter sensitivities. **A**: fCO afferent parameter sensitivity sorted by tiCS stimulus-evoked inputs (top: regular PAD type, middle: PAD release type, bottom: no PAD). It was distinguished between uni- and bidirectional velocity (V) or acceleration (A) dependence, and positive and negative position dependence (P). Σ: Combined parameter sensitivities for a given fCO afferent type. **B**: Fictive schematic depictions of exemplary changes in afferent action potential firing demonstrating the distinct sensitivities applied for fCO afferent characterization.

Position dependence in fCO afferents was no indicator for the type of tiCS-evoked effects. Both regular PAD and PAD release type responses were found in fCO afferents with positive position dependence (Fig. 5.3 A). Negative position dependence was only found in fCO afferents with regular PAD type responses, but sample size of these afferents was too low to be conclusive (N = 2). Positive position dependence was, however, correlated with unidirectional velocity sensitivity in fCO afferents. The two fCO afferents that showed no changes in membrane potential in response to tiCS stimuli were unidirectionally sensitive to velocity (Fig. 5.3 A, bottom row).

5.1.3.3 Presynaptic Inputs to Neuropilar Arborizations of Tibial Campaniform Sensilla Afferents

Presynaptic effects targeting the fCO have been the focus of this and other studies (e.g. Burrows and Matheson, 1994; Sauer et al., 1997; Stein and Schmitz, 1999), but it was unclear whether the situation in tiCS afferents is comparable. I therefore recorded from neuropilar arborizations of tiCS afferents to determine similarities, or differences, in the presynaptic processing of proprioceptive feedback in tiCS and fCO afferents (Fig. 5.4). For morphology of neuropilar tiCS G6A and G6B arborizations, see Suppl. Fig. 2.1.

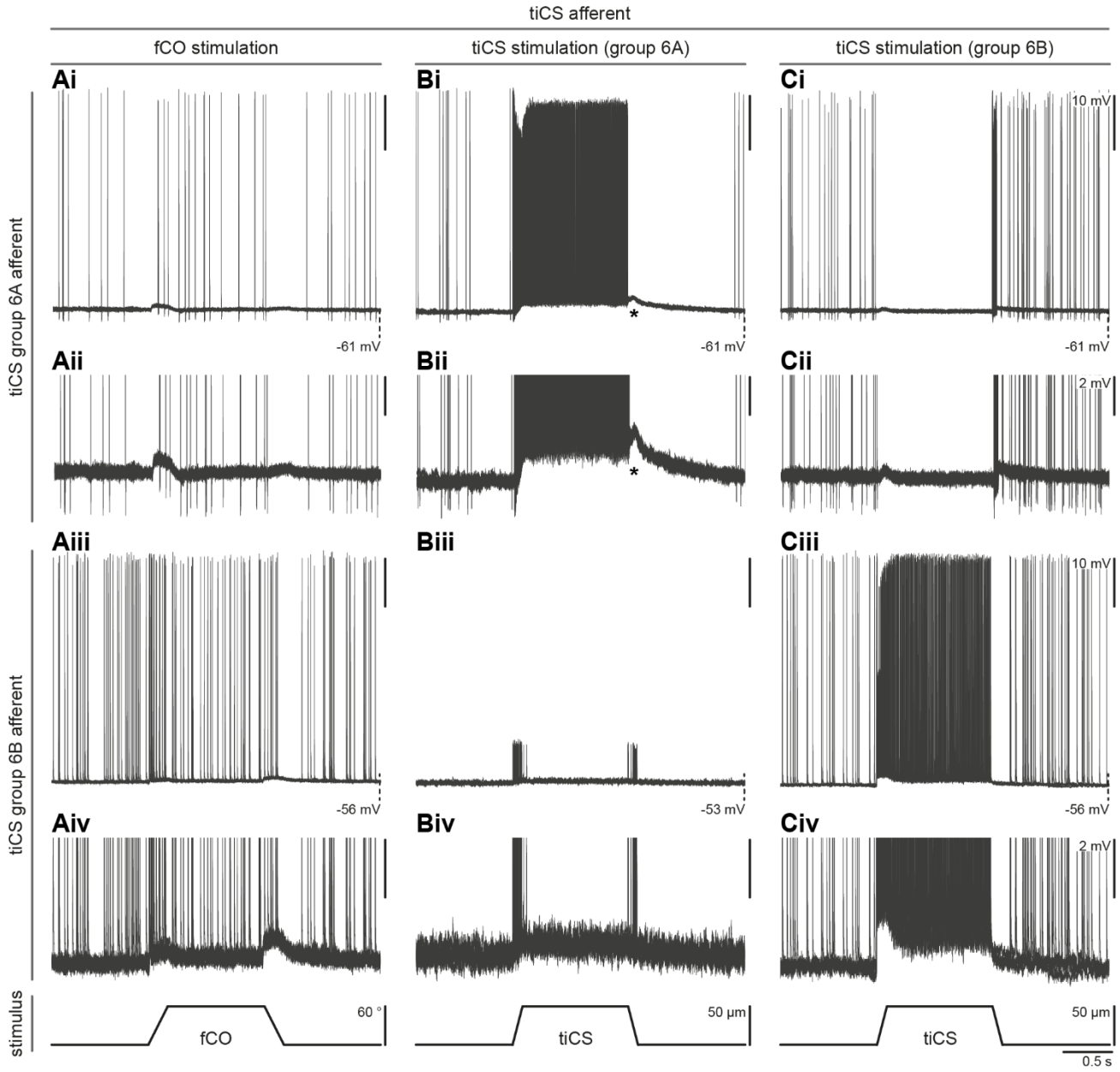

Figure 5.4: Presynaptic inputs to neuropilar arborizations of tiCS afferents of G6A (**i**, **ii**) and B (**iii**, **iv**). Presynaptic effects of fCO (**A**), and tiCS G6A (**B**) and G6B (**C**) stimulation on tiCS afferent activity. **A**: PADs resulting from activation of the fCO in tiCS G6A (**i**, **ii**) and G6B (**iii**, **iv**) afferents. **B**: PADs resulting from activation of tiCS G6A in tiCS G6A (**i**, **ii**) and G6B (**iii**, **iv**) afferents. **C**: PADs resulting from activation of tiCS G6B in tiCS G6A (**i**, **ii**) and G6B (**iii**, **iv**) afferents. **ii, iv**: Changes in membrane potential upon tiCS stimulation, enlarged view of **i**. **i**, **ii**, and **iii**, **iv** depict recordings from the same tiCS afferent, respectively. Exception: **Biii, Biv**. **i, iii**: tiCS afferent stimulus response. Asterisk: PAD in a G6A afferent induced by the off-response of G6B afferents. Action potential size in **Biii**, **iv** was decreased during the recording, probably due to an electrode-induced leak current, but action potential firing was unaltered. Scale 10 mV (**i, iii**), 2 mV (**ii**, **iv**). Membrane potentials indicated (**i**, **iii**). Bottom row: Stimulus traces. All panels: 5-10 sweeps of consecutive stimuli.

Presynaptic interaction between tiCS and the fCO was found to be reciprocal, i.e. tiCS activity modulated the membrane potential of fCO afferent arborizations (Fig. 5.1), and fCO stimulation elicited PADs in tiCS sensory afferents (Fig. 5.4 A, N = 9 / 12). Presynaptic effects onto tiCS afferents, however, showed the regular characteristics of presynaptic inhibition in all recordings. No evidence for PAD release type effects was found in tiCS afferents. Upon fCO stimulation, PADs were elicited in tiCS afferents of G6A (Fig. 5.4 Ai, ii, N = 4 / 5) and G6B (Fig. 5.4 Aiii, iv, N = 5 / 10, cf. Table 5.1).

Presynaptic inhibition in the form of PADs also occurred between tiCS afferents of the same group, i.e. between G6A afferents or between G6B afferents, respectively (Fig. 5.4 Bi, ii (G6A, N = 3 / 5), Ciii, iv (G6B, N = 5 / 10)), and between groups, i.e. from 6A to 6B, and vice versa (Fig. 5.4 Biii, iv (G6A onto 6B, N = 1 / 3), Ci, ii (G6B onto 6A, N = 2 / 4). Note that, due to experimental constraints, not all sensory stimuli could be tested in all recordings. One 6A and one 6B afferent out of 6 fully tested tiCS afferents showed no presynaptic effects to any type of sensory stimulation, neither from tiCS nor from fCO afferents. Most tiCS afferents were affected by combinations of presynaptic sources, e.g. from fCO and tiCS G6A or G6B afferents, or fCO and both tiCS groups. An example of these combinatory effects is shown in Figure 5.4 Bi and ii, where a tonic PAD during and an additional PAD at the end of the stimulus are visible (asterisk). The depicted 6A afferent therefore received tonic presynaptic inhibition from other 6A afferents while the stimulus was ongoing. At the end of the stimulus, the 6A afferent had already stopped its response in terms of action potential firing, and other 6A afferents will likely have had done so as well, leading to the conclusion that the additional PAD (Fig. 5.4 Bi, ii, asterisk) resulted from the off-response of a 6B afferent (cf. Fig. 5.4 Biii, iv). In summary, the results show that some tiCS afferents of both subgroups receive presynaptic inhibition from tiCS of the same and the other group, and from the fCO. This is comparable to the situation in the fCO, with the marked distinction that PAD release type effects were only found in fCO afferents as a result of tiCS afferent activation, not the other way around.

5.1.3.1 Presynaptic Interactions Within the Same & Between Two Proprioceptive Sense Organs

As the results presented above demonstrate, presynaptic interactions between sensory afferents of the same sense organ could be found both in fCO and tiCS afferents. Interactions between these sense organs were reciprocal, but asymmetrical, as both received presynaptic inhibition from each other, but only fCO afferents showed the upregulation by the PAD release type upon stimulation of tiCS. Table 5.1 summarizes these complex interactions, their prevalence in the set of recorded afferents, and the shape of the underlying respective regular PADs or PAD releases, respectively. It was distinguished between phasic-tonic (e.g. Fig. 5.4 Civ), phasic (e.g. Fig. 5.1 Ai), and tonic (e.g. Fig. 4.2 B) effects on afferent membrane potential. There was a clear difference in the presynaptic effects originating from fCO and tiCS afferents; PADs elicited by fCO stimulation were almost purely phasic, whereas regular PADs and PAD releases upon tiCS stimulation often had a tonic component (Table 5.1).

Table 5.1: Presynaptic interactions within the same and between two proprioceptive sense organs. Presynaptic inputs sorted in descending order by their source, i.e. whether originating from the fCO or tiCS and by their target afferents. Target afferents were subdivided ("type") into tiCS G6A and G6B ("source": fCO), into regular PAD and PAD release type ("source": tiCS, "target": fCO), or by the tiCS group from which the inputs originated ("source": tiCS, "target": tiCS 6A and 6B afferents). Numbers indicate the number of recorded afferents displaying these inputs out of the total number of respective afferents that were tested for the given sensory stimulus. Bottom rows: Numbers of respective inputs eliciting phasic-tonic, phasic, or tonic responses in the recipient afferent.

presynaptic inputs									
source	fCO			tiCS					
target	fCO afferent N = 27 / 28	tiCS afferent N = 9 / 15		fCO afferent N = 25 / 27		tiCS 6A afferent N = 4 / 5		tiCS 6B afferent N = 6 / 10	
type		tiCS 6A afferent N = 4 / 5	tiCS 6B afferent N = 5 / 10	regular PAD type N = 8 / 25	PAD release type N = 17 / 25	from tiCS 6A afferent N = 3 / 5	from tiCS 6B afferent N = 2 / 4	from tiCS 6A afferent N = 1 / 3	from tiCS 6B afferent N = 5 / 10
phasic - tonic	1	0	0	4	6	0	0	0	3
phasic	26	4	5	1	4	1	2	0	0
tonic	0	0	0	3	7	2	0	1	2

5.1.4 Discussion

Presynaptic afferent inhibition enables the gating of sensory inputs, and is one mechanism by which a sensorimotor network may control its gain (Burrows and Matheson, 1994; Wolf and Burrows, 1995; Clarac and Cattaert, 1996; Sauer et al., 1997; Torkkeli and Panek, 2002; Azim and Seki, 2019). While examples of presynaptic facilitation exist, these are usually mediated by mechanisms that differ from presynaptic inhibition (e.g. Siegelbaum et al., 1982; discussed in Clarac and Cattaert, 1996). Typically, presynaptic inputs involving GABAergic chloride conductances are considered to reduce the gain of sensory information that is of lesser relevance at a given moment. Thereby the gain, or salience, of relevant sensory feedback from other afferents is indirectly increased. It is important to note that this modulation of sensory gain is achieved by altering the amplitude of afferent action potentials. The information content of the firing pattern is usually not changed, only its impact on downstream networks due to the amount of transmitter released by action potentials of different amplitudes (Dudel and Kuffler, 1961).

The two types of inputs from tiCS onto fCO afferents shown here demonstrate that the mechanism underlying presynaptic inhibition could be used not only to downregulate fCO afferent gain (regular PAD type), but also for its upregulation (PAD release type, Fig. 5.1). The data suggests the hypothesis that the PAD release type responses in fCO afferents were the result of a disinhibition, i.e. a release from a tonic PAD, which equals a release from a tonic presynaptic inhibition. This is supported by the

observation that the amplitude of the presynaptically elicited hyperpolarization is increased, rather than decreased, when the afferent membrane is hyperpolarized by current injection. According to the PAD release hypothesis, the hyperpolarized afferent membrane is more negative than the reversal potential of chloride, thereby increasing the amplitude of the tonic PAD. Consequently, the hyperpolarization, thought to be the result of closing chloride channels and stopping the PAD, would appear to increase in amplitude. This is in accordance with the increased input resistance during the hyperpolarization, which, as a measure of membrane conductance, indicates the closing of ion channels. As a result of reduced membrane conductance, the shunt that the PAD effectively constitutes at this location on the afferent membrane would be removed, causing action potential amplitudes to increase, as was observed here.

Consistent with this hypothesis were the effects of blocking presynaptic PADs by the application of the $GABA_A$ antagonist PTX (Fig. 5.2). The overall membrane potential became more negative when the tonic PAD was blocked. As a result, the overall input resistance as the inverse measure of membrane conductance increased, and the amplitude of PAD release type effects decreased. The remaining hyperpolarization might have resulted from an incomplete block of presynaptic inhibition by PTX. The initial effects of PTX are typically observed 10 min following bath application, and it is difficult to maintain stable intracellular recordings from the fine afferent branches for much longer in addition to the required pre-application recording time.

These observations indicate that, despite their opposing effects on the fCO afferent membrane and action potential amplitude, the PAD release type responses found in this study might rely on the same cellular mechanisms as the regular PAD type responses that have been described before. Presynaptic effects of the regular PAD type decrease sensory gain transiently in response to, in this case, tiCS and fCO stimuli, whereas the gain of fCO afferents of the PAD release type was apparently constantly decreased and transiently released by tiCS activity.

The finding that proprioceptive information in fCO afferents was not only down-, but also upregulated broadens the possibilities of gating movement sensory feedback and of tuning the ensuing movement signal processing. It is therefore necessary to identify the type of information which is up- or downregulated to estimate the effects on downstream processing networks. fCO afferents can be characterized based on their sensitivity to tibial position, velocity, and acceleration (Büschges, 1994; Field and Matheson, 1998). Using these distinctions, it was possible to determine differences in the information content whose gain was in- or decreased (Fig. 5.3). Specifically, the gain of fCO afferents transmitting unidirectional information about changes in tibial position, i.e. velocity and acceleration, was increased. These sensory afferents not only carry information whether a movement has occurred, but also into which direction, whereas signals containing more general information from bidirectionally

sensitive afferents was suppressed. This indicates that in the presence of load, e.g. when the leg is in stance phase or encounters an external perturbation, movement signals containing information about the direction of movement become more relevant. Simultaneously, the relevance of non-directional information about movement is decreased. This must be considered together with the finding that fCO-mediated presynaptic inhibition was almost purely phasic, or present only during the velocity component of a movement, while most presynaptic effects from tiCS had a tonic component. The presynaptic modulation by load signals therefore represented a state-dependent-like effect while load is present. This effect was independent of the direction of load, i.e. whether tiCS G6A or G6B were activated. Movement signals, on the other hand, presynaptically transiently inhibited afferents as an update of changes in the status quo, i.e. phasically while the tibia was moving.

Drawing conclusions for walking must be done with caution, as all experiments were performed in the resting animal. Assuming, however, that the situation in the actively moving leg might be similar to the one observed here, the gain of load and movement afferents would be phasically decreased by fCO afferent-mediated presynaptic inhibition while the tibia was moving. During active movements, a large number of sensory signals is generated and the transient inhibition could prevent the system from being flooded with, and saturated by, sensory information. Once load is detected, the gain of more general fCO signals is decreased and directional information becomes more relevant. These distinct effects on sensory gain can be intuitively explained in the walking animal: Without load, during swing phase, deviations from the leg's trajectory will not have an effect on the walking animal as long as deviations into any direction do not significantly alter the duration or the location of the leg at the end of swing phase. During stance phase, however, in the presence of load, any deviation from the leg's trajectory will immediately impact walking kinematics, ground reaction forces, inter-leg coordination, and possibly even walking direction (cf. Dallmann et al., 2016; Dallmann et al., 2017). It must therefore be precisely compensated for, which requires information about the direction into which the deviation occurred. Furthermore, independent of walking, information about the direction of tibial movement can be used to infer the location, and possibly the strength, of an external perturbation. Berg et al. ruled out tiCS as the mediator of targeted searching movements around the location of an encountered perturbation, but tr/fCS might serve a similar purpose (Berg et al., 2013). In the inactive stick insect, velocity information is crucial for posture control and catalepsy (Bässler and Foth, 1982; Bässler, 1993). By increasing the gain of specific velocity information, load feedback might support this mechanism. It might also be the source of the phasic presynaptic inhibition of fCO afferents found in walking locusts (Wolf and Burrows, 1995). Furthermore, the complex interactions between load and movement afferents might explain some of the variability seen in the gain of movement processing in local premotor NSIs in Chapter 4 (Fig. 4.3).

No presynaptic effects of the PAD release type have been observed between fCO afferents themselves, between tiCS afferents, or from fCO afferents onto tiCS afferents. It must therefore be concluded that the presynaptic interactions between load and movement afferents are asymmetrical insofar that movement signal gain control in the presence of load is more differentiated than the reverse situation. The asymmetry of load and movement signal processing will be discussed in detail at a later point. Nevertheless, the complex pattern of presynaptic inhibition raises questions about the relevance of the upregulated fCO information for downstream processing that present possibilities for future research. Studies based on the data presented in this perspective Chapter 5 will have to substantiate the findings of the effects of blocking presynaptic inhibition with PTX, and investigate the source of the tonic PAD that is hypothesized to underly the PAD release type effects. In Chapter 4, one mechanism of how presynaptic afferent interactions influence downstream processing has been elucidated. Nevertheless, the complexity of the interactions suggests the presence of further possibilities by which the gating of sensory information might shape motor control.

The recordings of tiCS afferents shown here are the first extensive intracellular recordings of CS afferents, besides short excerpts of recordings in Chapter 4 and the work of Stein and Schmitz (1999). Increasing the number of these recordings will help to determine the specificity of presynaptic inhibition in these afferents. Aside from the presynaptic effects, an interesting observation was the high frequency of tiCS afferent responses in intracellular recordings, which seems to stand in contrast to the number of spikes identified on extracellular recordings of the ncr (cf. Chapter 2, Fig. 3.2, and Zill et al., 2011; Zill et al., 2012; Zill et al., 2013; Zill et al., 2017). Additional recordings form the individual tiCS afferents might also determine whether all of them have the same phasic-tonic response pattern that was found in this study.

5.2 Lateral Connectivity & Rhythmicity in the Network of Nonspiking Interneurons

5.2.1 Introduction

In Chapter 2, local premotor NSIs were established and introduced as a point of convergence within the premotor network (e.g. Burrows, 1987b; Laurent and Burrows, 1988; Laurent and Burrows, 1989b; Kittmann et al., 1996; Ludwar et al., 2005). In Chapter 3, differences between short- and long-latency sensory afferent inputs to NSIs were observed and used to infer mono- and polysynaptic connectivity between sensory afferents and NSIs. The results indicate that the different types of NSIs do not form a single layer within the premotor network, but are rather positioned at different levels of the sensory processing cascade. At this point, however, it is unclear whether individual NSIs that are part of different, or even the same, processing layer, are connected with each other to form a cross-linked network. Alternatively, NSIs could be positioned at different levels of parallel processing pathways without being synaptically connected, thereby essentially processing sensory information independently from each other.

A previous study on the locust has found unidirectional inhibitory connections between single pairs of NSIs that were not identified individually (Burrows, 1979). In Chapter 3, a double intracellular recording between NSIs E2 and E4 revealed reciprocal excitation (Fig. 3.3). Inferring the implications of synaptic connectivity on network function, however, requires more information on the extent of the interconnectivity, i.e. which NSIs are connected, and whether these connections are excitatory or inhibitory, unidirectional or reciprocal. A hypothetical network of interconnected NSIs that process distributed input from the same sense organs greatly increases the network's complexity, but potentially also its computational power. A parallel might be drawn to artificial neural networks, where the degree of interconnectivity and the number of layers increase the computational power of the network. This approach underlies the advanced capabilities of deep learning networks and artificial intelligence (Alzubaidi et al., 2021). Sensory signals would not be processed independently along parallel pathways, as synaptic connections between NSIs would cause the activity and sensory processing in a given NSI to depend on the activity of all NSIs that it is connected to.

These considerations led to questions about the coupling within the premotor NSI network. Assuming that synaptic connectivity between NSIs exists, how does this affect network coupling, i.e. the combined processing of the distributed inputs? In the following, initial data on the lateral connectivity within the NSI network will be presented. Specifically, simultaneous intracellular recordings from pairs of NSIs were used to reveal reciprocal excitation. Based on these experiments, the correlation between NSIs at rest was analyzed, leading to the discovery of relatively high-frequency rhythmic activity within specific NSIs in the absence of sensory stimuli.

5.2.2 Materials & Methods

Double and single electrode intracellular recordings from local premotor NSIs were performed according to the same procedures described in Chapter 3. Essentially, the recording procedure for double intracellular electrode experiments was the same as for single electrodes. Recording equipment was duplicated, and intracellular sharp electrodes were lowered through the ganglion sheath one after the other before searching for NSIs. Each NSI of a recorded pair was stained with a different dye (neurobiotin tracer (Vector Laboratories) or tetramethylrhodamine dextran (Invitrogen)) to allow for individual staining and identification.

Correlation of neural activity was analyzed between pairs of NSIs recorded simultaneously (cross-correlation, Fig. 5.6) or within single NSIs (auto-correlation, Fig. 5.7). In both cases, between 4 and 10 windows of 10 s duration were extracted from the recording traces. Only intervals of resting activity were included in the analysis, i.e. intervals during which the animal was not actively moving, no sensory stimuli were applied, no current was injected via the recording electrode, and no large fluctuations in membrane potential were observed. The remaining DC fluctuations were removed from the recording trace with Spike2 (CED). Traces were smoothed in Matlab (MathWorks). The results of this smoothing procedure were visually controlled for accuracy to avoid data distortion and maintain actual features of membrane potential oscillations while removing high-frequency noise. Z-scores were computed from smoothed data. Processed data was cross-correlated within each 10 s window between simultaneously recorded NSIs. For auto-correlation, each 10 s data trace was correlated with itself. Average traces show the average across all 10 s windows from the same recording. Auto-correlation frequency was calculated by measuring the period from the expected correlation peak of 1 at 0 ms to the first following peak. Average frequencies were calculated for each type of NSI, only NSIs in which rhythmicity was observed were included in the calculation of averages. Correlations were considered rhythmic if correlation strength showed peaks in addition to the auto-correlation peak at 0 ms. Fourier transformation was applied to raw, unprocessed data of the same 10 s windows for independent verification of correlation results.

5.2.3 Results

5.2.3.1 Reciprocal Excitation between Identified Premotor Nonspiking Interneurons

Different types of local premotor NSIs are part of the premotor network processing proprioceptive input from the leg and controlling motor output. To determine whether these NSIs form a network of interconnected neurons, simultaneous intracellular activity of 4 different pairs of NSIs was recorded (Fig. 5.5). NSIs were stained for unequivocal identification following each recording (Fig. 5.5 i, for morphology of identified NSIs, see also Suppl. Fig. 2.1). Depolarizing current was injected via one or the other recording electrode, and the effect on the respective other NSI's membrane potential was

recorded (Fig. 5.5 ii, iii). NSIs of types E2 / E4 (Fig. 5.5 A), E9 / E10 (B), I2 / E3 (C), and I3 / E3 (D) were recorded simultaneously, respectively. The pair E2 / E4 was recorded twice in different experiments, extracts from the second recording are included in Chapter 3. All recorded pairs exhibited reciprocal excitatory connections, i.e. each part of the pair was depolarized when positive current was injected into the respective other NSI.

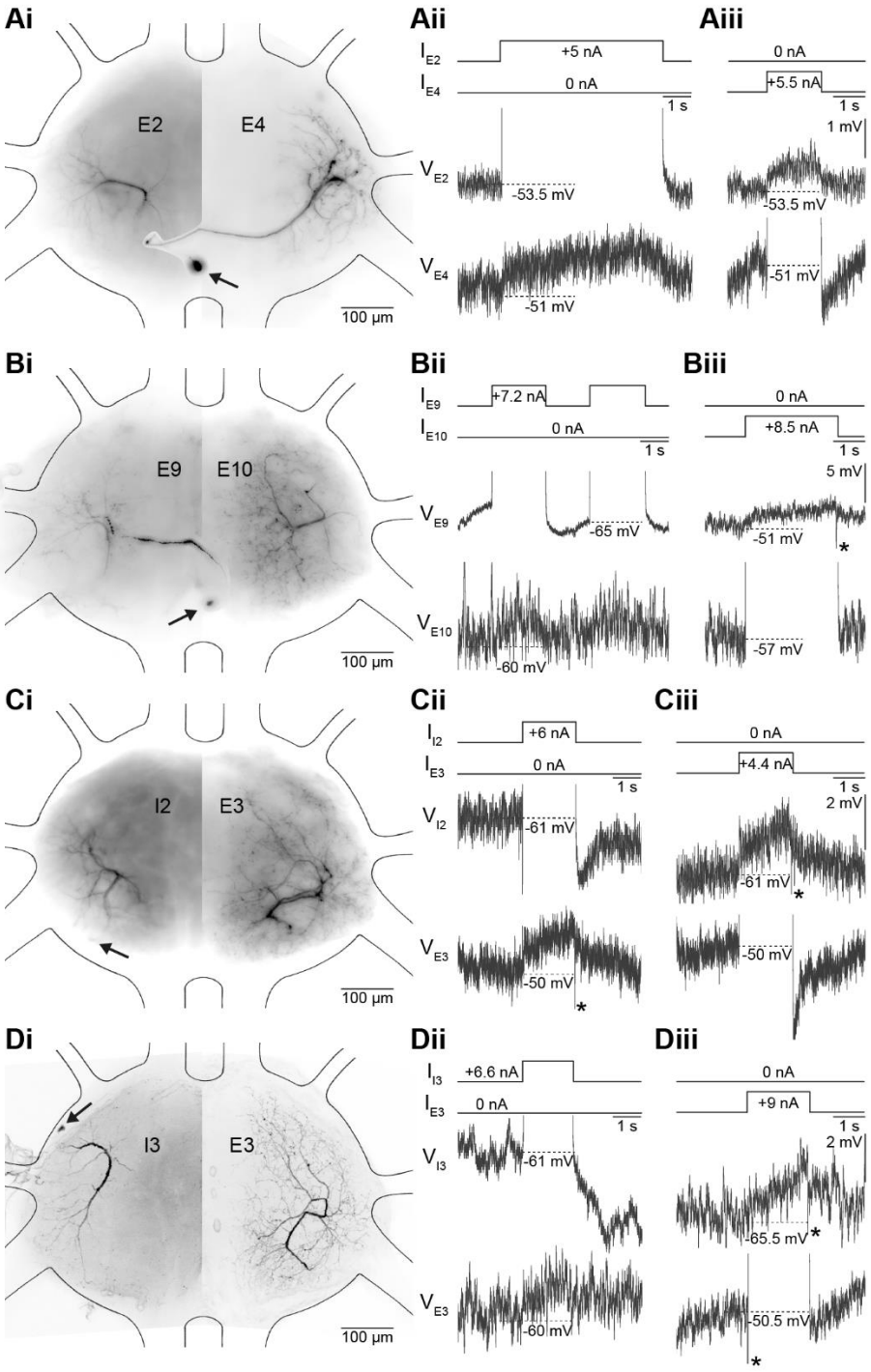

Figure 5.5: Reciprocal excitation between identified premotor NSIs. NSIs of types E2 / E4 (**A**), E9 / E10 (**B**), I2 / E3 (**C**), and I3 / E3 (**D**) were recorded simultaneously. Positive current injection into each NSI elicited a depolarization in the membrane potential of the respective other NSI. **i**: NSI morphology, NSIs on the left mirrored for this depiction, all NSIs were recorded from the neuropil of the same hemiganglion; location of somata indicated if detectable (arrow). **ii**, **iii**: Effects of current injection (I) on the respective other NSI's membrane potential (V_m). Resting membrane potentials indicated; asterisk: stimulation artifact.

NSIs show fast, small amplitude membrane potential fluctuations even in the absence of any external stimuli or apparent activity of the animal. To test whether the resting activity between NSIs was correlated, cross-correlation analysis between multiple 10 s windows of paired recordings was performed

(Fig. 5.6, for details on data processing and analysis, see Chapter 5.2.2). Both recorded E2 / E4 pairs showed a correlation peak with a temporal offset towards E4 (Fig. 5.6 A). Thus, the activity in E2 correlated with that of E4 with a time lag of 2.6 or 5.9 ms in both recordings.

The resting activity of E9 and E10 was not correlated (Fig. 5.6 B). E3, however, was rhythmically correlated with both I2 (Fig. 5.6 C) and I3 (D). The cross-correlation analysis revealed multiple peaks of increased correlation strength with a frequency of 31.3 and 28.6 Hz, respectively (Fig. 5.6 Ci, Di). The activity in E3 precede that of the simultaneously recorded NSI in both cases by 0.6 and 3.2 ms, respectively (Fig. 5.6 Cii, Dii).

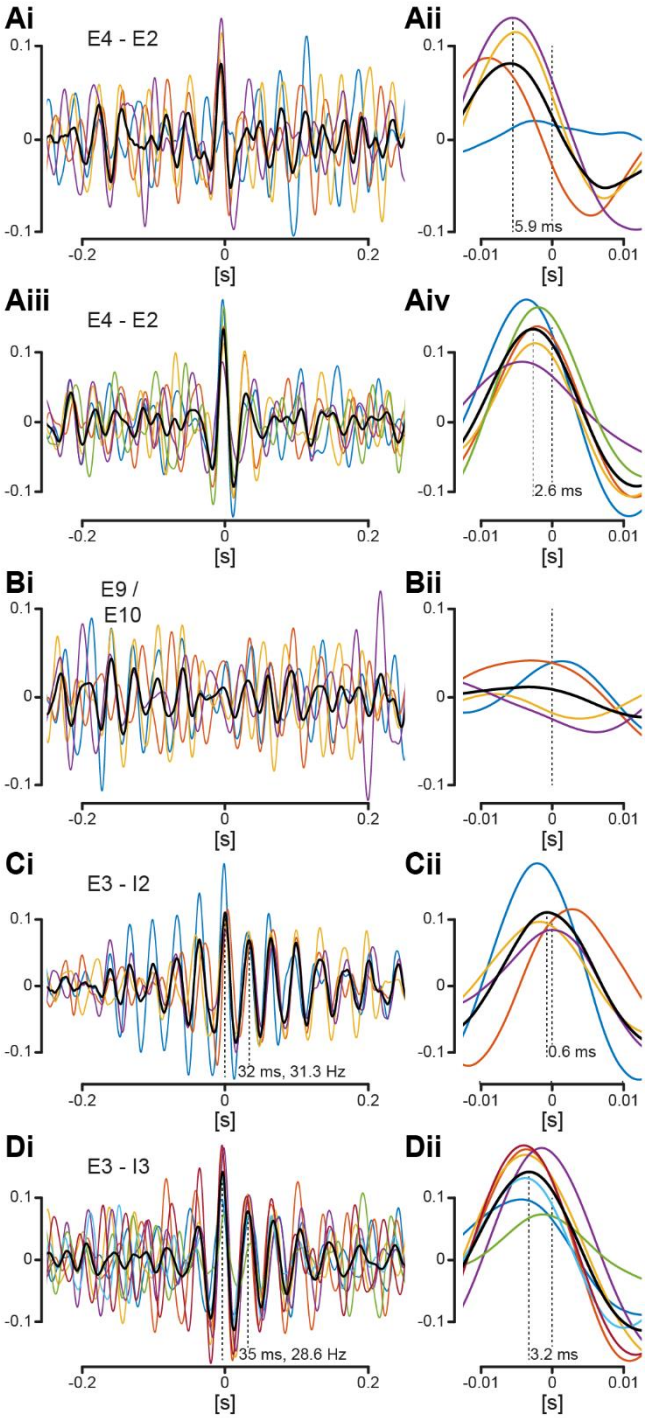

Figure 5.6: Cross-correlation between NSI resting activity in paired recordings. Simultaneous activity of NSIs E4 / E2 (**A**), E9 / E10 (**B**), E3 / I2 (**C**), and E3 / I3 (**D**) was cross-correlated (for details on data processing & analysis, see Chapter 5.2.2). Same recordings as Fig. 5.5, exception: for reciprocal excitatory effects of **Aiii**, **iv**, see Fig. 3.3. Correlation strength (y-axis) plotted against temporal offset (x-axis). Only data from inactive animals was included while no sensory stimuli or current injections were applied. Colored traces: data from individual 10 s windows; black trace: average. **ii** (**iv**): enlarged view of the area around 0 s in **i** (**iii**). Dashed lines in **ii** (**iv**): Temporal offset of cross-correlation peak from 0 s, offset length is indicated; the NSI whose activity precedes is named first in **i** (**iii**) (e.g. in A**i**, **ii**, E4 precedes E2 by 5.9 ms). Dashed lines in **Ci**, **Di**: Temporal distance between consecutive peaks of cross-correlation strength, period length and frequency are indicated.

5.2.3.2 Rhythmic Membrane Oscillations in Nonspiking Interneurons at Rest

The rhythmically correlated activity between NSIs shown in Figure 5.6 C, D raised the question whether the resting activity of a given NSI itself was also rhythmic. The presence or absence of rhythmicity in the activity of individual NSIs was determined by cross-correlating NSI activity with itself (auto-correlation, Fig. 5.7). No paired intracellular recordings were required for this analysis, thereby greatly increasing the sample size for each type of NSI. Auto-correlations were applied to NSIs of type E1 – 4, E9, E10, and I1 – 5 (Fig. 5.7). Auto-correlation results were complemented and supported by Fourier transformation regarding the presence or absence of frequency peaks in the single-sided amplitude spectrum (Fig. 5.7, insets in B).

The results were surprisingly consistent for a given type of NSI, both in whether or not auto-correlation showed rhythmicity, and, if so, at which frequency. With few exceptions, NSIs of type E1, E4, E9, and I3 showed rhythmicity in their auto-correlation at a narrow range of frequencies, typically around 30 Hz (Fig. 5.7 A, Bi, iv, vi, x). Note that in 3 recordings of E4, no rhythmicity was observed. A previous study has shown that two copies of E4 exist per hemiganglion, which might explain these seemingly heterogenous effects in E4 (Fig. A, Biv, v, Büschges and Wolf, 1995). A similar explanation might underly the effects in E9, which had previously also been stained twice in the same ganglion (data not shown). Note that rhythmicity in NSIs of type E9 was typically weak, indicated by only few additional peaks in the auto-correlation and a weak signal in the Fourier transformation (Fig. 5.7 Bvi). NSIs of type E2 showed a greater variability of frequencies that was on average lower than that of NSIs E1, E4, E9, and I3 (Fig. 5.7 A, Bii). NSIs of type I2 had on average a higher auto-correlation frequency (Fig. 5.7 A, Bix). Results for NSIs of type E10 were not consistent, as one recording showed rhythmicity, whereas two others did not (Fig. 5.7 A, Bvii). It is unknown whether multiple copies of E10 exist. NSIs E3, I1, I4, and I5 did not show rhythmicity in any recording, which was corroborated by the results of Fourier transformation (Fig. 5.7 A, Biii, viii, xi, xii).

The rhythmicity of membrane potential oscillations was also observed in the unprocessed intracellular recording traces, as shown for exemplary extracts from recordings of NSIs I2 and E3 in Figure 5.8. I2's membrane potential oscillated rhythmically with, in this example, an average frequency of 39.1 Hz (Fig. 5.8 A). The membrane potential of E3 also fluctuated, albeit with no detectable rhythmicity or pattern (Fig. 5.8 B).

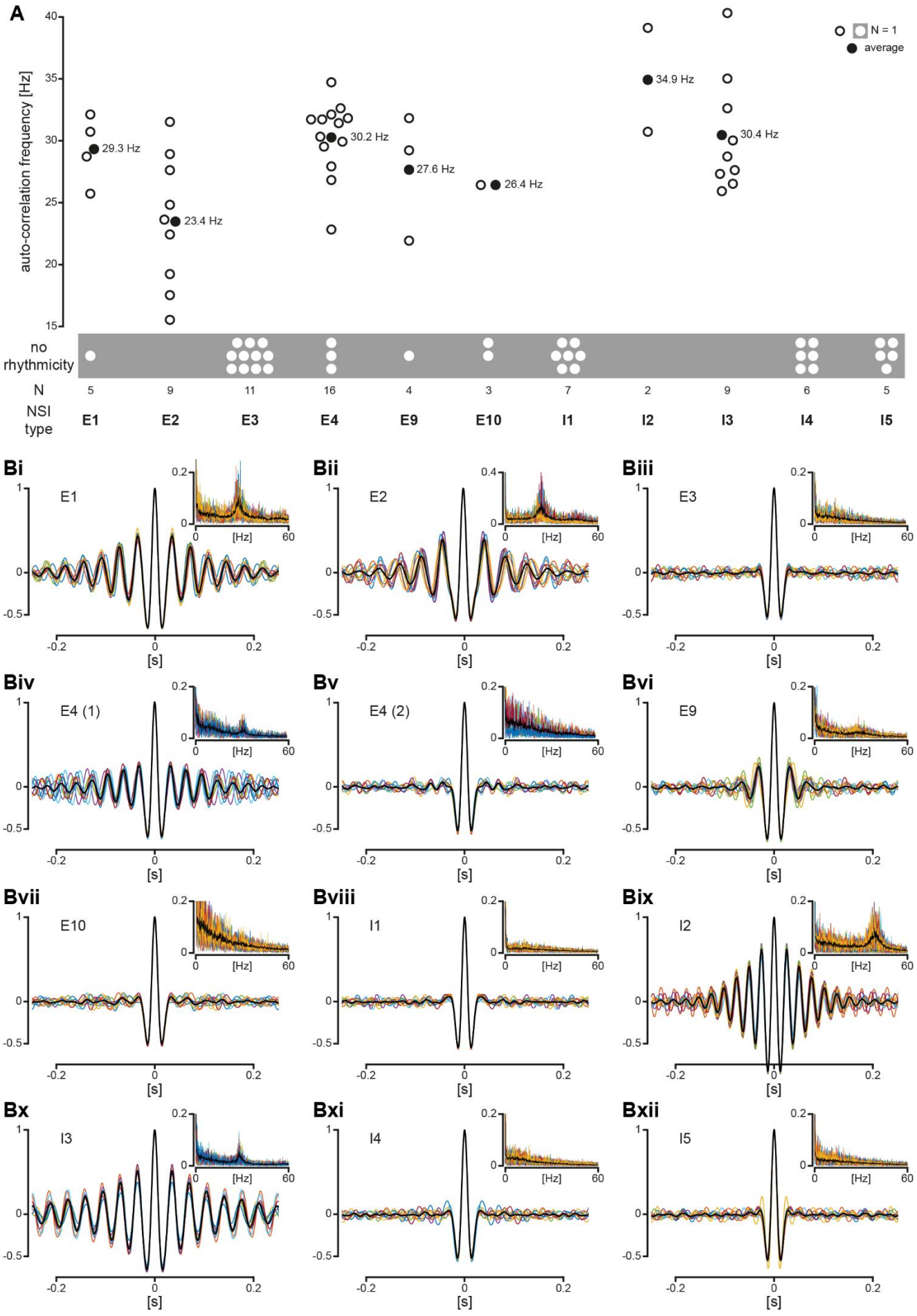
A
auto-correlation frequency [Hz]
N = 1
average
29.3 Hz
23.4 Hz
30.2 Hz
27.6 Hz
26.4 Hz
34.9 Hz
30.4 Hz
no rhythmicity
N
NSI type
E1
E2
E3
E4
E9
E10
I1
I2
I3
I4
I5
Bi
Bii
Biii
Biv
Bv
Bvi
Bvii
Bviii
Bix
Bx
Bxi
Bxii
[Hz]
[s]

Figure 5.7

Figure 5.7 (*previous page*): Rhythmic membrane oscillations in NSIs at rest. In the absence of external stimuli or self-generated movements, auto-correlation of the membrane potential showed rhythmic oscillations in specific types of NSIs. **A**: Auto-correlation frequency of individual types of NSIs; circles: individual NSIs, black dots: average frequency, white dots: no rhythmicity in auto-correlation. **B**: Exemplary auto-correlations for each NSI type; correlation strength (y-axis) plotted against temporal offset (x-axis). Only data from inactive animals was included while no sensory stimuli or current injections were applied. Insets: Fourier transformation of the same, but unprocessed, data as used for the respective correlation plot. Single-sided amplitude spectrum (y-axis) of frequency range up to 60 Hz. All plots: colored traces: data from individual 10 s windows; black trace: average.

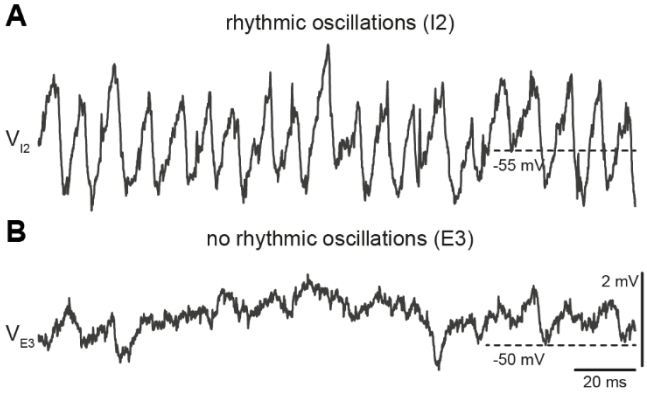

Figure 5.8: Exemplary intracellular traces of NSIs exhibiting rhythmic oscillations (**A**, I2), or non-rhythmic membrane fluctuations (**B**, E3). Correlation analysis of the NSIs depicted here are shown in Fig. 5.7 Biii (E3), Bix (I2). V: membrane potential; dashed line: resting membrane potential.

5.2.4 Discussion

Proprioceptive and other types of input are known to be distributed to the set of premotor NSIs that control leg movements (Büschges, 1990; Burrows, 1996). Typically, these are described as individual pathways, whose antagonistic properties, for example, are summarized to generate motor output or the weighting of which can be adapted to generate reflex reversal (Bässler and Büschges, 1998). In this study, the view of the NSI network as mostly independent, parallel pathways was tested and challenged by the results of paired double intracellular recording experiments. All recorded pairs of NSIs demonstrated reciprocal excitation (Fig. 5.5). Even in the absence of external stimuli or self-generated movements of the animal, the membrane potential fluctuations of some NSIs were correlated, including rhythmic correlations (Fig. 5.6). Additionally, a number of NSI types showed rhythmic oscillations of their membrane potential (Fig.s 5.7, 5.8). The frequencies of these rhythms, both within and between NSIs, covered the same narrow range and, with few exceptions, were consistent across animals.

A previous study had found inhibitory, unidirectional connections between premotor NSIs (Burrows, 1979), which stands in contrast to the reciprocal excitation reported here. In the experiments by Burrows, however, NSIs were not individually identified, therefore the results are not necessary contradictory. A larger sampling size of paired recordings will be required to determine the range of the interactions between premotor NSIs. Nevertheless, both Burrows' and the present study clearly show the presence of lateral connectivity within the NSI network. Reciprocal interconnections between NSIs

might have far-reaching implications for premotor processing and the sensory integration underlying motor control. Assuming two hypothetical NSIs, A and B, performing computations X and Y, respectively, then a reciprocal connection between A and B would result in signal computations in the order of X-Y, or Y-X, depending on whether signals are transmitted first to A or B. As described in Chapter 3, the functional connectivity of NSIs changed with the sensory context. In terms of sensory processing, this means that a different NSIs will receive short-latency, unprocessed sensory inputs depending on the sensory context. Note that for the sake of simplicity, presynaptic afferent effects on sensory signals are not considered here. To understand the effect of these alternative functional connections on network computation, knowledge about NSI interconnectivity is essential. Altering the order of computations might result in different outputs based on similar inputs and the same network components.

From the present data, no definite conclusion can be drawn as to whether the connections between NSIs were based on chemical or electrical synapses. Some NSIs were hyperpolarized when negative current was injected into their recorded partner, in addition to the excitatory effects upon depolarization shown in Figure 5.5. This is usually considered an indicator for an electrical synapse. Some NSIs, however, tonically release transmitter at their resting membrane potential (Burrows and Siegler, 1978), which would result in the same observation of seemingly excitatory and inhibitory effects onto the postsynaptic NSI. At present, chemical synapses seem to be the most likely hypothesis because changes in the membrane potential of the postsynaptic NSIs were small and did not indefinitely follow the amplitude of current injected into the presynaptic NSI, indicating saturation of chemical synapses.

Interestingly, local premotor NSIs were not only connected, i.e. their activity was not only correlated, when one of them was depolarized by current injection. E2 and E4, and E3 with both I2 and I3, showed correlating fluctuations of their membrane potential at rest. Specifically, activity in E3 was rhythmically correlated with, and preceded that of I2 and I3. It is important to note that the correlation of membrane fluctuations between NSIs per se does not allow inference of causality. All three NSIs could receive the same input, with different temporal shifts, from an unidentified source.

An indicator of causality, nevertheless, can be found in the activity and correlation of E3, which was rhythmically correlated with I2 and I3, but not rhythmic itself. The membrane potential of both I2 and I3, by contrast, showed rhythmic oscillations that were in a range similar to the rhythmic cross-correlation with E3. A possible hypothesis explaining these results suggests E3 as a reference point for I2 and I3. The frequency of the oscillations would represent a sort of metronome, or sampling frequency, at which I2 and I3 adjust their activity to match either a depolarization, hyperpolarization, or another, unknown state variable in E3. This form of rhythmic “sampling” of non-rhythmic E3 membrane oscillations by I2 and I3 could explain the time shift and rhythmicity in their correlation with E3, as well as the rhythmicity of their own activity. According to this hypothesis, E4 and E2, whose activity was

correlated without rhythmicity, and which themselves showed rhythmic oscillations, could play similar roles as I2 and I3. Both would be "sampling" from an unknown third NSI serving the same function as E3 for I2 and I3, causing their oscillations to be correlated, but not rhythmical. Following these explanations, E9 and E10 would not be part of the same oscillatory network, as their activity was not correlated and they showed only weak, or no rhythmicity in their membrane fluctuations.

These hypothetical considerations require further experimental support, and, potentially, computational circuit modeling. The large sampling size of individual NSIs, however, allows more definite conclusions on the presence of a strong rhythmicity in the membrane fluctuations of specific types of NSIs. NSIs of types E1, E2, E4, I2, and I3 showed strong rhythmicity in the absence of sensory input, and, with the exception of E2, their oscillations were restricted to a narrow range of frequencies around 30 Hz. The presence of this constant frequency across NSIs and animals and in the rhythmic cross-correlations between NSIs implies a functional relevance for the rhythmicity or its underlying cause.

Rhythmic oscillations, or synchronization, of networks are the focus of many studies on attention and sensory awareness in the vertebrate brain (review in Engel and Singer, 2001), and have also been reported in the olfactory and visual systems of locusts and *Drosophila melanogaster*, respectively (Laurent and Davidowitz, 1994; Grabowska et al., 2020). In the nervous system of *Drosophila melanogaster*, oscillatory activity in the range of 20-30 Hz is modulated with the salience of a stimulus, and can be linked to visual attention (van Swinderen and Greenspan, 2003; Grabowska et al., 2020). There are, however, crucial differences between these studies and the oscillations reported here. Most studies focus on sensory processing in the brain, while in this case rhythmicity occurred in the ventral nerve cord in the explicit absence of external stimulation. Oscillations therefore cannot be interpreted as a sign of focusing attention on a specific input, howsoever such a focusing would manifest in a proprioceptive network. Additionally, the network investigated here consists of nonspiking neurons. Thus, no immediate comparisons to rhythmic spiking networks with spike synchronization and coincidence detection can be drawn.

In this and the preceding Chapter 5.1, initial results are presented to provide starting points for hypothesis building and to guide future investigations. As discussed above, further questions need to be answered to fully understand the relevance of lateral connectivity between local premotor NSIs for sensorimotor processing. These include the origin of the oscillations, i.e. the mechanism, neuron, or network architecture that gives rise to the oscillations in membrane potential across and between NSI types. Rhythmic synchronization can be induced by common inputs to individual elements of the network, or by lateral connections within the network (Niebur et al., 2002). Synchronization via lateral connectivity can be based on recurrent inhibition, which does not seem applicable in the present case as recurrent connections were excitatory. Alternatively, it can be elicited by an intrinsic oscillator that

entrains the network, or by delayed mutual excitation, both of which represent possible hypothesis for the premotor network of the stick insect leg (Ritz and Sejnowski, 1997).

Another aspect to be investigated is the function of the synchronization. Here it will be important to know the source or the mechanism of the oscillations to determine whether they are the observable side effects of unknown network or neuron properties, or whether the oscillations themselves have a function. Synchronization facilitates the association of distributed networks, especially of networks integrating different parameters of a (sensory) input (König and Schillen, 1991; Ritz and Sejnowski, 1997). This difficulty, also known as binding problem, arises as a consequence of neuron assemblies that are required to process a given input parameter while other features of the information are superimposed onto the same network. Temporal coordination within a network is improved by synchronized oscillations, which can solve this binding problem (König and Schillen, 1991; Buzsáki and Draguhn, 2004).

Note again that in this case NSIs were synchronized in the absence of sensory processing, which might, however, be considered as a preparation for any incoming sensory inputs that will then require binding of a distributed network. Entraining the, in comparison to MNs and sensory afferents, "noisy" resting activity of premotor NSIs could prepare the network for incoming stimuli. This might be especially relevant in the context of distributed sensory input. If resting activity of the NSI network would be asynchronous, an incoming input will impinge onto, at this instant in time, more and less receptive NSIs. The weighting of the more receptive NSIs would be relatively larger in an unpredictable way, thus increasing the noise or instability of sensorimotor processing. A synchronized network could support input selection and have larger, and more tightly controlled, effects onto its postsynaptic targets (Buzsáki and Draguhn, 2004). Identifying the function of the network oscillations will also provide insights into the functional difference between NSIs that were found to be rhythmic and those that showed no rhythmicity in the auto-correlation analysis.

To approach these questions, further paired double intracellular NSI recordings will be required. The resulting cross-correlations between NSIs will help to establish the network architecture and potentially lead to the origin of the oscillatory patterns. The latter will have to be further characterized by input resistance measurements and during tonic current injections, which will determine whether they are based on synaptic inputs or NSI properties (cf. Laurent, 1993). Sensory stimuli can be used to test whether rhythmicity breaks down or is enhanced during actual sensorimotor processing. Pharmacological or physical blocking methods, i.e. blockers of GABAergic, glutamatergic, or cholinergic synaptic transmission and cutting of connectives and lateral nerves, will determine whether the oscillations emerge intrinsically from NSI properties, originate from tonic sensory, intersegmental, or local inputs, or are an emergent property of the NSI network itself.

6 General Discussion

6.1 Summary of Results & Ensuing Implications for Multimodal Proprioceptive Integration in Sensorimotor Networks

As a multimodal sense, proprioception depends on the integration of sensory feedback from distinct sense organs. Therefore, the nervous system is faced with the task of combining information of different sensory modalities and about different parameters of the same modality into a single coherent neuronal representation. This representation of the animal's proprioceptive context must be sufficiently detailed to enable appropriate motor responses, while remaining flexible enough for adaptive behavior in complex surroundings. In many experimental model organisms, such as mice, cats, and other vertebrates, populations of interneurons in the premotor networks of the spinal cord have been identified as major sites of signal integration, including proprioceptive sensory feedback (reviews in Pearson, 2004; Grillner, 2006; Jankowska, 2013a; Grillner and El Manira, 2020). Consequently, the starting point of this dissertation was to identify the neuronal point of convergence and integration of multimodal proprioceptive feedback in the premotor network of the stick insect leg.

In invertebrates, specifically large insects such as locusts and stick insects, single neuron recordings have demonstrated the existence of converging signal pathways onto single interneurons (e.g. Burrows, 1985, 1989; Laurent and Burrows, 1989b; Büschges et al., 1994; Burrows, 1996; Hess and Büschges, 1997). Furthermore, recent studies using the genetic toolkit of *Drosophila melanogaster* have identified interneuron populations as candidates for multimodal signal integration (Tuthill and Wilson, 2016b; Agrawal et al., 2020). In the premotor network of the stick insect leg, single neurons are identifiable and accessible to intracellular recordings in the semi-intact animal, while stimuli are applied to individual sense organs. In this dissertation, taking advantage of the accessibility of individual elements of the network, I analyzed the sensorimotor pathways of multimodal proprioceptive integration from sensory afferent input via the network of interneurons to the motor output. An advantage of studies on large insects is the possibility to record intracellular activity from neuropilar arborizations. Thereby it is possible to detect small changes in membrane potential that are not transmitted to the soma, which, in invertebrates, is typically not involved in electrical signal transmission (review in Matheson, 2002). Recordings from the neuropil can therefore detect small responses to sensory stimuli, and determine with higher confidence whether a neuron does or does not receive inputs from a given source than recordings from the soma.

Based on these methodological considerations, this dissertation's analysis of sensorimotor processing in different types of NSIs, but also in sensory afferents and MNs, was not restricted to predetermined individual neurons. Using this unbiased approach, single neuron responses to sensory stimuli were

combined with the analyses of network and population effects. Focusing on the sensorimotor control loop of the FTi joint, I analyzed the integration of two proprioceptive senses, load and movement, against the backdrop of established information on movement feedback transmission (Burrows, 1987a; Burrows et al., 1988; Büschges, 1990, 1994). In the many years of previous research on large insects, movement signal processing has been established to be distributed and antagonistic (Büschges, 1990; Sauer et al., 1996), and the role of the premotor circuit and specifically local premotor NSIs in motor control has been demonstrated repeatedly (e.g. Burrows, 1980 (MN recruitment); Büschges and Schmitz, 1991 (resistance reflex); Büschges et al., 1994 (walking); Büschges, 1995 (rhythmicity); Kittmann et al., 1996 (leg reflexes & voluntary movements); Bässler and Büschges, 1998 (review); von Uckermann and Büschges, 2009 (walking); Berg et al., 2015 (searching)). In addition, the relevance of load feedback for motor output has been studied extensively (e.g. Zill et al., 1981; Schmitz, 1993; Zill et al., 2004; Zill et al., 2012; Zill et al., 2013, 2015; Haberkorn et al., 2019).

Based on this wealth of information, local premotor NSIs were hypothesized to be the most likely candidate for spatial summation of load and movement signals. And indeed, NSIs that are part of the FTi joint control loop by coordinating the activity of ExtTi MNs were established as a point of convergence for proprioceptive signals from movement (fCO) and multiple load sense organs (tr/fCS, tiCS) in Chapter 2 (Fig. 6.1 A). Similar to fCO signals (Büschges, 1990), load signals from the stimulated groups of CS (groups 1-6) were distributed onto all NSIs of the FTi control network that were found in the unbiased search, including 3 types of NSIs that were characterized for the first time in this study. NSIs integrated feedback signaling movement of the tibia (fCO) and load feedback from the same (tiCS) and adjacent (tr/fCS) leg segments, i.e. load within and orthogonal to the leg plane (cf. Zill et al., 2012). Additionally, antagonistic processing, i.e. signal transmission along parallel pathways that support or oppose the final motor output, was found to not only apply to movement signals (Büschges, 1990; Sauer et al., 1996) but also to load feedback. Intriguingly, these findings implicate not only a few specific NSIs in the integration of load and movement feedback, but show that the NSI network as a whole is the point of convergence. Consequently, multimodal proprioceptive integration must be analyzed, and can only be understood, by looking at network activity and populations of neurons.

To determine whether signal integration in the network controlling leg movements is as homogeneous as the spatial summation in Chapter 2 suggested, the timing of load and movement signal processing was analyzed (Chapter 3). Although both types of feedback converged onto the same NSI network (spatial summation), there was a persistent time difference in their signal transmission to and within the premotor circuit (temporal summation, Fig. 6.1 B). Signals elicited by fCO stimulation were transmitted to the ventral nerve cord with a shorter latency than CS signals. tr/fCS signal transmission was faster than tiCS, but did not reach fCO values despite comparable distance between the sense organ's

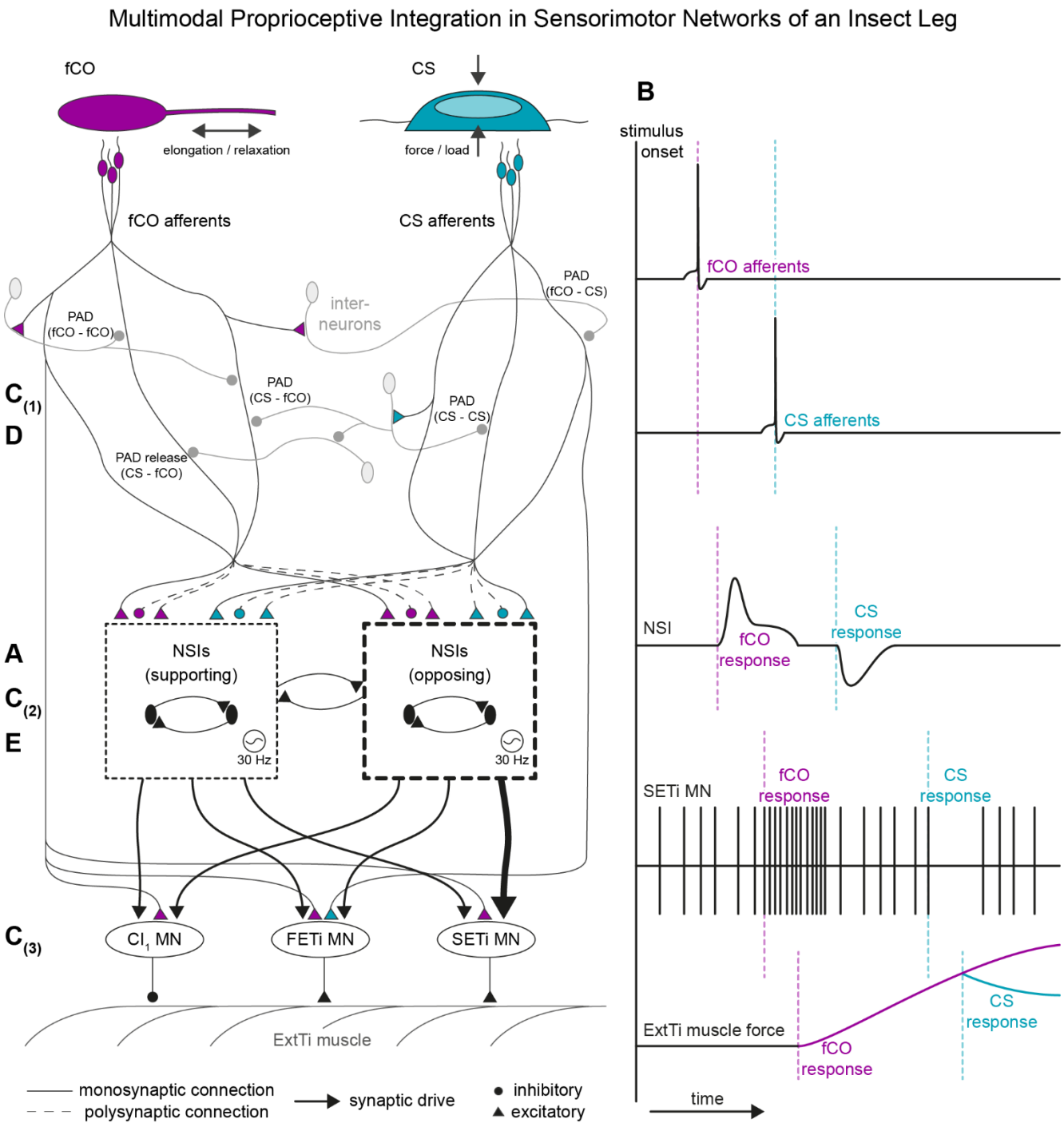

Figure 6.1: Multimodal proprioceptive integration in sensorimotor networks of an insect leg. Schematic depiction of results presented in this dissertation. Proprioceptive information from load (CS) and movement (fCO) sense organs is distributed into an antagonistic network of local premotor NSIs (**A**). Movement signal transmission along sensorimotor pathways is faster than load processing (**B**). Load signals alter movement signal gain in NSIs and MNs by presynaptic afferent inhibition (**C**$_{(1)\text{-}(3)}$). Presynaptic interactions between load and movement afferents are widespread and diverse (**D**). The premotor NSI network is connected by reciprocal excitation and synchronized 30 Hz oscillations (**E**).

position on the leg and the central premotor networks. Notably, the delay of load signals was already present at the level of sensory afferent projections within the neuropil, persisted within the premotor NSI network, and was functionally relevant as it affected ExtTi MN output and muscle force. Short-latency, i.e. potentially monosynaptic, connections from fCO to NSIs were common, whereas short-latency CS connectivity was more specific and, apart from NSI type E1, restricted to either tiCS or tr/fCS, but not both. Similar results were found for connections between sensory afferents and MNs; while short-latency fCO connections were found in all three ExtTi MNs, tiCS elicited fast excitation only in FETi but not in SETi or CI_1. Functional connectivity, i.e. which elements of the NSI network were the first to respond to a sensory input, depended on the sensory context of the leg and, therefore, on the applied sensory stimuli. This was supported by reciprocal excitation between a pair of NSIs, indicating that NSIs may switch positions within the signal processing cascade depending on the sensory context. The findings in Chapter 3 demonstrate a temporal hierarchy of sensory processing that had not been previously observed in proprioceptive integration. Despite the homogeneous distribution of load and movement signals onto the entire NSI network (Chapter 2), their integration was markedly different with regard to temporal summation and monosynaptic connectivity. These findings provide experimental support for the hypothesis that both sensory modalities fulfill distinct roles in motor control, and that proprioceptive integration is asymmetric (see also Chapter 6.3). Specifically, it could indicate a network that processes detailed movement information and which is tuned, or modified, by load feedback.

This hypothesis was tested in Chapter 4. It was found that load and movement feedback were not processed independently, and their network effects could not be described by simple linear signal summation (Fig. 6.1 C, Chapter 4). Multimodal signal interaction occurred at the earliest neuronal stage via presynaptic afferent inhibition from load (tiCS) onto movement (fCO) afferents that reduced fCO afferent action potential size (Fig. 6.1 $C_{(1)}$). In postsynaptic NSIs, signals from both sense organs were summed nonlinearly, and sensorimotor gain of movement responses was altered. The effects were neuron-specific and depended on movement stimulus parameters (velocity / amplitude). Notably, the amplitude dependence was upregulated in NSIs opposing the movement reflex response in the ExtTi MN SETi (Fig. 6.1 $C_{(2)}$). Consistently, SETi amplitude dependence was reduced. This is the first time that experimental results provide a mechanism for how a distributed, antagonistic network can be modified and shaped into a (temporarily) dedicated network by the presence of feedback from another sensory modality (Fig. 6.1 $C_{(3)}$). Load was therefore able to tune movement signal processing, establishing a mechanism by which presynaptic inhibition can shift the balance of an antagonistic, distributed network in a context-dependent way. If found to be present not only in the inactive, but also in the walking animal, sensory feedback-dependent contextualization at the local level will have far-reaching

implications for our understanding of how the swing and stance phase of walking are coordinated (see Chapters 4.7, 6.2, & 6.3 for further discussions).

Further in-depth analysis of the presynaptic afferent interactions between tiCS and fCO afferents identified a complementary mechanism to presynaptic inhibition (Fig. 6.1 D, Chapter 5.1). Harnessing the machinery of regular presynaptic inhibition mediated by PTX-sensitive PADs, the gain of fCO afferents transmitting unidirectional information about tibial movement was upregulated by a release from tonic presynaptic inhibition. The PAD release type effects were mediated by load stimuli and effectively represented a disinhibition of the respective fCO afferent. Regular, PAD-mediated presynaptic inhibition also occurred in tiCS afferents, evoked by fCO or other tiCS afferent activity, but no upregulation of signal gain was observed in tiCS afferents. Additionally, fCO afferent-mediated effects were mostly transient, whereas load-evoked effects were tonic. Thus, presynaptic afferent signal gain control of load and movement afferents was asymmetric and more complex than previously known. The majority of sensory afferent signals was modulated presynaptically. Consequently, the postsynaptic premotor network will receive sensory inputs that for the most part have already been contextualized and modified by other sensory and non-sensory inputs (cf. Burrows and Matheson, 1994; Wolf and Burrows, 1995; Sauer et al., 1997). The upregulation of salient sensory inputs by a release from tonic presynaptic inhibition presents a complimentary mechanism to the downregulation of less relevant information by means of regular presynaptic inhibition. This bidirectional modulation of sensory gain broadens the possibilities for how sensory input can be weighted as it enters the premotor network. Lateral connections between sensory afferents thereby constitute a first signal processing layer that determines the signal gain of information which is passed on to the downstream network.

Lateral connectivity was not only present at the sensory input level of the premotor network, but also between premotor NSIs (Fig. 6.1 E, Chapter 5.2). Supporting the hypothesis formulated in Chapter 3 that NSIs might change their position within the signal processing cascade depending on the current sensory context, reciprocal excitatory connections were found between pairs of NSIs in simultaneous intracellular recordings. Additionally, fluctuations of their membrane potential in the absence of external stimuli were correlated between individual pairs, with some of the correlations showing rhythmicity. The frequency of these rhythmic cross-correlations was similar to that of rhythmic oscillations that specific types of NSIs demonstrated consistently. NSI rhythmicity, or the absence thereof, was consistent across recordings of a given type of NSI. The results suggest the existence of a mechanism for synchronizing NSI network activity, thereby potentially increasing network coupling and processing strength. NSIs lie at the center of spatial summation of load and movement integration (Chapter 2), of the effects of temporally shifted summation on motor output (Chapter 3), and are the mediators of load-induced gain control of movement signal processing (Chapter 4). Therefore, gaining insights into

the mechanisms and functions of premotor NSI network interactions will deepen our understanding of the computations underlying sensorimotor processing.

In the following, I will discuss the relevance of the findings of this dissertation in the context of an antagonistic network architecture, with a specific focus on how such a network may be tuned to achieve specific outputs. I will also highlight the conceptual differences of load and movement feedback, and how these are reflected at different stages of the sensorimotor processing cascade. Finally, I will expand on the importance of understanding proprioception not as a summation of individual sensory modalities, but as a multimodal sense that emerges from the nonlinear interaction of sensory signals.

6.2 Multimodal Proprioceptive Integration in an Antagonistic Network

Movement feedback from the fCO is processed by a distributed, antagonistic network. The signals are transmitted and processed through multiple, parallel pathways before impinging on the ExtTi MNs. The responses of these individual pathways, together with their effects on downstream MNs, either support or oppose the motor response to the initial sensory stimulus (Büschges, 1990; Sauer et al., 1996). This type of network architecture is thought to confer behavioral flexibility. By shifting the weighting between individual pathways, the same set of neurons may partake in multiple behaviors, such as different walking directions, searching behavior, or reflex reversals (discussed in Bässler and Büschges, 1998; Büschges and El Manira, 1998). A similar network structure is expected to underly locomotor control in cats and other vertebrates, confirming its advantages for signal processing in local networks (Duysens et al., 1990; cf. Pearson, 1993).

To reduce the complexity of the system, previous studies have focused mainly on the processing of single sensory modalities. Under natural conditions, however, the nervous system simultaneously receives proprioceptive signals from more than one sense organ. As it is shown in this dissertation (Chapter 2), load feedback does not reduce the complexity of sensorimotor processing by its immediate actions on the membrane potential of NSIs. For example, by exciting resistance reflex opposing pathways and thereby supporting a reflex reversal, the antagonistic movement pathways could hypothetically be sorted, but at the cost of reducing flexibility by hardwiring load onto a movement processing network. Instead, load added another level of complexity by being distributed and eliciting antagonistic responses in the same pathways that movement feedback occupies. The effects of load signals on the membrane potential of local premotor NSIs by themselves did not sort the antagonism of the fCO-induced network responses. They can therefore only to some extent explain how load alters the strength of movement-feedback reflexes (Schmitz and Stein, 2000) or increases the likelihood of a reflex reversal to occur (Akay and Büschges, 2006). Note that the experiments by Akay and Büschges

(2006) were done on the group of CS on the femur (group 5), but preliminary data showed a similar effect of tiCS on the occurrence of the active reaction (see Suppl. Table 6.1).

These findings indicate a more complex integration of load signals into movement feedback processing than simple linear signal summation at the NSI membrane. Reflex reversal in the presence of exclusive fCO feedback depends on shifting the weighting of pathways presynaptic to the NSI network (Driesang and Büschges, 1996). Presynaptic inhibition of individual fCO afferents might mediate this shift (cf. Wolf and Burrows, 1995; Sauer et al., 1997), suggesting that load signals could act on movement processing via the same mechanism. Stimulation of tr/fCS (Stein and Schmitz, 1999) and tiCS (Chapters 4 & 5.1) was indeed found to alter presynaptic action potential size in fCO afferents. Consequently, not only the absolute membrane potential was altered in postsynaptic NSIs by the immediate, mono- or polysynaptic, action of CS afferents, but also the gain of the NSI's movement responses was altered in the presence of load. Interestingly, specifically the amplitude dependency, or gain, of NSIs opposing the resistance reflex was increased, independent of the sign of the NSI's response to CS stimuli. The resulting decrease in SETi amplitude dependence reduced the strength of the resistance reflex, indicating a shift towards a reflex reversal and an active response. In the stick insect, the active response to an elongation of the fCO consists of two parts. In the first part, SETi activity stops and is reinitiated during the second part (review in Bässler and Büschges, 1998). The reflex reversal, from resistance reflex and SETi activation to active response and SETi inactivation, can therefore be seen as an extreme case of altered gain, one in which the gain is completely reversed. Under this regard, the network effects of load on movement signal processing described in Chapter 4 might very well explain the increased likelihood of occurrence of reflex reversals described by Akay and Büschges (2006). Gain reversals were in fact observed in some NSIs (Chapter 4, Figure 4.3).

Although themselves distributed onto and processed by antagonistic pathways, load signals coordinated, by their action on movement signal processing, the balance between antagonistic movement processing pathways. By increasing the gain of specific pathways, load dedicated the network towards a specific behavioral response in the sensory context of multimodal proprioceptive feedback. This is very likely to be one of many mechanisms by which load influences network processing, and by which the antagonistic network can be tuned. In fact, the results presented in this dissertation indicate the complexity of the interactions by highlighting the distinct effects of load on the movement response of individual ExtTi MNs (FETi, SETi, CI_1, Fig. 4.4), the dependence of the effects on movement stimulus parameters, and the diversity of the effects on individual NSIs (Fig. 4.3). These effects are complemented, and at least partially caused by, the diverse presynaptic interactions that were found between proprioceptive afferents, which in- or decrease load and movement signal gain before these signals are processed by the local network. Additionally, the effect of timing delays in load signal transmission will result in load signals from the, in terms of milliseconds, more distant past affecting the processing

of relatively more recent movement signals. The shift in time might have important implications for proprioceptive processing by determining which sensory signals are combined by the network.

The modulation of movement feedback gain in the premotor network in the presence of load signals via presynaptic inhibition establishes one way to tune a distributed, antagonistic network. Future lines of study include the possibility of load effects themselves being dependent on the behavioral context. Furthermore, the presynaptic modulation of both load and movement signal gain raises the question which and how other signals contribute to the control of proprioceptive sensorimotor gain. In locusts and crayfish, for example, presynaptic afferent inhibition is modulated during (fictive) locomotion (El Manira et al., 1991; Wolf and Burrows, 1995). It will therefore be essential to investigate how the findings of this dissertation translate to the actively walking animal.

6.3 Distinct Roles of Movement & Load for Multimodal Proprioceptive Integration

During walking, a stepping leg encounters continuously changing joint movements, load, and forces (Dallmann et al., 2016; Zill et al., 2018). These activate distinct load and movement sense organs, whose signals are summed spatially within the network of local premotor NSIs (Chapter 2). The temporal summation within the premotor network is shifted insofar that load signals are processed later than the corresponding (i.e. simultaneously elicited) movement signals (Chapter 3). The temporal shift may have strong implications for multimodal proprioceptive integration in sensorimotor networks, including: 1) Delayed load signals arrive in time to tune ongoing movement processing; 2) load and movement feedback have distinct roles in the sensorimotor network; 3) the delay of load signals has a functional purpose in proprioceptive signal processing. The first point has been highlighted in Chapter 6.2, the second and third will be discussed in the following.

Despite their convergence onto the same set of premotor NSIs, load and movement feedback may serve distinct roles in sensorimotor control. This view is supported by the distinct timing of signal transmission from CS and fCO afferents. The temporal shift between load and movement feedback will result in spatial summation of multimodal proprioceptive signals from different time points, i.e. more recent movement signals with preceding load signals. Moreover, it may affect the sensorimotor gain control described in Chapter 4 in a similar manner. In these experiments, responses to ongoing, repetitive load stimuli were analyzed to avoid effects caused by the timing discrepancy. Under natural conditions, varying load stimuli will affect ongoing movement processing. In Chapter 4, the reverse situation of movement feedback effects on load processing were not tested; however, these are likely to exist as well, since presynaptic inhibitory effects of fCO stimuli on tiCS afferents were also found (Chapter 5.1). Nevertheless, any effects of movement signals on load feedback processing will be distinct from the reverse situation. Because of their timing, fCO signals may act on load processing pathways before, or only shortly after, the load signal has been perceived. Thus, load feedback may tune *ongoing*

movement processing, whereas movement feedback may prime a network *before* load processing has started. Furthermore, only movement signal gain was not only down- but also upregulated in the presence of load, whereas all effects on load signal gain were inhibitory. Load-mediated effects on sensory afferent signaling were mostly tonic, signaling state-like changes of the sensory context, while movement-dependent changes in sensory gain were transient. Taken together, the results presented in this dissertation provide clear evidence that load and movement feedback processing is asymmetric and not equivalent for both modalities.

The temporal asymmetry between load and movement feedback and the distinct modulation of their presynaptic signal gain may also indicate separate roles of these proprioceptive modalities for behavior. All the experiments presented in this dissertation were performed in inactive, i.e. resting animals (for details on behavioral state-dependency in the stick insect premotor network, see Bässler and Büschges, 1998). The results might therefore not directly apply to walking, but it is a reasonable assumption that distinct delays in sensory afferent transmission times from the periphery to the central nervous system will be independent of the behavioral state. Given the temporal differences between load and movement feedback, the premotor networks will either be required to compensate for them, or assign distinct roles to individual modalities during walking. In accordance with this hypothesis, the fast feedback from movement sense organs is thought to be relevant for phase transitions, whereas the slower load signals are considered to support ongoing muscle activation, e.g. support the activation of retractor muscles as load increases during the stance phase of forward walking (Pearson, 1993; Büschges et al., 2008; Rosenbaum et al., 2010).

In addition to temporal aspects, load and movement themselves are very different sensory modalities. They are described by distinct physical parameters of different complexity not only for signal interpretation by the premotor network, but also for experimental designs. Movement signals from the fCO represent a comparatively straightforward parameter space. They essentially consist of a single variable (FTi position) over time, its derivatives (velocity and acceleration) and combinations thereof, including vibration sensitivity (Büschges, 1994; Field and Matheson, 1998; Mamiya et al., 2018). This information can be immediately derived from the action of a single joint, whose movement stretches the fCO apodeme, providing a direct correlation between apodeme elongation and FTi joint angle over a wide range of the natural parameter space (Weiland et al., 1986; Weiland and Koch, 1987). The only additional information necessary to describe the movement of the FTi joint is a corollary discharge to distinguish between self-generated and passive movements. Opposed to this, load feedback presents a stark contrast, as neural activity in CS afferents represents a much more integrated signal. The neural activity of a single CS depends on material properties and shape of its cap, collar, and other surrounding structures (Sane and McHenry, 2009). It is influenced by its position on the leg and its orientation relative to the acting forces (Zill and Moran, 1981a, b; Cocatre-Zilgien and Delcomyn, 1999; Zill et al.,

2004; Dinges et al., 2021), the force distribution across the cuticle (Kaliyamoorthy et al., 2001), and other parameters (for detailed discussion of CS mechanics and morphology, see Dinges, 2021; Dinges et al., 2021). The neural activity of a group of CS thereby represents the integrated information about internal muscle forces, gravitational forces, ground reaction forces, external perturbations, and any other type of force that distorts the cuticle (Zill et al., 2004). Additionally, the forces measured by a given group of CS may have originated on a different leg segment. Especially tr/fCS are considered to act as integrators of overall leg loading (Höltje and Hustert, 2003; Zill et al., 2012). These aspects stand in stark contrast to the mathematically easier definable parameter space of the fCO.

Based on these different complexities of the parameter space of the fCO and CS, it stands to reason that fCO afferents provide a sufficiently unambiguous signal that can be applied for the precise control of phase transitions during locomotion. At the level of the premotor network, the complex and ambiguous CS signal potentially provides more general information on the general state of the system that have broader effects on network processing. The latter idea is supported by the temporal delays and network-wide effects of load feedback on movement signal processing (Chapter 3 & 4). Note that this argument does not preclude targeted effects of individual (groups of) CS on specific MN pools. The information necessary for decoding load feedback at the network level, however, might be provided by the simultaneous signaling of other proprio- and exteroceptive sense organs, such as the fCO or hair plates and fields. Load signal processing, and its impact on the processing of other sensory modalities, would thereby need to be contextualized by behavior or movement, or the absence thereof, in order to be decoded by the network.

Following the argument of “not a bug, but a feature”, the temporal delay of load relative to movement signals might serve a functional purpose in the network. This hypothesis is supported by the finding that signals from tr/fCS are slower than fCO signals, despite a similar distance from both sense organs to the premotor network. The delay does not seem to be imposed by physical restraints on the system, as could be argued for the more distal tiCS. Even though invertebrates do not have myelinated axons, load signals could be transmitted fast enough to be processed simultaneously with movement feedback. Multimodal signal transmission could be synchronized by altering afferent axon diameter and thereby altering transmission velocity, or by sending fCO signals through neuronal delay lines inserted prior to the premotor circuit (Hodgkin, 1954; Hartline and Colman, 2007). The absence of these compensating mechanisms is indicative of a functional purpose for delayed load signals. The functional relevance of differential timing of sensory signals has not been investigated in proprioception, but there are examples from other systems where signal delays are integrated into circuit function. In the auditory system of many vertebrates, the timing difference between signals from the right and the left ear is used for coincidence detection to infer the location of an acoustic signal source (Joris et al., 1998), auditory signals are send through a parallel delay line and integrated by a coincidence detector

that is integral for song pattern recognition in crickets (Hedwig and Sarmiento-Ponce, 2017), and a similar mechanism underlies visual motion detection (Reichardt, 1987).

In the control of leg movements, the functional relevance could be approached by examining with which other signals, from other sense organs or other signals sources such as central pattern generators, load feedback coincides because of its delay. An interesting notion is the idea of delay lines serving as a very short short-term memory which, in the present case, stores information about load encountered in the past to compare it to, or integrate it with, more recent movement signals. In future experiments, the effects of temporal delay on sensorimotor processing could be tested by applying movement stimuli as they occur during the stepping cycle simultaneously or time-shifted with naturalistic torque stimuli (cf. Zill et al., 2018; Zill et al., 2021).

6.4 Proprioception as a Multimodal Sense

The results presented in this dissertation support and extend the view of proprioception as a multimodal, integrative sense. It is constituted by the convergence of signals from distinct sources, mainly load and movement sense organs. These sensory signals must be interpreted by the central nervous system to form one coherent representation of the proprioceptive context of a limb, i.e. its proprioceptive signal space. The way in which these signals from different sense organs are integrated is especially important since the information about an electrical signal's source lies solely within its neural pathway (Adrian, 1932). As soon as their neuronal signal pathways merge, load and movement feedback become virtually indistinguishable for the nervous system. Therefore, as it was shown here, the convergence of proprioceptive modalities must be specific and involve more complex mechanisms than signal summation.

Specifically, the population of local premotor NSIs was found to be a major point of convergence. These neurons also receive signals from other elements of the nervous system, such as exteroceptive sensory afferents (Laurent and Burrows, 1988), spiking local and intersegmental interneurons (Burrows, 1987b; Laurent and Burrows, 1989b; Kittmann et al., 1996; Ludwar et al., 2005), and other NSIs (Chapters 3, 5.2; Burrows, 1979). NSIs thereby act as general signal integrators in the premotor network of the insect leg, a task to which interneurons using graded potentials are well suited (for details on the advantages of graded transmission in information processing, see reviews in Siegler, 1984; Burrows, 1989). An in-depth understanding of the sensory processing and computations performed by the NSI network requires further information about their interconnectivity. Initial data on this topic is given in Chapter 5.2, which also identified 30 Hz oscillations of the NSI resting membrane potential. These consistent oscillations of similar frequency across specific types of NSIs apparently originate from an underlying synchronizing mechanism in the NSI network. Determining the source and function of the synchronization might provide crucial information for understanding how a single network can process

multimodal inputs from various sources that contain a multitude of information about distinct parameters. This challenge, the so-termed binding problem, contrasts the requirements for network flexibility by distributed, multimodal processing with maintaining network coherence, e.g. eliciting reproducible motor responses to given inputs.

The integration of proprioceptive load and movement information into one common framework can be understood on a behavioral, as well as on the circuit level. Both sensory modalities are not completely separable; they are concurrently elicited by many stimuli, for example, a flexion of the tibia while the tarsus has ground contact. Nor do they provide entirely redundant information. In the example of tibial flexion, CS and fCO afferents will signal an increased joint flexion. The fCO signal, however, will contain information about joint angle, velocity, and acceleration (Büschges, 1994; Field and Matheson, 1998). In contrast, CS feedback indicates the source of the stimulus by the identity of the signaling CS, e.g. external perturbation, ground contact, and / or internally generated muscle forces (Zill et al., 2004). Multimodal proprioceptive sensory signals thereby complement each other's information by representing different aspects of the limb's proprioceptive space. In the premotor network, this is reflected by the context-dependent processing of one of these modalities in the presence of the other (Chapter 4).

In experimental paradigms on insect proprioception, the senses of load and movement are typically treated separately. The separation allows to analyze the individual effects and the underlying circuitry, and presents one of the advantages of invertebrate model organisms. In vertebrates, studies of this kind are impeded by the anatomical situation of the sense organs. Golgi tendon organs and muscle spindles are positioned in series, which complicates the search for stimulation paradigms that exclusively activate one sensory modality and not the other (discussed in Proske and Gandevia, 2012; Jankowska, 2013b). The situation in vertebrates highlights the advantages of exclusive mechanical stimuli in insects. However, the separate effects and the neural circuits identified by stimuli targeting single sense organs on the insect leg must be merged to understand how, under natural conditions, proprioceptive integration occurs. Ultimately, load feedback most likely will only be understood in the context of movement in the premotor network, since load acting on the limb will also alter its position. To some extent, this statement also holds for the reverse situation of movement in the context of load feedback, because most movements of the leg will be accompanied by altered load signaling.

The results presented in this dissertation provide a first step to understanding how the central nervous system integrates multimodal proprioceptive input. The complexity of the evoked motor responses and of the underlying neuronal responses clearly demonstrate that proprioceptive integration is more than the sum of its constituent parts.

6.5 Conclusion & Perspectives

The context-dependency of proprioceptive processing and the resulting motor output reveal a highly nonlinear system. Open lines of inquiry for future studies include the relevance of lateral connections at different levels of the premotor network, the functional implications of the temporal difference between load and movement sensory signals in the walking animal, and computational consequences of the specificity found in the connectivity from sensory afferents to individual local premotor NSIs and MNs.

Combined experimental and computational approaches may shed further light on the functional connectivity of the NSI network itself. This specifically includes the implications of a network that is synchronized by fast membrane oscillations and whose individual neurons change their functional position within the circuit depending on the sensory context, i.e. the combination of simultaneously elicited sensory signals. These investigations will also require more details on the lateral connectivity within the NSI network. Initial results and previous studies (Chapters 3, 5.2; Burrows, 1979) indicate the presence of reciprocal connections between NSIs. Depending on the membrane properties and computational processes of individual neurons, altering the functional position of a computational unit, i.e. a NSI, within the network could alter and determine the resulting downstream processing cascade. In other words, the order of NSIs that a signal passes through represents the order of computations that the signal will be subjected to, thereby determining the network's motor output. Altering the order of computations will affect signal processing and network output and could be an efficient way to employ the same network in different behavioral contexts. Furthermore, as discussed in Chapter 5.2, synchronizing NSI oscillations might strengthen the network's output. By de- or increasing coupling strength between distinct sets of NSIs, signal processing could be altered. This last effect would provide an alternative approach to the historical discussion of dedicated *versus* distributed pathways (Burrows, 1996; Sauer et al., 1996; Büschges et al., 2000), as it could serve as a mechanism for selective, i.e. dedicated, attention in a distributed network.

All computations and integrations presented and proposed in this dissertation depend on the input signals that the premotor network receives. It is therefore essential for our understanding of proprioception to identify if and how these signals represent the "raw" information as sent from the sense organs, or whether they have already been preprocessed. This and other studies have presented evidence for presynaptic interactions between sensory afferents of different modalities (Chapter 5.1, Stein and Schmitz, 1999). The modulatory effects on movement signal gain shown in Chapter 5.1 demonstrate that these interactions might be more complex than previously thought, emphasizing the need for further investigations of this stage of the local network.

In this dissertation I have investigated the interaction of the two main proprioceptive senses involved in the control of leg movements and posture. I have identified their point, or rather network, of convergence in the premotor network of local premotor NSIs (Chapter 2), illuminated the temporal course of their signal processing and transmission from sensory afferents to muscle fibers (Chapter 3), and presented a mechanism for local, context-dependent proprioceptive integration and sensorimotor control (Chapter 4). Initial data emphasize the relevance of lateral connectivity between sensory afferents and within the layer of NSIs for proprioceptive signal processing and provide insights into network computations underlying motor output and behavior (Chapter 5). The results on spatial summation, temporal differences, and sensory gain control of load and movement feedback provide a framework for multimodal proprioceptive integration. The underlying mechanisms of distributed processing, distinct lateral and horizontal connectivity, transmission times, and context-dependent sensory processing controlled by presynaptic afferent interactions will guide not only future studies on invertebrate systems, but might also be applicable to vertebrate motor control.

The results of this dissertation provide a new perspective on the flexibility of sensorimotor processing and posture control. Sensorimotor networks in vertebrates and invertebrates clearly consist of more than a number of separate reflex arcs from a sensory modality to its effector muscle. This study opens up new avenues of questions regarding proprioceptive signal integration. It emphasizes that the nervous systems of invertebrates are by no means simple and how their study provides valuable insights into general aspects of sensorimotor processing and proprioceptive integration for both vertebrates and invertebrates.

7 List of Figures

8 List of Tables

9 References

Adrian ED (1932) The Mechanism of Nervous Action: Electrical Studies of the Neurone, 1959 Edition. London: Oxford University Press.

Agrawal S, Dickinson ES, Sustar A, Gurung P, Shepherd D, Truman JW, Tuthill JC (2020) Central processing of leg proprioception in Drosophila. Elife 9.

Akay T (2002) The Role of Sensory Signals for Interjoint Coordination in Stick Insect Legs. In: Mathematisch-Naturwissenschaftliche Fakultät: University of Cologne.

Akay T, Büschges A (2006) Load signals assist the generation of movement-dependent reflex reversal in the femur-tibia joint of stick insects. Journal of Neurophysiology 96:3532-3537.

Akay T, Bässler U, Gerharz P, Büschges A (2001) The Role of Sensory Signals From the Insect Coxa-Trochanteral Joint in Controlling Motor Activity of the Femur-Tibia Joint. Journal of Neurophysiology 85:594-604.

Akay T, Haehn S, Schmitz J, Büschges A (2004) Signals From Load Sensors Underlie Interjoint Coordination During Stepping Movements of the Stick Insect Leg. Journal of Neurophysiology 92:42-51.

Akay T, Tourtellotte WG, Arber S, Jessell TM (2014) Degradation of mouse locomotor pattern in the absence of proprioceptive sensory feedback. Proc Natl Acad Sci U S A 111:16877-16882.

Akay T, Ludwar B, Göritz ML, Schmitz J, Büschges A (2007) Segment specificity of load signal processing depends on walking direction in the stick insect leg muscle control system. Journal of Neuroscience 27:3285-3294.

Alzubaidi L, Zhang J, Humaidi AJ, Al-Dujaili A, Duan Y, Al-Shamma O, Santamaría J, Fadhel MA, Al-Amidie M, Farhan L (2021) Review of deep learning: concepts, CNN architectures, challenges, applications, future directions. J Big Data 8:53.

Azim E, Seki K (2019) Gain control in the sensorimotor system. Curr Opin Physiol 8:177-187.

Bässler D, Büschges A, Meditz S, Bässler U (1996) Correlation between muscle structure and filter characteristics of the muscle-joint system in three Orthopteran insect species. Journal of Experimental Biology 199:2169-2183.

Bässler U (1976) Reversal of a Reflex to a Single Motoneuron in the Stick Insect *Carausius morosus**. Biol Cybern 24:47-49.

Bässler U (1983a) Neural Basis of Elementary Behaviour in Stick Insects, 1 Edition. Heidelberg, Germany: Springer Berlin Heidelberg.

Bässler U (1983b) The Neural Basis of Catalepsy in the Stick Insect *Cuniculina Impigra** 3. Characteristics of the Extensor Motor Neurons. Biological Cybernetics 46:159-165.

Bässler U (1986) Afferent control of walking movements in the stick insect *Cuniculina impigra*. J Comp Physiol A 158:351-362.

Bässler U (1988) Functional Principles of Pattern Generation for Walking Movements of Stick Insect Forelegs: The Role of the Femoral Chordotonal Organ Afferences. Journal of Experimental Biology 136:125-147.

Bässler U (1993) The femur-tibia control system of stick insects - a model system for the study of the neural basis of joint control. Brain Research Reviews 18:207-226.

Bässler U, Foth E (1982) The Neural Basis of Catalepsy in the Stick Insect *Cuniculina Impigra** 1. Catalepsy as a Characteristic of the Femur-Tibia Control System. Biol Cybern 45:101-105.

Bässler U, Büschges A (1998) Pattern generation for stick insect walking movements—multisensory control of a locomotor program. Brain Research Reviews 27:65-88.

Bässler U, Storrer J, Saxer K (1982) The Neural Basis of Catalepsy in the Stick Insect *Cuniculina Impigra** 2. The Role of the Extensor Motor Neurons and the Characteristics of the Extensor Tibiae Muscle. Biol Cybern 46:1-6.

Beenhakker MP, Kirby MS, Nusbaum MP (2007) Mechanosensory gating of proprioceptor input to modulatory projection neurons. J Neurosci 27:14308-14316.

Berg E (2014) Adaptive Motor Control: Neuronal Mechanisms Underlying (Targeted) Searching Movements. In: Mathematisch-Naturwissenschaftliche Fakultät: University of Cologne.

Berg E, Büschges A, Schmidt J (2013) Single Perturbations Cause Sustained Changes in Searching Behavior in Stick Insects. Journal of Experimental Biology 216:1064-1074.

Berg E, Hooper SL, Schmidt J, Büschges A (2015) A leg-local neural mechanism mediates the decision to search in stick insects. Current Biology 25:2012-2017.

Berry M, Pentreath V (1976) Criteria for distinguishing between monosynaptic and polysynaptic transmission. Brain Research:1-20.

Bidaye SS, Bockemühl T, Büschges A (2018) Six-legged walking in insects: how CPGs, peripheral feedback, and descending signals generate coordinated and adaptive motor rhythms. Journal of Neurophysiology 119:459-475.

Burrows M (1979) Graded Synaptic Interactions Between Local Premotor Interneurons of the Locust. Journal of Neurophysiology 42:1108-1123.

Burrows M (1980) The Control of Sets of Motoneurones by Local Interneurones in the Locust. Journal of Physiology 298:213-233.

Burrows M (1985) The Processing of Mechanosensory Information by Spiking Local Interneurons in the Locust. Journal of Neurophysiology 54:463-478.

Burrows M (1987a) Parallel Processing of Proprioceptive Signals by Spiking Local Interneurons and Motor Neurons in the Locust. Journal of Neuroscience 7:1064-1080.

Burrows M (1987b) Inhibitory Interactions Between Spiking and Nonspiking Interneurons in the Locust. Journal of Neuroscience 7:3282-3292.

Burrows M (1989) Processing of Mechanosensory Signals in Local Reflex Pathways of the Locust. Journal of Experimental Biology 146:209-227.

Burrows M (1996) The Neurobiology of an Insect Brain. Oxford, UK: Oxford University Press.

Burrows M, Siegler MVS (1976) Transmission without spikes between locust interneurones and motoneurones. Nature 262:222-224.

Burrows M, Siegler MVS (1978) Graded Synaptic Transmission Between Local Interneurones And Motor Neurones In The Metathoracic Ganglion Of The Locust. Journal of Physiology 285:231-255.

Burrows M, Pflüger JH (1988) Positive feedback loops from proprioceptors involved in leg movements of the locust. Journal of Comparative Physiology A 163:425-440.

Burrows M, Laurent G (1993) Synaptic Potentials in the Central Terminals of Locust Proprioceptive Afferents Generated by Other Afferents from the Same Sense Organ. Journal of Neuroscience 13:808-819.

Burrows M, Matheson T (1994) A Presynaptic Gain Control Mechanism among Sensory Neurons of a Locust Leg Proprioceptor. Journal of Neuroscience 14:272-282.

Burrows M, Laurent G, Field LH (1988) Proprioceptive Inputs to Nonspiking Local Interneurons Contribute to Local Reflexes of a Locust Hindleg. J Neurosci 8:3085-3093.

Büschges A (1989) Processing of Sensory Input from the Femoral Chordotonal Organ by Spiking Interneurones of Stick Insects. Journal of Experimental Biology 144:81-111.

Büschges A (1990) Nonspiking Pathways in a Joint-Control Loop of the Stick Insect *Carausius morosus*. Journal of Experimental Biology 151:133-160.

Büschges A (1994) The Physiology of Sensory Cells in the Ventral Scoloparium of the Stick Insect Femoral Chordotonal Organ. Journal of Experimental Biology 189:285-292.

Büschges A (1995) Role of Local Nonspiking lnterneurons in the Generation of Rhythmic Motor Activity in the Stick Insect. Journal of Neurobiology 27:488-512.

Büschges A, Schmitz J (1991) Nonspiking Pathways Antagonize the Resistance Reflex in the Thoraco-Coxal Joint of Stick Insects. Journal of Neurobiology 22:224-237.

Büschges A, Wolf H (1995) Nonspiking Local Interneurons in Insect Leg Motor Control I. Common Layout and Species-Specific Response Properties of Femur-Tibia Joint Control Pathways in Stick Insect and Locust. Journal of Neurophysiology 73:1843-1860.

Büschges A, Wolf H (1996) Gain Changes in Sensorimotor Pathways of the Locust Leg. Journal of Experimental Biology 199:2437-2445.

Büschges A, El Manira A (1998) Sensory pathways and their modulation in the control of locomotion. Current Opinion in Neurobiology 8:733-739.

Büschges A, Gruhn M (2007) Mechanosensory Feedback in Walking: From Joint Control to Locomotor Patterns. In: Insect Mechanics and Control pp 193-230.

Büschges A, Kittmann R, Schmitz J (1994) Identified nonspiking interneurons in leg reflexes and during walking in the stick insect. Journal of Comparative Physiology 174:685-700.

Büschges A, Sauer AE, Bässler U (2000) Flexibility of a Proprioceptive Feedback System Results from its "Parliamentary" (Distributed) Organization. In: Prerational Intelligence: Adaptive Behavior and

Intelligent Systems Without Symbols and Logic (Cruse H, Dean J, Ritter H, eds). Dordrecht: Springer.

Büschges A, Akay T, Gabriel JP, Schmidt J (2008) Organizing network action for locomotion: insights from studying insect walking. Brain Research Reviews 57:162-171.

Buzsáki G, Draguhn A (2004) Neuronal Oscillations in Cortical Networks. Science 304:1926-1929.

Cattaert D, El Manira A (1999) Shunting versus Inactivation: Analysis of Presynaptic Inhibitory Mechanisms in Primary Afferents of the Crayfish. Journal of Neuroscience 19:6079-6089.

Cattaert D, Libersat F, El Manira A (2001) Presynaptic Inhibition and Antidromic Spikes in Primary Afferents of the Crayfish: A Computational and Experimental Analysis. Journal of Neuroscience 21:1007-1021.

Clarac F, Cattaert D (1996) Invertebrate presynaptic inhibition and motor control. Experimental Brain Research 112:163-180.

Cocatre-Zilgien JH, Delcomyn F (1999) Modeling stress and strain in an insect leg for simulation of campaniform sensilla responses to external forces. Biol Cybern 81:149-160.

Combes D, Meyrand P, Simmers J (1999) Dynamic Restructuring of a Rhythmic Motor Program by a Single Mechanoreceptor Neuron in Lobster. Journal of Neuroscience 19:3620-3628.

Confais J, Kim G, Tomatsu S, Takei T, Seki K (2017) Nerve-Specific Input Modulation to Spinal Neurons during a Motor Task in the Monkey. J Neurosci 37:2612-2626.

Czarkowska J, Jankowska E, Sybirska E (1981) Common Interneurones in Reflex Pathways from Group Ia and Ib Afferents of Knee Flexors and Extensors in the Cat. Journal of Physiology 310:367-380.

Dallmann CJ, Dürr V, Schmitz J (2016) Joint torques in a freely walking insect reveal distinct functions of leg joints in propulsion and posture control. Proc Biol Sci 283.

Dallmann CJ, Hoinville T, Dürr V, Schmitz J (2017) A load-based mechanism for inter-leg coordination in insects. Proc Biol Sci 284.

Dallmann CJ, Karashchuk P, Brunton BW, Tuthill JC (2021) A leg to stand on: computational models of proprioception. Current Opinion in Physiology.

De Serres SJ, Yang JF, Patrick SK (1995) Mechanism for reflex reversal during walking in human tibialis anterior muscle revealed by single motor unit recording. Journal of Physiology 488:249-258.

Deliagina TG, Zelenin PV, Orlovsky GN (2012) Physiological and circuit mechanisms of postural control. Curr Opin Neurobiol 22:646-652.

Dinges GF (2021) Morphology of Leg Campaniform Sensilla and Their Role in *Drosophila melanogaster* Walking. In: Mathematisch-Naturwissenschaftliche Fakultät: University of Cologne.

Dinges GF, Chockley AS, Bockemühl T, Ito K, Blanke A, Büschges A (2021) Location and arrangement of campaniform sensilla in Drosophila melanogaster. J Comp Neurol 529:905–925.

Dörr H, Heß D, Gramoll S (1996) Interstitial Voltage and Potassium Concentration in the Mesothoracic Ganglion of a Stick Insect at Rest and During Neuronal Activation. Journal of Insect Physiology 42:967-974.

Driesang RB, Büschges A (1993) The neural basis of catalepsy in the stick insect. IV. Properties of nonspiking interneurons. Journal of Comparative Physiology 173:445-454.

Driesang RB, Büschges A (1996) Physiological changes in central neuronal pathways contributing to the generation of a reflex reversal. Journal of Comparative Physiology 179:45-57.

Dudel J, Kuffler SW (1961) Presynaptic Inhibition at the Crayfish Neuromuscular Junction. Journal of Physiology 155:543-562.

Duysens J, Clarac F, Cruse H (2000) Load-Regulating Mechanisms in Gait and Posture: Comparative Aspects. Physiological Reviews 80:83-133.

Duysens J, Trippel M, Horstmann GA, Dietz V (1990) Gating and reversal of reflexes in ankle muscles during human walking. Experimental Brain Research 82:351-358.

Edwards DH, Prilutsky BI (2017) Sensory Feedback in the Control of Posture and Locomotion. In: Neurobiology of Motor Control: Fundamental Concepts and New Directions, 1 Edition (Hooper SL, Büschges A, eds), pp 263-304: John Wiley & Sons, Inc.

El Manira A, DiCaprio RA, Cattaert D, Clarac F (1991) Monosynaptic Interjoint Reflexes and their Central Modulation During Fictive Locomotion in Crayfish. European Journal of Neuroscience 3:1219-1231.

Engel AK, Singer W (2001) Temporal binding and the neural correlates of sensory awareness. Trends in Cognitive Sciences 5:16-21.

Field LH, Matheson T (1998) Chordotonal Organs of Insects. In: Advances in Insect Physiology, 1st Edition (Evans P, ed): Academic Press.

Fink AJ, Croce KR, Huang ZJ, Abbott LF, Jessell TM, Azim E (2014) Presynaptic inhibition of spinal sensory feedback ensures smooth movement. Nature 509:43-48.

Fisher KM, Zaaimi B, Edgley SA, Baker SN (2021) Extensive Cortical Convergence to Primate Reticulospinal Pathways. J Neurosci 41:1005-1018.

Florey E (1963) Acetylcholine in invertebrate nervous systems. Canadian Journal of Biochemistry and Physiology 41:2619-2626.

Follmann R, Goldsmith CJ, Stein W (2018) Multimodal sensory information is represented by a combinatorial code in a sensorimotor system. PLoS Biol 16:e2004527.

Forssberg H, Grillner S, Rossignol S (1975) Phase dependent reflex reversal during walking in chronic spinal cats. Brain Research 85:103-107.

Frank K, Fuortes MGF (1957) Presynaptic and postsynaptic inhibition of monosynaptic reflexes. Fed Proc 16:39.40.

Frith CD, Blakemore S-J, Wolpert DM (2000) Explaining the symptoms of schizophrenia: Abnormalities in the awareness of action. Brain Research Reviews 31:357-363.

Gebehart C (2018) Processing of Load Signals by Local Premotor Interneurons in the Stick Insect *Carausius morosus*. In: Department of Biology: University of Cologne.

Gebehart C, Schmidt J, Büschges A (2021) Distributed Processing of Load and Movement Feedback in the Premotor Network Controlling an Insect Leg Joint. Journal of Neurophysiology 125:1800-1813.

Goldammer J, Büschges A, Schmidt J (2012) Motoneurons, DUM cells, and sensory neurons in an insect thoracic ganglion: a tracing study in the stick insect Carausius morosus. Journal of Comparative Neurology 520:230-257.

Gorassini MA, Prochazka A, Hiebert GW, Gauthier MJA (1994) Corrective Responses to Loss of Ground Support During Walking I. Intact Cats. J Neurophysiol 71:603-610.

Grabowska MJ, Jeans R, Steeves J, van Swinderen B (2020) Oscillations in the central brain of Drosophila are phase locked to attended visual features. Proc Natl Acad Sci U S A 117:29925-29936.

Graham D, Bässler U (1981) Effects of afference sign reversal on motor activity in walking stick insects (*Carausius morosus*). J Exp Biol 91:179-193.

Grillner S (2006) Biological pattern generation: the cellular and computational logic of networks in motion. Neuron 52:751-766.

Grillner S (2021) The execution of movement: a spinal affair. J Neurophysiol 125:693-698.

Grillner S, El Manira A (2020) Current Principles of Motor Control, with Special Reference to Vertebrate Locomotion. Physiol Rev 100:271-320.

Haberkorn A, Gruhn M, Zill SN, Büschges A (2019) Identification of the origin of force-feedback signals influencing motor neurons of the thoraco-coxal joint in an insect. J Comp Physiol A Neuroethol Sens Neural Behav Physiol 205:253-270.

Hartline DK, Colman DR (2007) Rapid conduction and the evolution of giant axons and myelinated fibers. Curr Biol 17:R29-35.

Hasenpusch J, Brock PD (2006) Studies on the Australian stick insect genus *Ctenomorpha Gray* (Phasmida: Phasmatidae: Phasmatinae), with the description of a new large species. Zootaxa 1282:1-15.

Hedwig B, Sarmiento-Ponce EJ (2017) Song pattern recognition in crickets based on a delay-line and coincidence-detector mechanism. Proc Biol Sci 284.

Hellekes K, Blincow E, Hoffmann J, Büschges A (2012) Control of reflex reversal in stick insect walking: effects of intersegmental signals, changes in direction, and optomotor-induced turning. J Neurophysiol 107:239-249.

Hengstenberg R (1977) Spike Responses Of 'Non-Spiking' Visual Interneurone. Nature 270.

Hess D, Büschges A (1997) Sensorimotor Pathways Involved in Interjoint Reflex Action of an Insect Leg. Journal of Neurobiology 33:891-913.

Hess D, Büschges A (1999) Role of Proprioceptive Signals from an Insect Femur-Tibia Joint in Patterning Motoneuronal Activity of an Adjacent Leg Joint. Journal of Neurophysiology 81:1856-1865.

Hodgkin AL (1954) A Note on Conduction Velocity. J Physiol 125:221-224.

Hofmann T, Bässler U (1982) Anatomy and physiology of trochanteral campaniform sensilla in the stick insect, *Cuniculina impigra*. Physiological Entomology 7:413-426.

Hofmann T, Koch UT, Bässler U (1985) Physiology of the Femoral Chordotonal Organ in the Stick Insect, *Cuniculina impigra*. Journal of Experimental Biology 114:207-223.

Höltje M, Hustert R (2003) Rapid mechano-sensory pathways code leg impact and elicit very rapid reflexes in insects. J Exp Biol 206:2715-2724.

Hooper SL, Guschlbauer C, von Uckermann G, Büschges A (2007) Slow temporal filtering may largely explain the transformation of stick insect (Carausius morosus) extensor motor neuron activity into muscle movement. Journal of Neurophysiology 98:1718-1732.

Hooper SL, Guschlbauer C, Blümel M, Rosenbaum P, Gruhn M, Akay T, Büschges A (2009) Neural control of unloaded leg posture and of leg swing in stick insect, cockroach, and mouse differs from that in larger animals. Journal of Neuroscience 29:4109-4119.

Hustert R, Pflüger JH, Bräunig P (1981) Distribution and Specific Central Projections of Mechanoreceptors in the Thorax and Proximal Leg Joints of Locusts. Cell and Tissue Research 216:97-111.

Imai F, Yoshida Y (2018) Molecular mechanisms underlying monosynaptic sensory-motor circuit development in the spinal cord. Dev Dyn 247:581-587.

Ivanenko YP, Grasso R, Lacquaniti F (2000) Influence of Leg Muscle Vibration on Human Walking. J Neurophysiol 84:1737-1747.

Jami L (1992) Golgi Tendon Organs in Mammalian Skeletal Muscle: Functional Properties and Central Actions. Physiological Reviews 72:623-666.

Jankowska E (2013a) Spinal Interneurons. In: Neuroscience in the 21st Century (Pfaff DW, ed), pp 1189-1224.

Jankowska E (2013b) Spinal Reflexes. In: Neuroscience in the 21st Century (Pfaff DW, ed), pp 1189-1224.

Jankowska E, McCrea DA (1983) Shared Reflex Pathways from Ib Tendon Organ Afferents and Ia Muscle Spindle Afferents in the Cat. Journal of Physiology 338:99-111.

Joris PX, Smith PH, Yin TCT (1998) Coincidence Detection in the Auditory System: 50 Years after Jeffress. Neuron 21:1234-1238.

Kaliyamoorthy S, Zill SN, Quinn RD, Ritzmann RE, Jongung C (2001) Finite element analysis of strains in a Blaberus cockroach leg during climbing. In: Proceedings 2001 IEEE/RSJ International Conference on Intelligent Robots and Systems. Expanding the Societal Role of Robotics in the the Next Millennium (Cat. No.01CH37180), pp 833-838.

Keller CH, Heilgenberg H (1989) From distributed sensory processing to discrete motor representations in the diencephalon of the electric fish, *Eigenmannia*. J Comp Physiol A 165:565-576.

Kistemaker DA, Van Soest AJ, Wong JD, Kurtzer I, Gribble PL (2013) Control of position and movement is simplified by combined muscle spindle and Golgi tendon organ feedback. Journal of Neurophysiology 109:1126-1139.

Kittmann R (1997) Neural Mechanisms of Adaptive Gain Control in a Joint Control Loop: Muscle Force and Motoneuronal Activity. J Exp Biol 200:1383-1402.

Kittmann R, Schmitz J, Büschges A (1996) Premotor Interneurons in Generation of Adaptive Leg Reflexes and Voluntary Movements in Stick Insects. Journal of Neurobiology 31:512-531.

Koch SC, Del Barrio MG, Dalet A, Gatto G, Gunther T, Zhang J, Seidler B, Saur D, Schule R, Goulding M (2017) RORbeta Spinal Interneurons Gate Sensory Transmission during Locomotion to Secure a Fluid Walking Gait. Neuron 96:1419-1431 e1415.

König P, Schillen TB (1991) Stimulus-Dependent Assembly Formation of Oscillatory Responses: I. Synchronization. Neural Computation 3:155-166.

Krasne FB, Bryan JS (1973) Habituation: Regulation through Presynaptic Inhibition. Science 182:590-592.

Laurent G (1993) A Dendritic Gain Control Mechanism in Axonless Neurons of the Locust, *Schistocerca americana*. Journal of Physiology 470:45-54.

Laurent G, Burrows M (1989a) Intersegmental Interneurons Can Control the Gain of Reflexes in Adjacent Segments of the Locust by Their Action of Nonspiking Local Interneurons. Journal of Neuroscience 9:3030-3039.

Laurent G, Burrows M (1989b) Distribution of Intersegmental Inputs to Nonspiking Local Interneurons and Motor Neurons in the Locust. Journal of Neuroscience 9:3019-3029.

Laurent G, Davidowitz H (1994) Encoding of Olfactory Information with Oscillating Neural Assemblies. Science 265:1872-1875.

Laurent GJ, Burrows M (1988) Direct excitation of nonspiking local interneurones by exteroceptors underlies tactile reflexes in the locust. Journal of Comparative Physiology A 162:563-572.

Liessem S, Kowatschew D, Dippel S, Blanke A, Korsching S, Guschlbauer C, Hooper SL, Predel R, Buschges A (2021) Neuromodulation can be simple: myoinhibitory peptide, contained in dedicated regulatory pathways, is the only neurally-mediated peptide modulator of stick insect leg muscle. J Neurosci.

Lockery SR, Kristan WB, Jr. (1990) Distributed processing of sensory information in the leech. II. Identification of interneurons contributing to the local bending reflex. Journal of Neuroscience 10:1816-1829.

Ludwar B, Westmark S, Büschges A, Schmidt J (2005) Modulation of membrane potential in mesothoracic moto- and interneurons during stick insect front-leg walking. J Neurophysiol 94:2772-2784.

Lutz EM, Tyrer NM (1988) Immunohistochemical Localization of Serotonin and Choline Acetyltransferase in Sensory Neurones of the Locust. Journal of Comparative Neurology 267:335-342.

Mamiya A, Gurung P, Tuthill JC (2018) Neural Coding of Leg Proprioception in Drosophila. Neuron 100:636-650 e636.

Marquardt F (1940) Beiträge zur Anatomie der Muskulatur und der peripheren Nerven von Carausius (Dixippus) morosus. Zool Jb Abt Anat Ont 66:63-128.

Matheson T (2002) Invertebrate Nervous Systems. In: eLS.

McComas AJ (2016) Hypothesis: Hughlings Jackson and presynaptic inhibition: is there a big picture? J Neurophysiol 116:41-50.

Mendes CS, Bartos I, Akay T, Márka S, Mann RS (2013) Quantification of gait parameters in freely walking wild type and sensory deprived Drosophila melanogaster. Elife 2:e00231.

Miroschnikow A, Schlegel P, Schoofs A, Hueckesfeld S, Li F, Schneider-Mizell CM, Fetter RD, Truman JW, Cardona A, Pankratz MJ (2018) Convergence of monosynaptic and polysynaptic sensory paths onto common motor outputs in a Drosophila feeding connectome. Elife 7.

Mulloney B, Smarandache-Wellmann C, Weller C, Hall WM, DiCaprio RA (2014) Proprioceptive feedback modulates coordinating information in a system of segmentally distributed microcircuits. J Neurophysiol 112:2799-2809.

Newland P, Emptage N (1996) The central connections and actions during walking of tibial campaniform sensilla in the locust. Journal of Comparative Physiology 178:749-762.

Niebur E, Hsiao SS, Johnson KO (2002) Synchrony: a neuronal mechanism for attentional selection? Current Opinion in Neurobiology 12:190-194.

Noah A, Quimby L, Frazier F, Zill S (2001) Force detection in cockroach walking reconsidered: discharges of proximal tibial campaniform sensilla when body load is altered. Journal of Comparative Physiology A: Sensory, Neural, and Behavioral Physiology 187:769-784.

Pearson K (1993) Common Principles of Motor Control in Vertebrates and Invertebrates. Annu Rev Neurosci 16:265-297.

Pearson KG (1995a) Proprioceptive regulation of locomotion. Current Opinion in Neurobiology 5:786-791.

Pearson KG (1995b) Reflex Reversal in the Walking Systems of Mammals and Arthropods. In: Neural Control of Movement (W.R. F, U. P, eds). Boston, MA: Springer.

Pearson KG (2004) Generating the walking gait: role of sensory feedback. In: Brain Mechanisms for the Integration of Posture and Movement, pp 123-129.

Phelps JS, Hildebrand DGC, Graham BJ, Kuan AT, Thomas LA, Nguyen TM, Buhmann J, Azevedo AW, Sustar A, Agrawal S, Liu M, Shanny BL, Funke J, Tuthill JC, Lee WA (2021) Reconstruction of motor control circuits in adult Drosophila using automated transmission electron microscopy. Cell.

Pringle JWS (1938) Proprioception in Insects. II. The Action of the Campaniform Sensilla on the Legs. Journal of Experimental Biology 15:114-131.

Prochazka A, Gillard D, Bennett DJ (1997) Implications of Positive Feedback in the Control of Movement. J Neurophysiol 77:3237-3251.

Proske U, Gandevia SC (2012) The proprioceptive senses: their roles in signaling body shape, body position and movement, and muscle force. Physiol Rev 92:1651-1697.

Putney J, Conn R, Sponberg S (2019) Precise timing is ubiquitous, consistent, and coordinated across a comprehensive, spike-resolved flight motor program. Proc Natl Acad Sci U S A.

Reichardt W (1987) Evaluation of optical motion information by movement detectors. J Comp Physiol A 161:533-547.

Ritz R, Sejnowski TJ (1997) Synchronous oscillatory activity in sensory systems: new vistas on mechanisms. Current Opinion in Neurobiology 7:536-546.

Rosenbaum P (2013) Motor flexibility: neuronal control of walking direction and walking speed in an insect. In: Mathematisch-Naturwissenschaftliche Fakultät: Universität zu Köln.

Rosenbaum P, Wosnitza A, Büschges A, Gruhn M (2010) Activity patterns and timing of muscle activity in the forward walking and backward walking stick insect Carausius morosus. Journal of Neurophysiology 104:1681-1695.

Rudomin P, Schmidt RF (1999) Presynaptic inhibition in the vertebrate spinal cord revisited. Experimental Brain Research 129:1-37.

Sane SP, McHenry MJ (2009) The biomechanics of sensory organs. Integrative and Comparative Biology 49:i8-i23.

Santuz A, Akay T, Mayer WP, Wells TL, Schroll A, Arampatzis A (2019) Modular organization of murine locomotor pattern in the presence and absence of sensory feedback from muscle spindles. J Physiol 597:3147-3165.

Sauer AE, Büschges A, Stein W (1997) Role of Presynaptic Inputs to Proprioceptive Afferents in Tuning Sensorimotor Pathways of an Insect Joint Control Network. Journal of Neurobiology 32:359-376.

Sauer AE, Driesang RB, Büschges A, Bässler U (1995) Information processing in the femur-tibia control loop of stick insects 1. The response characteristics of two nonspiking interneurons results fom parallel excitatory and inhibitory inputs. Journal of Comparative Physiology A 177:145-158.

Sauer AE, Driesang RB, Büschges A, Bässler U (1996) Distributed Processing on the Basis of Parallel and Antagonistic Pathways Simulation of the Femur-Tibia Control System in the Stick Insect. Journal of Computational Neuroscience 3:179-198.

Scheffer LK et al. (2020) A connectome and analysis of the adult Drosophila central brain. Elife 9.

Schmitz J (1993) Load-Compensating Reactions in the Proximal Leg Joints of Stick Insects During Standing and Walking. Journal of Experimental Biology 183:15-33.

Schmitz J, Stein W (2000) Convergence of Load and Movement Information onto Leg Motoneurons in Insects. Journal of Neurobiology 43:424-436.

Schmitz J, Büschges A, Delcomyn F (1988) An Improved Electrode Design for En Passant Recording from Small Nerves. Comparative Biochemistry and Physiology 91:769-772.

Schmitz J, Büschges A, Kittmann R (1991) Intracellular Recordings from Nonspiking Interneurons in a Semiintact, Tethered Walking Insect. Journal of Neurobiology 22:907-921.

Schmitz J, Gruhn M, Büschges A (2015) The role of leg touchdown for the control of locomotor activity in the walking stick insect. J Neurophysiol 113:2309-2320.

Schmitz J, Gruhn M, Büschges A (2019) Body side-specific changes in sensorimotor processing of movement feedback in a walking insect. J Neurophysiol 122:2173-2186.

Schomburg ED, Behrends HB (1978) Phasic Control of the Transmission in the Excitatory and Inhibitory Reflex Pathwas from Cutaneous Afferents to α-Motoneurones during Fictive Locomotion in Cats. Neuroscience Letters 8:277-282.

Sherrington CS (1907) On the Proprio-ceptive System, Especially in its Reflex Aspect. Brain 29:467-485.

Siegelbaum SA, Camardo JS, Kandel ER (1982) Serotonin and cyclic AMP close single K^+ channels in Aplysia sensory neurones. Nature 299:413-417.

Siegler MVS (1981) Postural Changes Alter Synaptic Interactions Between Nonspiking Interneurons and Motor Neurons of the Locust. Journal of Neurophysiology 46:310-323.

Siegler MVS (1984) Local Interneurones and Local Interactions in Arthropods. Journal of Experimental Biology 112:253-281.

Siegler MVS, Burrows M (1983) Spiking Local Interneurons as Primary Integrators of Mechanosensory Information in the Locust. Journal of Neurophysiology 50:1281-1295.

Smarandache-Wellmann C, Weller C, Mulloney B (2014) Mechanisms of coordination in distributed neural circuits: decoding and integration of coordinating information. J Neurosci 34:793-803.

Sponberg S, Daniel TL (2012) Abdicating power for control: a precision timing strategy to modulate function of flight power muscles. Proc Biol Sci 279:3958-3966.

Spors H, Albeanu DF, Murthy VN, Rinberg D, Uchida N, Wachowiak M, Friedrich RW (2012) Illuminating vertebrate olfactory processing. J Neurosci 32:14102-14108.

Stein W, Sauer AE (1998) Modulation of sensorimotor pathways associated with gain changes in a posture-control network of an insect. Journal of Comparative Physiology 183:489-501.

Stein W, Schmitz J (1999) Multimodal Convergence of Presynaptic Afferent Inhibition in Insect Proprioceptors. Journal of Neurophysiology 82:512-514.

Stein W, Büschges A, Bässler U (2006) Intersegmental transfer of sensory signals in the stick insect leg muscle control system. J Neurobiol 66:1253-1269.

Stein W, Straub O, Ausborn J, Mader W, Wolf H (2008) Motor pattern selection by combinatorial code of interneuronal pathways. J Comput Neurosci 25:543-561.

Stolz T, Diesner M, Neupert S, Hess ME, Delgado-Betancourt E, Pflüger HJ, Schmidt J (2019) Descending octopaminergic neurons modulate sensory-evoked activity of thoracic motor neurons in stick insects. J Neurophysiol 122:2388-2413.

Szczecinski NS, Bockemühl T, Chockley AS, Büschges A (2018) Static stability predicts the continuum of interleg coordination patterns in Drosophila. J Exp Biol 221.

Thoreson WB, Mangel SC (2012) Lateral interactions in the outer retina. Prog Retin Eye Res 31:407-441.

Torkkeli PH, Panek I (2002) Neuromodulation of arthropod mechanosensory neurons. Microsc Res Tech 58:299-311.

Tuthill JC, Wilson RI (2016a) Mechanosensation and Adaptive Motor Control in Insects. Current Biology 26:R1022-R1038.

Tuthill JC, Wilson RI (2016b) Parallel Transformation of Tactile Signals in Central Circuits of Drosophila. Cell 164:1046-1059.

Tuthill JC, Azim E (2018) Proprioception. Curr Biol 28:R194-R203.

van Swinderen B, Greenspan RJ (2003) Salience modulates 20–30 Hz brain activity in *Drosophila*. Nature Neuroscience 6:579-586.

von Reyn CR, Breads P, Peek MY, Zheng GZ, Williamson WR, Yee AL, Leonardo A, Card GM (2014) A spike-timing mechanism for action selection. Nat Neurosci 17:962-970.

von Uckermann G, Büschges A (2009) Premotor interneurons in the local control of stepping motor output for the stick insect single middle leg. Journal of Neurophysiology 102:1956-1975.

Weidler D, Diecke F (1969) The Role of Cations in Conduction in the Central Nervous System of the Herbivorous Insect *Carausius Morosus*. Zeitschrift für vergleichende Physiologie 64:372-399.

Weiland G, Koch UT (1987) Sensory Feedback During Active Movements of Stick Insects. Journal of Experimental Biology 133:137-156.

Weiland G, Bässler U, Brunner M (1986) A Biological Feedback Control System with Electrotonic Input: The Artificially Closed Femur-Tibia Control System of Stick Insects. Journal of Experimental Biology 120:369-385.

Weiler J, Gribble PL, Pruszynski JA (2021) Spinal stretch reflexes support efficient control of reaching. J Neurophysiol 125:1339-1347.

Windhorst U (2007) Muscle proprioceptive feedback and spinal networks. Brain Res Bull 73:155-202.

Wittenberg G, Kristan WB, Jr. (1992a) Analysis and Modeling of the Multisegmental Coordination of Shortening Behavior in the Medicinal Leech II. Role of Identified Interneurons. Journal of Neurophysiology 68:1693-1707.

Wittenberg G, Kristan WB, Jr. (1992b) Analysis and Modeling of the Multisegmental Coordination of Shortening Behavior in the Medicinal Leech I. Motor Output Pattern. Journal of Neurophysiology 68:1683-1692.

Wolf H, Burrows M (1995) Proprioceptive Sensory Neurons of a Locust Leg Receive Rhythmic Presynaptic Inhibition during Walking. Journal of Neuroscience 15:5623-5636.

Wolf H, Büschges A (1995) Nonspiking Local Interneurons in Insect Leg Motor Control II. Role of Nonspiking Local Interneurons in the Control of Leg Swing During Walking. Journal of Neurophysiology 73:1861-1875.

Zia S, Cody F, O'Boyle D (2000) Joint Position Sense Is Impaired by Parkinson's disease. Ann Neurol 47:218-228.

Zill S, Schmitz J, Büschges A (2004) Load sensing and control of posture and locomotion. Arthropod Structure & Development 33:273-286.

Zill SN, Moran DT (1981a) The Exoskeleton and Insect Proprioception. I. Responses of Tibial Campaniform Sensilla to External and Muscle-Generated Forces in the American Cockroach, *Periplaneta americana*. Journal of Experimental Biology 91:1-24.

Zill SN, Moran DT (1981b) The Exoskeleton and Insect Proprioception. III. Activity of Tribal Campaniform Sensilla During Walking in the American Cockroach, *Periplaneta Americana*. Journal of Experimental Biology 94:57-75.

Zill SN, Moran DT, Varela FG (1981) The Exoskeleton and Insect Proprioception. II. Reflex Effects of Tibial Campaniform Sensilla in the American Cockroach, *Periplaneta americana*. Journal of Experimental Biology 94:43-55.

Zill SN, Büschges A, Schmitz J (2011) Encoding of force increases and decreases by tibial campaniform sensilla in the stick insect, Carausius morosus. Journal of Comparative Physiology 197:851-867.

Zill SN, Schmitz J, Chaudhry S, Büschges A (2012) Force encoding in stick insect legs delineates a reference frame for motor control. Journal of Neurophysiology 108:1453-1472.

Zill SN, Chaudhry S, Büschges A, Schmitz J (2013) Directional specificity and encoding of muscle forces and loads by stick insect tibial campaniform sensilla, including receptors with round cuticular caps. Arthropod Structure & Development 42:455-467.

Zill SN, Chaudhry S, Büschges A, Schmitz J (2015) Force feedback reinforces muscle synergies in insect legs. Arthropod Structure & Development 44:541-553.

Zill SN, Dallmann CJ, Büschges A, Chaudhry S, Schmitz J (2018) Force dynamics and synergist muscle activation in stick insects: the effects of using joint torques as mechanical stimuli. J Neurophysiol 120:1807-1823.

Zill SN, Dallmann CJ, Szczecinski NS, Büschges A, Schmitz J (2021) Evaluation of force feedback in walking using joint torques as 'naturalistic' stimuli. Journal of Neurophysiology.

Zill SN, Neff D, Chaudhry S, Exter A, Schmitz J, Büschges A (2017) Effects of force detecting sense organs on muscle synergies are correlated with their response properties. Arthropod Structure & Development 46:564-578.

10 Supplementary Material

10.1 Supplementary Material Chapter 2

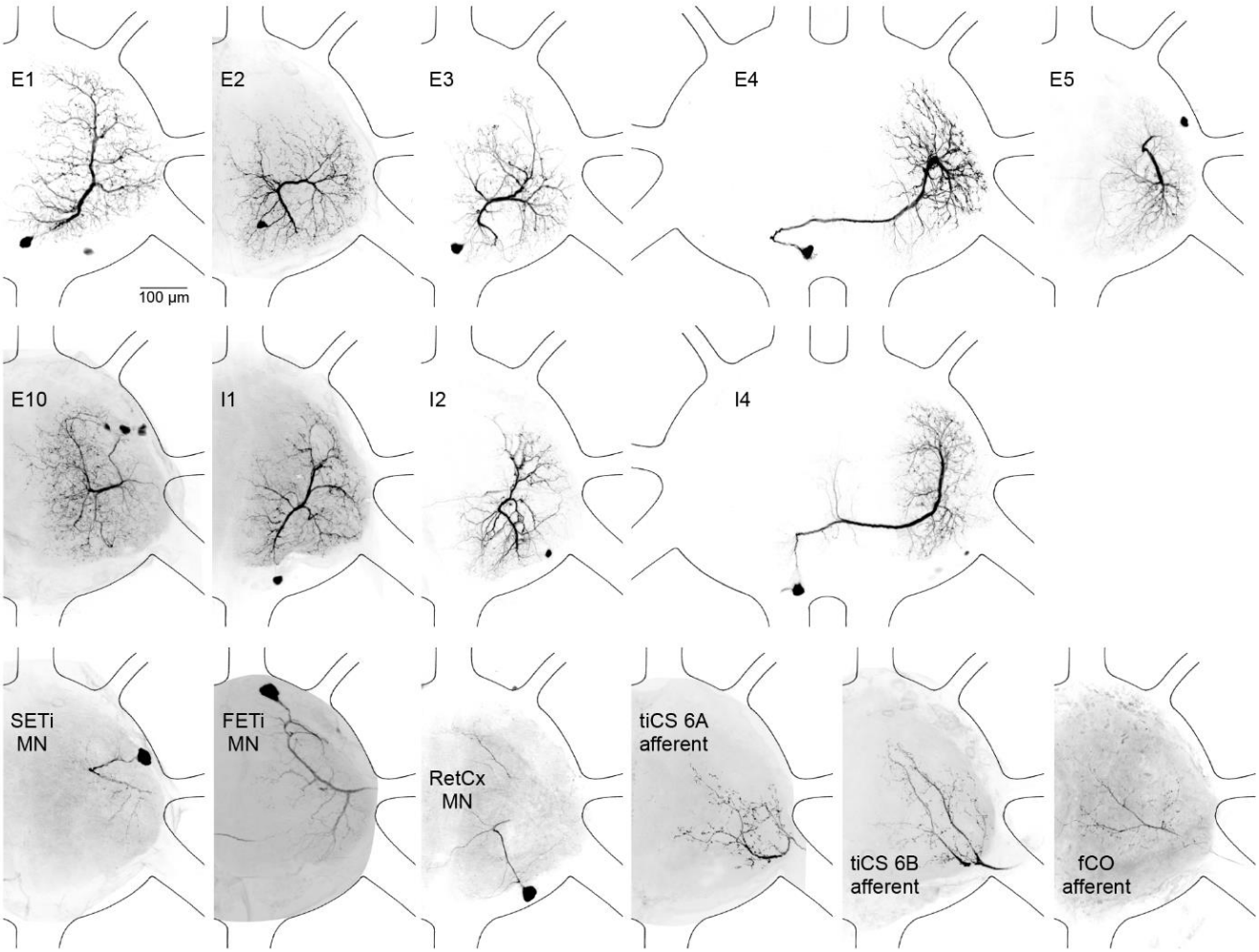

Supplementary Figure 2.1: Morphology of identified NSIs, MNs, and sensory afferents included in this dissertation. All neurons were stained following intracellular recording by iontophoretic injection of neurobiotin tracer (see Chapter 2, Materials and Methods). Morphology was used to complement physiology for neuron identification. NSIs were identified based on previously published characteristics. (Büschges, 1990; Driesang and Büschges, 1993; Büschges et al., 1994; Sauer et al., 1995, 1996; Rosenbaum, 2013; Berg, 2014). Note that NSI E10 was originally named E9 by T. Akay and first recorded by R.A. DiCaprio (personal communication in Akay, 2002), but was relabeled E10, for details see Chapter 2, Discussion (Akay, 2002). Axons of SETi and FETi MNs project through nl3; axons of RetCx MNs project into nl5 via the ncr; tiCS & fCO afferents project through the ncr. Scale bar given in E1.

Supplementary Table 2.1: Number of recorded NSIs. (N/N): number of recordings with qualitatively the same response / total number of recordings. (N): number of recordings with qualitatively the same response, equals the total number of experiments. (N_{total}): total number of recordings of each type of NSI.

NSI	N_{total}	N_{fCO}	$N_{tiCS\ dorsal}$	$N_{tiCS\ ventral}$	$N_{tr/fCS\ anterior}$	$N_{tr/fCS\ posterior}$
E1	7	7	4	2	2	3
E2	8	8	5	1	3	4
E3	12	9/12	7	2/3	2	2
E4	22	22	9/10	3	9/10	9/11
E9	3	3	2	2	1	1
I1	11	11	3	3	7	6/7
I3	10	10	6	2/3	1	2
I4	6	6	3	2	1	3
I5	6	6	4	3	1	2

10.2 Supplementary Material Chapter 3

Supplementary Table 3.1: Number of recordings (N), number of stimulus runs per recording (n, each stimulus run depicts average of 5-10 consecutive stimuli), average, standard deviation and raw data of Fig.s 3.1 – 3.4. Data for Fig. 3.2 E in Suppl. Table 3.2. [1]includes anterior & posterior stimulus direction; [2]includes dorsal & ventral stimulus direction; [3]each; [4]suprathreshold, fCO stimulus; [5]suprathreshold, tiCS stimulus; [6]fCO stimulus; [7]tiCS stimulus; [8]50 ms; [9]stimulus, [10]frequency of combined tiCS & fCO stimuli normalized to exclusive fCO stimuli.

figure	N (number of recordings)	n (number of stimulus runs per recording)	average	standard deviation	raw data [ms]
1 Bi	1	100			
1 Bii – A*	7	100	9.13	0.54	8.64
					9.36
					8.64
					8.64
					9.20
					10.08
					9.36
1 Bii – A'	7	100	4.27	0.33	4.16
					4.64
					4.24
					3.92
					3.84
					4.64
					4.48
1 Ci – fCO	3	2 - 7	2.52	0.20	2.72
					2.73
					2.4
					2.48
					2.33
					2.33

					2.40
					2.40
					2.47
					2.52
					2.95
1 Ci – tr/f CS [1]	5	2 - 7	5.94	0.93	6.56
					7.19
					7.34
					6.16
					6.24
					6.01
					4.54
					5.27
					5.04
					6.24
					4.80
1 Ci – tiCS A* [2]	5	1 - 2	6.76	1.65	5.75
					7.19
					4.55
					8.81
					7.52
1 Ci – tiCS A' [2]	6	2	2.08	1.16	3.6
					3.52
					1.11
					1.12
					1.53
					1.59
1 Di – fCO	9	1	4.33	0.59	3.2
					4.64
					4.00
					4.64
					4.00
					4.1
					5.28
					4.66
					4.5
	6	1	11.76	0.71	11.37

1 Di – tiCS					13.1
					11.38
					12.01
					11.51
					11.21
2 Aii – Dii [3]	1	5 (every tiCS spike above threshold in 5 consecutive stimuli)			
3 C – SETi [4]	10	1	12.27	1.97	10.24
					12.77
					14.34
					14.66
					8.92
					12.57
					12.84
					13.47
					9.68
					13.24
3 C – SETi [5]	10	1	48.70	4.31	53.79
					53.21
					48
					51.28
					43.8
					43.02
					46.91
					45.2
					54.94
					46.88
3 C – E4 [6]	10	1	5.62	0.20	5.74
					5.34
					5.30
					5.77
					5.49
					5.64
					5.79
					5.60
					5.90
					5.68

3 C – I5 [8]	2	1	18.30	0.42	18.00
					18.60
4 D - F	5	1	29.8	9.5	29.9
					25.2
					30.9
					18.7
					44.5
			fCO [Hz]	fCO + tiCS [Hz]	nor-mal-ized[11]
4 A [8]	11	1	100	120	1.2
			60	40	0.67
			20	40	2
			60	40	0.67
			60	60	1
			100	100	1
			120	120	1
			120	120	1
			120	120	1
			120	120	1
			120	120	1
4 A [9]	11	1	35.71	40.71	1.14
			22.86	25.00	1.09
			10.71	13.57	1.27
			16.43	15.71	0.96
			17.86	19.29	1.08
			28.57	32.14	1.13
			60.71	65.71	1.08
			32.86	36.43	1.11
			4.29	6.43	1.50
			30.71	24.29	0.79
			32.14	42.87	1.33
4 B [8]	11	1	100	100	1
			60	40	0.67
			60	40	0.67
			60	60	1
			80	80	1
			100	80	0.8
			60	80	1.33
			100	100	1
			60	60	1
			100	80	0.8
			60	60	1
4 B [9]	11	1	39.29	22.86	0.58
			20	16.43	0.82
			21.43	8.57	0.40
			14.29	10.7	0.75
			22.14	15	0.68
			40	34.29	0.86
			32.86	17.86	0.54
			47.14	41.43	0.88
			52.86	35	0.66
			57.14	33.57	0.59
			39.29	22.86	0.58
(4 D-F see above)					

Supplementary Table 3.2 (*following pages*): Latency data [ms] of sensory afferents, NSIs, and MNs to sensory stimuli in Fig. 3.2 E. Raw data from individual recordings (average of 5-10 consecutive stimuli), average / standard deviation, and normalized latency. Latency data was normalized by subtracting the average transmission time from stimulus onset to recording site B plus the standard deviation (see Fig. 3.1 E; fCO: 4.9 ms; tr/fCS: 8.8 ms; tiCS: 12.5 ms; for details, see Chapter 3). Each data point within one sensory modality from a different recording. NSIs E4 and I5 show depolarizations in response to fCO elongation and relaxation (E4) or to dorsal and ventral tiCS stimulation (I5). Data for different stimulus directions was pooled in Fig. 3.2 E, but separated in Fig. 3.3 C; the subset of data from Fig. 3.2 E used in Fig. 3 C is duplicated in Suppl. Table 3.1.

neuron type	fCO stimulation, excitation	average / standard deviation	normalized	fCO stimulation, inhibition	average / standard deviation	normalized	tr/fCS stimulation, excitation	average / standard deviation	normalized	tr/fCS stimulation, inhibition	average / standard deviation	normalized	tiCS stimulation, excitation	average / standard deviation	normalized	tiCS stimulation, inhibition	average / standard deviation	normalized
fCO afferent	3.20	4.31 / 0.71	-1.70															
	4.64		-0.26															
	4.00		-0.90															
	4.10		-0.80															
	5.28		0.38															
	4.66		-0.24															
tiCS afferent	11.37	11.76 / 0.71	6.47															
	13.10		8.20															
	11.38		6.48															
	12.01		7.11															

	11.51		6.61																
	11.21		6.31																
E1	5.00	6.08 / 0.63	0.10				8.90	10.35 / 2.01	0.10				13.50	12.30 / 1.70	1.00	79.70	53.05 / 18.29	67.20
	6.24		1.34				12.64		3.84				11.10		-1.40	40.50		28.00
	6.44		1.54				9.50		0.70							41.70		29.20
	6.10		1.20													50.30		37.80
	6.60		1.70															
E2	5.00	6.20 / 1.08	0.10	12.70	12.16 / 3.30	7.80	20.98	23.23 / 4.14	12.18				24.90	29.44 / 10.19	12.40			
	7.30		2.40	10.58		5.68	28.00		19.20				22.10		9.60			
	5.81		0.91	10.80		5.90	20.70		11.90				19.50		7.00			
	6.40		1.50	17.60		12.70							38.90		26.40			
	5.14		0.24	9.09		4.19							41.78		29.28			
	7.55		2.65															
E3	6.15	5.83 / 0.46	1.25	8.10	11.81 / 2.29	3.20	27.20	30.68 / 4.91	18.40				13.30	13.18 / 0.92	0.80	57.11	60.59 / 4.91	44.61
	4.90		0.00	15.29		10.39	34.15		25.35				13.30		0.80	64.06		51.56
	6.42		1.52	13.60		8.70							14.30		1.80			
	6.04		1.14	11.67		6.77							13.82		1.32			
	5.40		0.50	11.22		6.32							12.90		0.40			
	5.70		0.80	13.60		8.70							13.93		1.43			
	5.80		0.90	10.30		5.40							11.42		-1.08			
	6.16		1.26	9.50		4.60							12.46		-0.04			
	5.90		1.00	13.04		8.14												
E4	5.74	6.02 / 0.50	0.84				9.80	11.72 / 2.46	1.00	14.04	18.27 / 7.14	5.24	21.15	20.98 / 0.25	8.65	22.33	24.00 / 4.27	9.83
	5.34		0.44				9.53		0.73	13.10		4.30	20.80		8.30	26.90		14.40

	5.30		0.40				13.91		5.11	18.63		9.83				25.60		13.10
	5.77		0.87				14.80		6.00	13.03		4.23				20.10		7.60
	5.49		0.59				10.54		1.74	15.54		6.74				19.82		7.32
	5.64		0.74							34.80		26.00				20.20		7.70
	5.79		0.89							17.14		8.34				21.78		9.28
	5.60		0.70							19.90		11.10				32.50		20.00
	5.90		1.00													26.80		14.30
	5.68		0.78															
	6.09		1.19															
	6.28		1.38															
	6.63		1.73															
	6.23		1.33															
	5.98		1.08															
	6.32		1.42															
	6.80		1.90															
	6.55		1.65															
	7.14		2.24															
	6.20		1.30															
E9	13.30	10.83 / 3.49	8.40	12.30	11.43 / 1.23	7.40	22.70	19.86 / 2.64	13.90				14.41	14.46 / 0.06	1.91	25.20	20.23 / 7.03	12.70
	8.37		3.47	10.56		5.66	17.48		8.68				14.50		2.00	15.26		2.76
							19.40		10.60									
I1	6.02	6.14 / 0.15	1.12	10.00	14.52 / 2.77	5.10	8.28	11.44 / 4.47	-0.52	10.88	17.15 / 5.44	2.08				16.80	19.09 / 2.69	4.30
	6.30		1.40	14.70		9.80	14.60		5.80	19.86		11.06				17.40		4.90
	6.24		1.34	15.70		10.80				20.70		11.90				19.25		6.75

	6.00		1.10	17.50		12.60										18.42		5.92
				14.70		9.80										23.60		11.10
I3	6.00	6.33 / 0.54	1.10				15.73	15.73	6.93				21.60	28.16 / 5.10	9.10			
	6.18		1.28										32.42		19.92			
	5.60		0.70										27.60		15.10			
	5.80		0.90										25.20		12.70			
	7.16		2.26										33.98		21.48			
	6.07		1.17															
	6.60		1.70															
	5.60		0.70															
	6.94		2.04															
	6.20		1.30															
	6.80		1.90															
	7.10		2.20															
	6.24		1.34															
I4	5.00	6.18 / 1.04	0.10				41.61	25.56 / 22.70	32.81	13.83	24.81 / 10.44	5.03				28.21	27.82 / 10.32	15.71
	5.83		0.93				9.51		0.71	34.60		25.80				26.30		13.80
	7.80		2.90							26.00		17.20				15.81		3.31
	5.80		0.90													40.96		28.46
	6.45		1.55															
I5	6.25	6.33 / 0.19	1.35	13.00	11.03 / 1.36	8.10	27.10	20.73 / 7.15	18.30				12.50	14.71 / 2.94	0.00			
	6.56		1.66	9.70		4.80	22.10		13.30				11.50		-1.00			
	6.25		1.35	9.84		4.94	13.00		4.20				13.26		0.76			
	6.09		1.19	11.60		6.70							14.40		1.90			

	6.49		1.59	11.00		6.10							18.00		5.50			
													18.60		6.10			
SETi MN	6.10	6.01 / 0.35	1.20	12.39	15.80 / 4.28	7.49							45.61	38.21 / 10.47	33.11	32.30	31.67 / 3.39	19.80
	5.62		0.72	14.41		9.51							30.80		18.30	34.70		22.20
	6.30		1.40	20.60		15.70										28.00		15.50
FETi MN	5.62	5.92 / 0.36	0.72	16.87	14.29 / 1.87	11.97	48.20	48.20	39.40				13.70	14.32 / 1.82	1.20			
	6.49		1.59	12.60		7.70							12.10		-0.40			
	5.60		0.70	13.30		8.40							15.16		2.66			
	6.00		1.10	14.40		9.50							16.30		3.80			
	5.90		1.00															
Cl_1 MN	4.81	5.33 / 0.75	-0.09										24.09	21.15 / 4.16	11.59			
	5.29		0.39										18.20		5.70			
	4.82		-0.08															
	6.40		1.50															
RetCx MN	22.60	37.95 / 21.71	17.70	11.98	14.39 / 3.26	7.08	11.89	14.11 / 4.02	3.09				32.90	35.43 / 2.37	20.40	23.70	20.51 / 4.51	11.20
	53.30		48.40	13.10		8.20	15.20		6.40				37.60		25.10	17.32		4.82
				18.10		13.20	19.24		10.44				35.80		23.30			
							10.10		1.30									

10.3 Supplementary Material Chapter 6

Supplementary Table 6.1: Likelihood of occurrence of the active reaction in response to fCO stimuli in the presence and absence of tiCS ramp stimuli. Animals were decerebrated, and dissected for tiCS and fCO stimulation as described in Chapter 2, Materials and Methods. ExtTi MN activity was recorded from nerve F2. The animals were activated by repeated tactile stimulation of the abdomen, ExtTi MN responses were defined as active reactions according to established criteria (Bässler, 1976, 1986, 1988; Driesang and Büschges, 1993; Schmitz et al., 2019). Likelihood of occurrence to combined stimuli was normalized to the occurrence during exclusive fCO stimuli.

likelihood of occurrence for the active reaction			number of stimuli per stimulus paradigm	stimulated tiCS group
exclusive fCO stimulus [%]	combined fCO + tiCS stimulus [%]	normalized combined fCO + tiCS stimulus		
65	82.5	1.27	40	6B
65	70.9	1.09	110	6B
70	67.5	0.96	40	6B
38	74	1.95	50	6B
81.4	84.3	1.04	70	6B
38.6	96.7	2.51	60	6B
77.1	88.6	1.15	70	6B
60	70	1.17	10	6B
77	70	0.91	100	6A
45	72.5	1.61	40	6A
15	25	1.67	20	6A
	average	1.39		
	standard deviation	0.49		

11 Acknowledgements

When writing a dissertation, you are told to write “I did”, because it is your work, your project, your own first contribution to scientific knowledge. This now is the section where I am finally allowed to admit that “we did”, and to thank everyone that supported me along the way.

I want to thank my Doktorvater, Prof. Ansgar Büschges, who encouraged and supported me since my B.Sc. studies. Thank you for being an enthusiastic supervisor and a true mentor. Despite a busy schedule, you always found time to come to the setup and record nonspikers when I was convinced that E4 simply did not exist in stick insects any more. It was your lecture during the B.Sc. main module that sparked my curiosity in neuroscience – I did not understand half of it, but thought this much enthusiasm must have a valid reason.

I am very grateful to the members of the Büschges lab. In between scientific discussions, retreats, Mauerbier, paella, and a pandemic I have made great friends, and your support was indispensable. A special thanks goes to the Büro Buddies; Gesa, for always being ready to listen, independent of time and outside temperature, and for getting through this together, Alex, for showing me how to stand up for my own (scientific) opinion, regardless of who I am talking to, and Sander, for having the wildest oscillating work-life-balance and showing me that working on weekends is fun, too, as long as you oscillate back to the life-side of the balance often enough. All of you were an important part of my PhD, and the source of definitely too many nicknames – Sincerely, Stick Insect the Empty Chair.

A huge thank you also to Dr. Till Bockemühl, who helped me develop concrete analyses when all I had were fuzzy ideas, and for helping me when Matlab was saying no. Thank you to Dipl.-Ing. Micha (Günther) Dübbert for making my ideas work, and for endless rounds of trouble shooting – even though trouble occasionally shot back. I want to thank PD Dr. Jochen Schmidt, because his door was always open, even if I just wanted to discuss the latest addition to my electrophysiological cabinet of curiosities. Thank you also to Mehrdad Ghanbari for technical support, and Dr. Christoph Guschlbauer, for showing me the ways of the muscle force.

I am very grateful to the members of my TAC, Prof. Dr. Silvia Daun and Prof. Dr. Abdel El Manira, for their valuable input and fruitful, motivating discussions, and to Dr. Eugenia Chiappe, for her time and commitment as my mentor, and for shaping my diffuse ideas about academia into a concrete notion of what is going on here. I am also very grateful to Prof. Dr. Sasha Zill, who is the most contagiously enthusiastic scientist I know, and Dr. Nick Szczecinski, whose questions about the NSI network made me sit down and think (which might be just as useful as contagious enthusiasm).

I have wanted to become a scientist since I was twelve years old and read a book about marine scientists on a boat. The main reason why I am a giant step closer to this goal (the scientist, not the boat), today, 15 years later, are my parents, Beate and Achim Gebehart, and my brother Robin. I was never told to maybe study something a bit more financially sensible, or to have a plan B, or to reconsider my choice. I am the child of two business economics graduates, but they never made me feel pressure to follow in their steps – they helped me find my own path, supported me when the going was rough, and told me when I needed to sit down and take a breath. Thank you for more than I can put into words. And thank you, Robin, for sitting through dinners talking about insects, and dissections, and other topics that might not be generally accepted as dinner-appropriate. No acknowledgements would be complete without our dog Kim, who was a non-certified cuddle expert and could lift even the darkest mood with a hearty sneeze and her enthusiastic ignorance of whatever real-world problem was knocking on the door.

There are many more people that should be mentioned here, and I hope they will forgive me that they are not – space is limited, time is fleeting and all that, but I am grateful whether or not I put it down on paper. To all of you out there who supported me, made me believe in myself, or just gave me a pat on the back when I needed it, feel deeply acknowledged. Because not “I did”, but “we did”.

12 Data Storage & Availability

This dissertation project involved the acquisition of primary data and subsequent analyses.

Experimental protocols are included in the dissertation. All analysis protocols were custom-written using Matlab (Mathworks) or Spike2 (CED) if not indicated otherwise.

Primary data, analysis protocols, and all additional information are archived using the Tivoli Storage Manager Client (IBM) of the Regional Computing Centre of the University of Cologne, and are available from C. Gebehart or Prof. Dr. A. Büschges upon reasonable request.

13 Funding

This project was funded by the Deutsche Forschungsgemeinschaft (DFG, German Research Foundation, grant 233886668 / GRK1960 to Ansgar Büschges and Corinna Gebehart), and supported by the Studienstiftung des deutschen Volkes (to Corinna Gebehart).

14 Erklärung

Hiermit versichere ich an Eides statt, dass ich die vorliegende Dissertation selbstständig und ohne die Benutzung anderer als der angegebenen Hilfsmittel und Literatur angefertigt habe. Alle Stellen, die wörtlich oder sinngemäß aus veröffentlichten und nicht veröffentlichten Werken dem Wortlaut oder dem Sinn nach entnommen wurden, sind als solche kenntlich gemacht. Ich versichere an Eides statt, dass diese Dissertation noch keiner anderen Fakultät oder Universität zur Prüfung vorgelegen hat; dass sie - abgesehen von unten angegebenen Teilpublikationen und eingebundenen Artikeln und Manuskripten - noch nicht veröffentlicht worden ist sowie, dass ich eine Veröffentlichung der Dissertation vor Abschluss der Promotion nicht ohne Genehmigung des Promotionsausschusses vornehmen werde. Die Bestimmungen dieser Ordnung sind mir bekannt. Darüber hinaus erkläre ich hiermit, dass ich die Ordnung zur Sicherung guter wissenschaftlicher Praxis und zum Umgang mit wissenschaftlichem Fehlverhalten der Universität zu Köln gelesen und sie bei der Durchführung der der Dissertation zugrundeliegenden Arbeiten und der schriftlich verfassten Dissertation beachtet habe und verpflichte mich hiermit, die dort genannten Vorgaben bei allen wissenschaftlichen Tätigkeiten zu beachten und umzusetzen. Ich versichere, dass die eingereichte elektronische Fassung der eingereichten Druckfassung vollständig entspricht.

Teilpublikation:

Gebehart C, Schmidt J, Büschges A (2021) Distributed Processing of Load and Movement Feedback in the Premotor Network Controlling an Insect Leg Joint. Journal of Neurophysiology 125: 1800-1813. doi: 10.1152/jn.00090.2021.

Corinna Gebehart Köln, den 01.07.2021

You can’t possibly be a scientist if you mind people thinking that you’re a fool.

Douglas Adams